SYNTHESIS OF FLUORESCENT POLYMERS WITH PENDANT TRIAZOLE-QUINOLINE GROUPS *VIA* RAFT POLYMERIZATION

J.M.V. Ngororabanga

2014

SYNTHESIS OF FLUORESCENT POLYMERS WITH PENDANT TRIAZOLE-QUINOLINE GROUPS *VIA* RAFT POLYMERIZATION

By

J. M.V. Ngororabanga

A dissertation submitted in fulfilment of the requirements for the Masters degree in chemistry to be awarded at the Nelson Mandela Metropolitan University

January 2014

Supervisor: Dr. N. Mama
Co-Supervisor: Prof. C. W. McCleland

Dedication

To my mother, siblings and friends

Acknowledgements

I would like to acknowledge the following people and institutions that made it possible for me to complete this project;

- The almighty God for the gift of life
- My supervisor, Dr. N. Mama for proposing the project and for her constant guidance and support
- My co-supervisor, Prof. C. W. McCleland for his input and valued advice
- National Research Fund (NRF) and Nelson Mandela Metropolitan University (NMMU) for funding and giving the opportunity and facilities to carry out the project
- Mr. H. marchand, H. Schalekamp and E. Bashman for their technical assistance
- Fellow students and friends at Nelson Mandela Metropolitan University
- My mother and siblings for their endless love and motivation.

Abstract

In this study, fluorescent polymers with pendant quinoline groups were synthesized by reversible addition-fragmentation chain transfer polymerization (RAFT) from a fluorescent quinoline-based vinyl monomer, synthesized in multiple steps from *p*-nitroaniline and crotonaldehyde. The structures of the synthesized vinyl monomer and polymers were confirmed by NMR and FT-IR spectroscopy, X-ray studies and modeling stdies.

The photophysical properties of the synthesized quinoline compounds and resulting polymers were investigated. In order to evaluate the binding potential of our quinoline-based polymer in the presence of transition metal ions, preliminary studies on a complexation of quinoline-based polymers with Zn, Cd, Hg, Fe, and Ni were carried out. The investigation of fluorescence properties of the complexes showed fluorescence quenching for Fe(II), and fluorescence enhancement for the remaining ions [Zn(II), Cd(II), Hg(II), and Ni(II)].

Table of contents

List of figures

Selected abbreviations

OLED: Organic light emitting diodes

TMS: Trimethylsilyl

TBPA: Tris(4-bromophenyl)aminium hexachloroantimonate

CuAAC: Cu(I)-catalysed azide-alkyne cycloaddition

THF: Tetrahydrofuran

DMF: *N*,*N*-dimethyl formamide

DMSO: Dimethyl sulfoxide

VSEPR: Valence Shell electron pair repulsion

UV-vis: Ultraviolet-visible

AIBN: 2,2'-azobisisobutyronitrile

CRP: Controlled/''Living'' radical polymerization

NMP: Nitroxide mediated polymerization

ATRP: Atomic transfer radical polymerization

RAFT: Reversible addition-fragmentation chain transfer polymerization

PRE: Persistence radical effect

TEMPO: 2,2,6,6-tetramethylpiperidinyl-1-oxy

CSIRO: Commonwealth Scientific and Industrial Research organization

CTA: Chain transfer agent

ATRA: Atomic transfer radical addition

PET: Photoinduced electron transfer

ICT: Intermolecular charge transfer

FRET: Fluorescence resonance energy transfer

([H-NMP]$^+$ HSO$_4$: *N*-methyl-2-pyrrolidinium bisulfate

DFT: Density field theory

CPDB: 2-(2-cyanopropyl)-dithiobanzoate

TLC: Thin layer chromatography

EPA: Environment protection agency

PMDETA: *N,N,N′,N″,N″*-Pentamethyldiethylenetriamine

PTSA: *p*-toluene sulfonic acid

DCM: Dichloromethane

NaAsc: Sodium ascorbate

HOAc: acetic acid

Rt: Room temperature

TG: Thermogravimetry

DTG: Derivative thermogravimetry

GPC: Gel Permission Chromatography

DMA: N,N-dimethylaniline

PMMA: Poly(methyl methacrylate)

Chapter 1

Introduction

1.1. Overview

For the past few decades quinolone derivatives (Figure **1.1a**) have been well known as building blocks of many synthetic and natural occurring compounds that exhibit a wide range of therapeutic and biological activities**.**[1,2,3] Those compounds have been introduced in clinical practice as anti-inflammatory, anti-fungal, anti-malarial, antiasthmatic, antihypertensive, and tyrosine kinase inhibiting agents.[4,5] An interesting example of a quinoline-containing naturally occurring compound is quinine (Figure **1.1b**), the antimalarial drug isolated from cinchona bark.

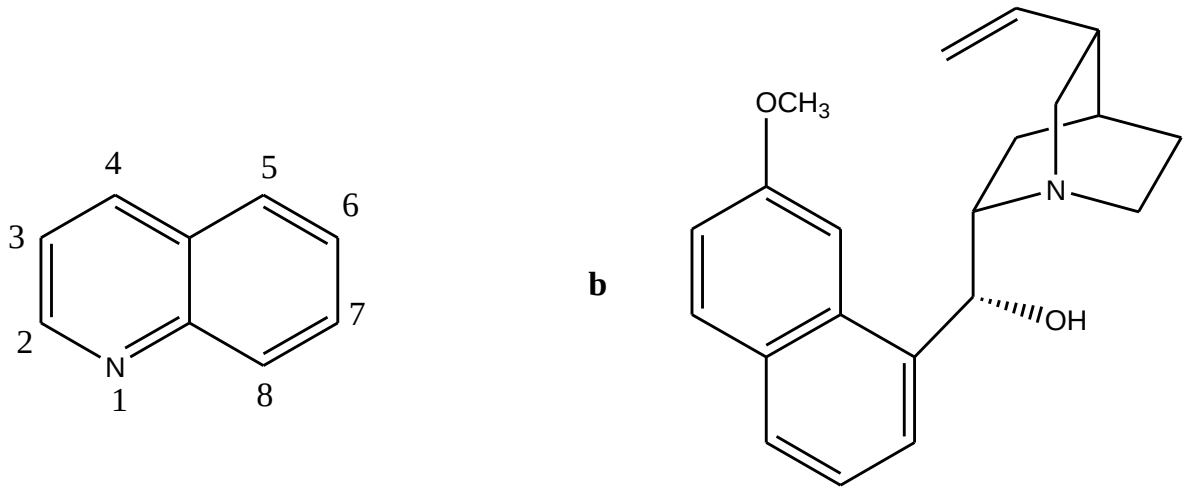

1 **2**

Figure 1.1: a) Quinoline skeleton and its numbering b) Quinine structure

The development of cheap organic compounds which aimed to replace costly inorganic materials in electronic devices has extended the applications of quinoline-containing compounds, with many quinoline-containing low molecular weight compounds and polymers being synthesized for various electrophotonic applications.

Besides the low cost associated with organic materials, they also exhibit faster response times under excitation than their analogous inorganic materials, and their emission wavelengths can be easily tuned through structural modification.

Compared to their low molecular weight counterparts, quinoline-based polymers have received much attention due to their easy processing or spin casting from solution. The first report on quinoline-based polymers was published by Stille and Coworker in the 1970's,[6] and the Friedländer reaction involving high-yielding condensation reaction of aromatic amines or ketones with ketomethylene species, was used for quinoline ring formation as shown in Scheme **1.1**.

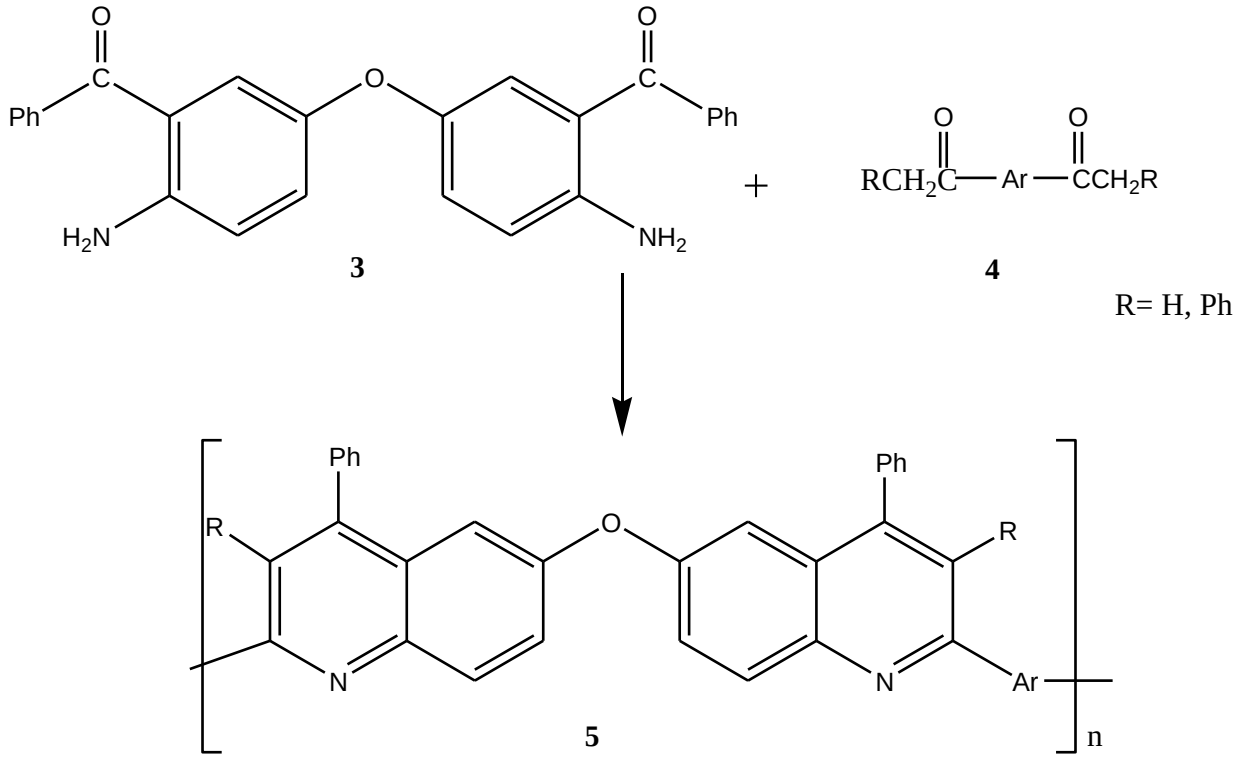

Scheme 1.1: Quinoline-based polymers published by Stille

Quinoline-based polymers are known to exhibit excellent thermal and oxidative stabilities, high electron mobilities, low relative permittivity, good mechanical strength, low moisture absorption, high photoluminescence efficiencies and film forming properties, and these features allow them to be used in electroluminescence devices,[7] organic photovoltaic cells,[8] electrochromic cells,[9] chemosensors[10] and non–linear optics.[11]

Due to the presence of *N*-heterocycles either in the main chain or as part of pendant chains, quinoline-containing polymers have proved to be important materials in semiconductor manufacturing, where they can act as *n*-type polymeric semi-conductors.[12,13] The latter are involved in the fabrication of more efficient and high-performance plastic electronic and optoelectronic devices.

In the past few decades quinoline-based polymers and their derivatives have been among the most studied and successful classes of polymeric material for organic light emitting diodes (OLED).[14,15] This attracted the attention of many researchers intending to design and synthesize quinoline-based polymers with improved photophysical properties and processability. Among the synthetized quinoline polymers are non-linear and linear polymers as shown in Figure **1.2**

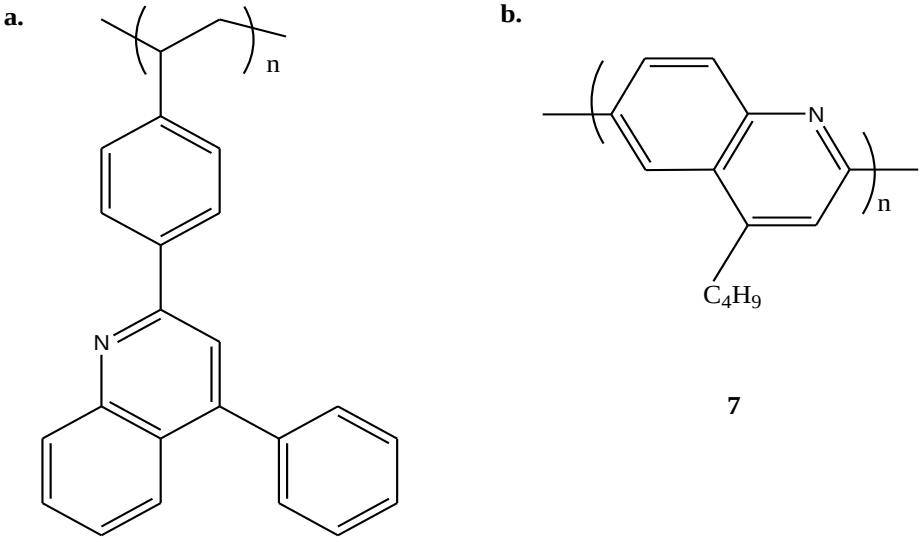

6 **7**

Figure 1.2: a) Polystyrene-supported phenyl quinoline[16] b) Poly(4-butylquinoline)[17]

Recently, due to developments in polymer science which aimed to produce polymeric materials that fit the targeted properties, various new types of monomers and synthetic processes have been designed.

Among the newly designed monomers are included a new class of vinyl monomer "functionalized 4-vinyl-1,2,3-triazoles''(Figure **1.3**) in which the properties of the triazole ring system as well as inherent properties of classical vinyl monomers such polarity, aromaticity, and structural diversity, are combined within one structural unit.[18]

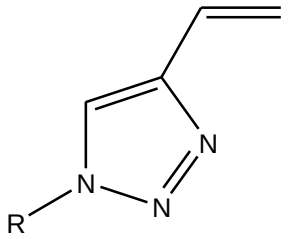

8

Figure 1.3: 4-vinyl-1,2,3-triazoles derivative

The design of this novel type of vinyl monomer relies on efficient synthesis for the basic monomer unit and its easy functionalization. Since the synthetic methods and design of the basic monomer unit is mediated by quantitative, insensitive and regioselective Cu(I)-catalyzed Huisgen's 1,3-dipolar cycloaddition of alkynes with azides (the"Click reaction''), this new class of compounds has become a focus of much research in polymer and materials science intending to develop libraries of new synthetic polymers with an extended range of functional groups and improved physical properties.[19] The main attractive properties of these polymers are their high stabilities originated from the triazole ring, and large dipole moments. [20]

The early synthesis of 4-vinyl-1,2,3-triazole containing monomers involved the reaction between a suitable organic azide and trimethylsilyl (TMS)-protected vinyl acetylene under click conditions as shown in the Scheme **1.2**.[21]

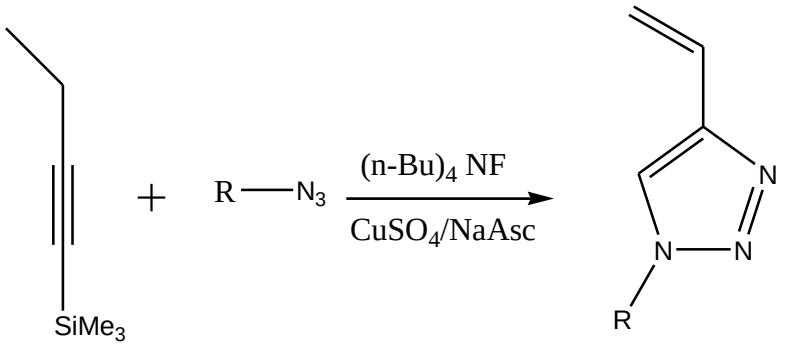

9 **8**

Scheme 1.2: Early synthetic method for 4-vinyl-1,2,3-triazole containing monomers

This high-yielding reaction exhibited a number of limitations including difficulty in the preparation and handling of trimethylsilyl (TMS)-protected vinyl acetylene, as well as costly starting materials. Recently, the use trimethylsilyl (TMS)-protected vinyl acetylene has been overtaken by more readily available alkynes or alkyl halides, resulting in intermediate species **11** which undergoes elimination or Wittig reaction to afford the desired monomer as shown in Scheme **1.3**.[22]

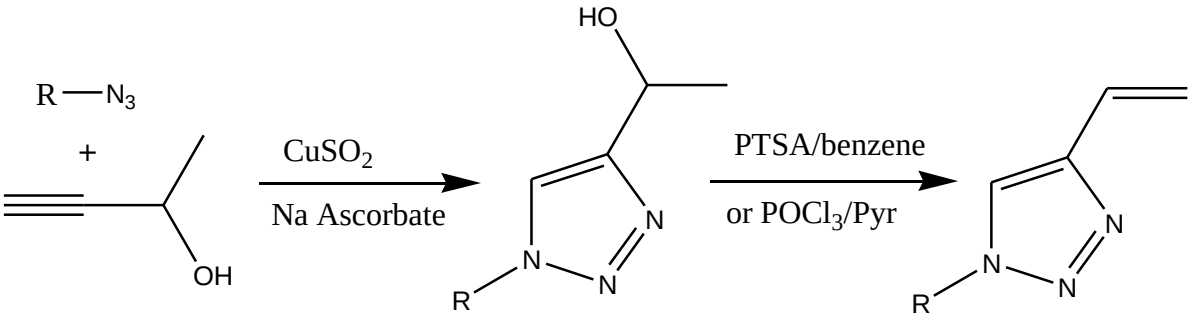

10 **11** **12**

Scheme 1.3: Recent synthetic procedure for 4-vinyl-1,2,3-triazoles derivative

Generally, vinyl monomers can be polymerized *via* conventional free radical polymerization techniques which offer a number of advantages compared to other polymerization techniques, such as impurity tolerance, moderate reaction temperature, and the availability of multiple polymerization processes.

Despite those advantages conventional free radical polymerization lacks molecular weight control and results in polymers with high molecular weight distribution. Since the properties of the polymers depend on molecular weight distribution and number of incorporated monomers, living or controlled free radical polymerization which offers molecular weight control has become the preferred polymerization technique for these novel vinyl monomers. In this work conventional free radical polymerization and a well-known controlled system "reversible addition fragmentation chain transfer polymerization (RAFT) was investigated.

1.2. Synthesis of quinoline and its derivatives

Heterocyclic containing compounds including quinoline derivatives have received much attention due to their wide range of physiological and pharmaceutical applications. Though quinolines and their derivatives are well-known in medicinal chemistry as building blocks for various naturally occurring products[23] and drugs[24] they have also been applied in a wide range of studies such as polymer science, organic electronics, and optoelectronics, owing to their outstanding mechanical properties.[25] Several quinoline-based copolymers including diblock and triblock have been studied for their ability to undergo hierarchical self-assembly into nano and microstructures with superior electronic and photonic functions.[26] Quinolines have also found application in various bioorganic and bioinorganic processes.[27] Due to their extensive scientific, medicinal and industrial applications, their synthesis has attracted much attention and a number of synthetic methodologies have been developed. Existing methodologies for quinoline synthesis include the Combes,[28] Pfitzinger,[29] Doebner Van Muller,[30] Gould Jacobs,[31] Skraup[32] and Friedländer annulation methods.[33]

Due to its accessibility, Friedländer annulation has proved to be a facile and extensively used synthetic method for polysubstituted quinolines compounds. A typical reaction involves a condensation reaction of *O*-aminoaryl aldehydes or ketones with an appropriate carbonyl derivative compound having a reactive α-methylene group. This leads to the formation of an intermediate species which undergoes cyclocondensation to give quinolines as shown in Scheme **1.5.**

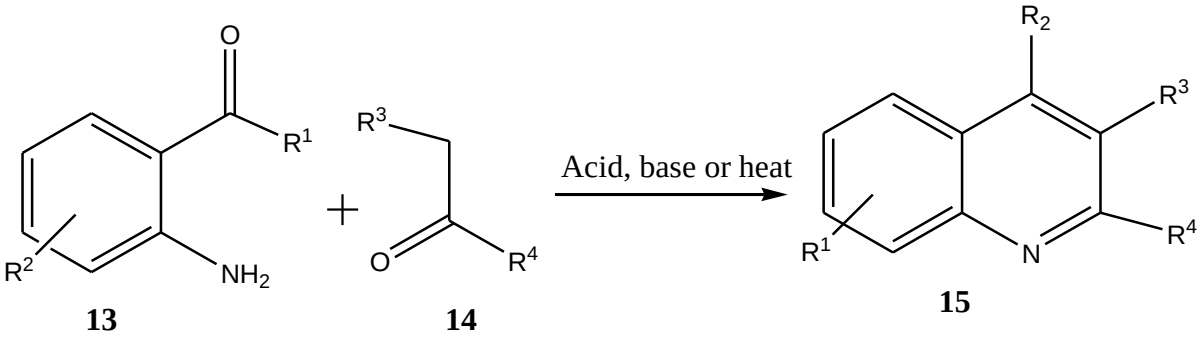

13 **14** **15**

Scheme 1.4: Friedländer reaction.

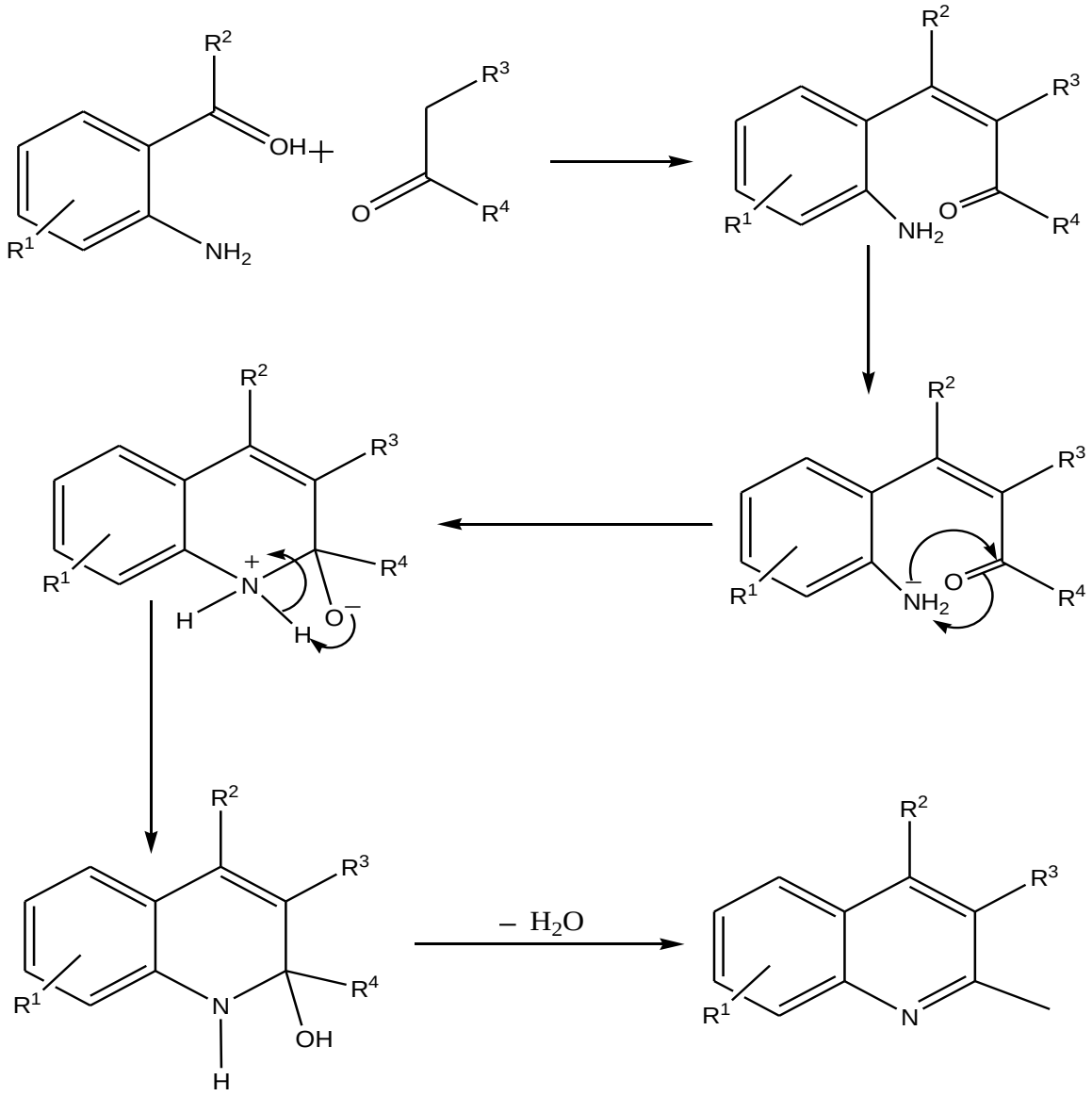

Scheme 1.5: Friedländer reaction mechanism

Most existing methodologies for quinoline synthesis through the Friedländer reaction involve alcohol or basic medium,[34] the presence of Brϕnsted or Lewis acids,[35,36] inorganic salts,[37] ionic liquid catalysts[38]and in some cases under microwavable irradiation.[39]

However, most of the synthetic procedures exhibited significant drawbacks such as harsh reaction conditions, high temperature requirements, low yields, work-up procedure problems, difficulty in handling carbonyl compounds, and the use of costly and non-environmentally friendly catalysts. Recently a number of catalyst-free, efficient and environmentally friendly methods for the synthesis of quinolines from readily available compounds have been developed. According to green chemistry protocols which aim to develop environmentally benign reactions, a number of catalyst-free reactions in aqueous medium have been designed. The latter includes successful Ugi or Passemi aqueous and catalyst-free reactions.[40,41] In the same context a new catalyst-free Friedländer reaction which produces quinolines from readily available α-aminobenzaldehyde and ketones (Scheme **1.6**) in aqueous medium has been developed.[42]

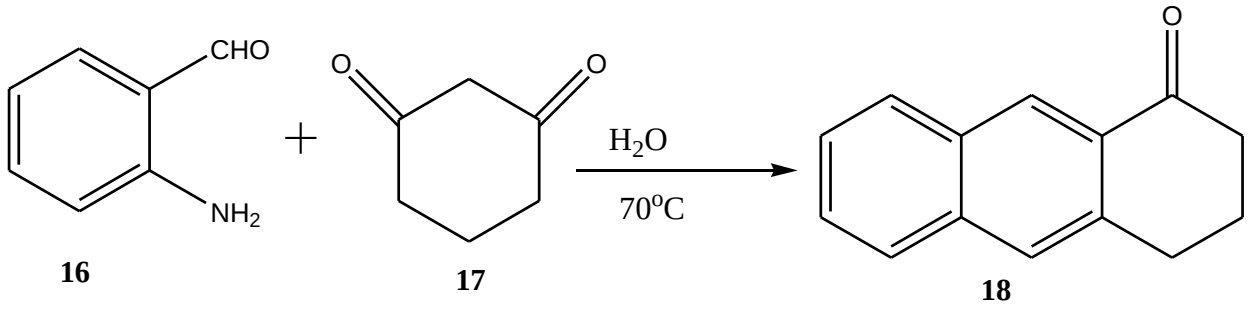

16 **17** **18**

Scheme 1.6: Aqueous medium Friedländer quinoline synthesis reaction from aminobenzaldehyde and ketones

The advantages of this method over the existing ones include highly efficient reactions, waste minimization and the use of an environmental friendly solvent (H_2O).

The development of sonochemistry brought about a new solvent-free reaction for the synthesis of quinoline derivatives. The typical reaction as shown in Scheme **1.7** involves a one-step procedure in which the synthesis of quinoline derivatives is achieved by means of solid-supports such as silica chloride under sonic condition.[43]

This system offers some economic and environmental advantageous over those which take place in solution phase, such as less toxicity, easy preparation and handling, relatively less time-consuming purification and the use of inexpensive catalysts.

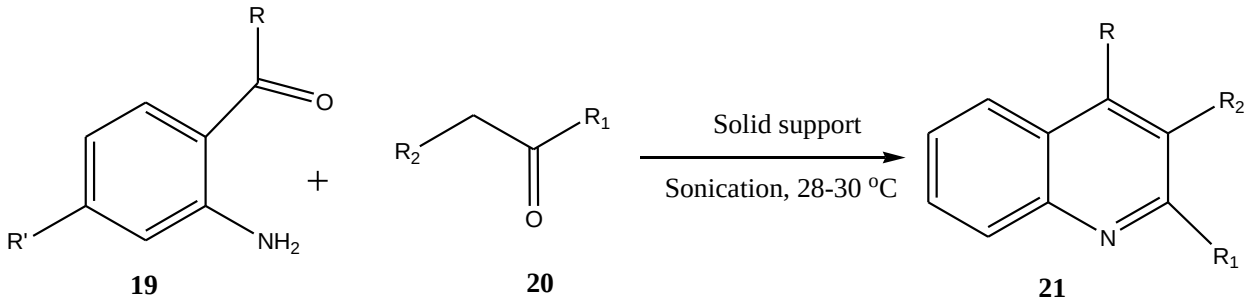

19 **20** **21**

Scheme 1.7: Quinoline synthesis under sonic condition

Due to their abilities to selectively catalyse cleavage of C-C bonds, transition metals have found application in the synthesis of quinolones.[44,45] Recent reports include a regioselective, inexpensive, and efficient $FeCl_3$ promoted tandem reaction to produce 3-arylquinoline from accessible and affordable compounds, aniline and styrene oxide, *via* C-C cleavage and C-H activation as shown in Scheme **1.8**.[46]

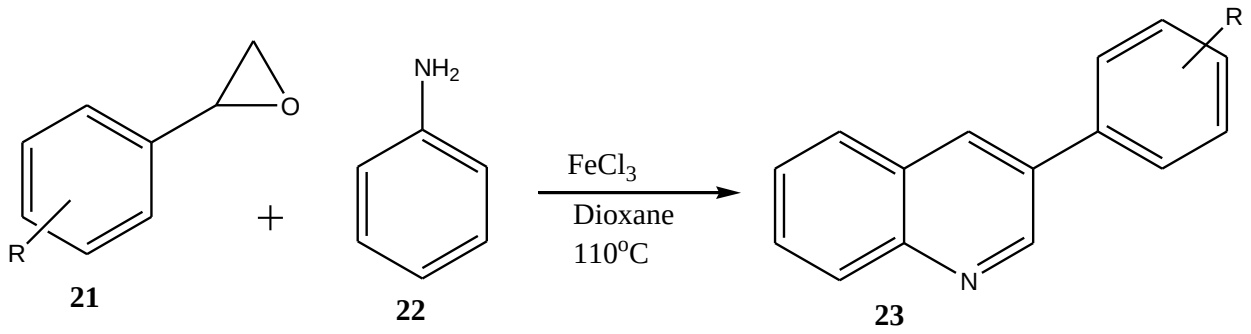

21 **22** **23**

Scheme 1.8: $FeCl_3$ promoted tandem reaction for 3-arylquinoline synthesis

Efforts have been made to optimize the reaction conditions, and some reactions that produce quinolines at room temperature have been reported.

An interesting example is the synthesis of 2-alkylquinoline **27** derivatives from aromatic amines **25** and substituted 3-ethoxycyclobutanone **26** *via* a one-step, regioselective and Lewis acid promoted [3+3] annulation reaction as shown in Scheme **1.9**.[47]

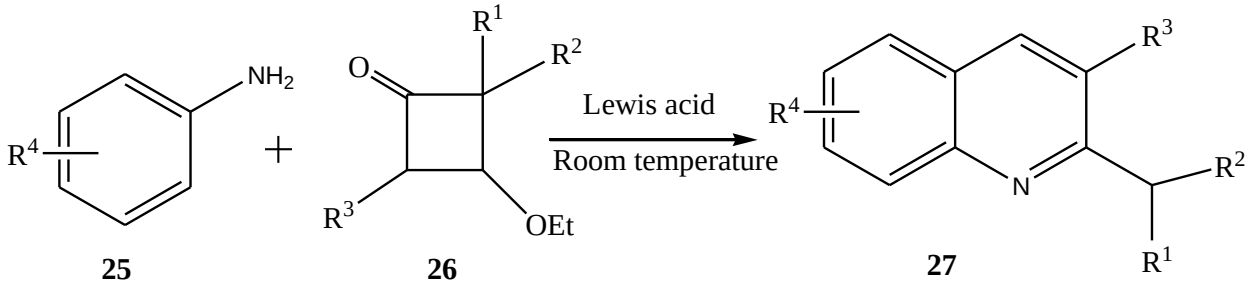

25 **26** **27**

Scheme 1.9: One step 2-alkyl quinoline derivatives synthesis at room temperature

In another case, quinoline derivatives were synthesised using a Lewis acid catalyzed reaction of the glycine derivatives **23** and styrene **24** in the presence of the persistent radical cation salt tris(4-bromophenyl)aminium hexachloroantimonate ($TBPA^{+\cdot}$) as shown in Scheme **1.10.**

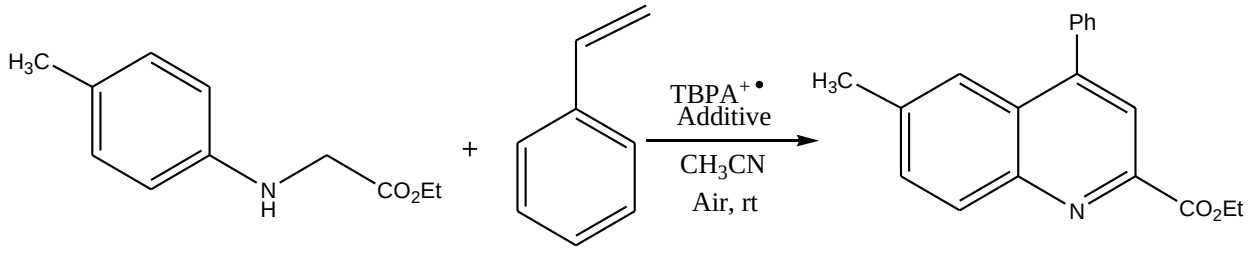

23 **24** **25**

Scheme 1.10: $TBPA^{+\cdot}$-promoted reaction of glycine derivatives and styrene. [48]

Further studies showed that the use of electron-rich styrene can improve the reaction yields together with the use of $InCl_3$ as a Lewis acid.

1. 3. 1,2,3-Triazole formation

Due to the wide range of applications of 1,2,3-triazole in industry as well as the inherent biological activity of this heterocyclic ring system, the synthesis of 1,2,3-triazole containing compounds has become the subject of interest in academia and industry where triazole containing compounds have been investigated as dye stuffs, auxiliaries in fibre finishes, photostabilizers, photographic materials and agrochemicals.[49] Thus several synthetic approaches for their synthesis have been developed. The early approaches included the well-known Huisgen cycloaddition of azides and alkynes (Scheme **11**).[50] The latter has not been given much attention due to the required reaction conditions of elevated temperature, long reaction time and also the lack of regioselectivity when unsymmetrical alkynes without highly electron-withdrawing groups are used.

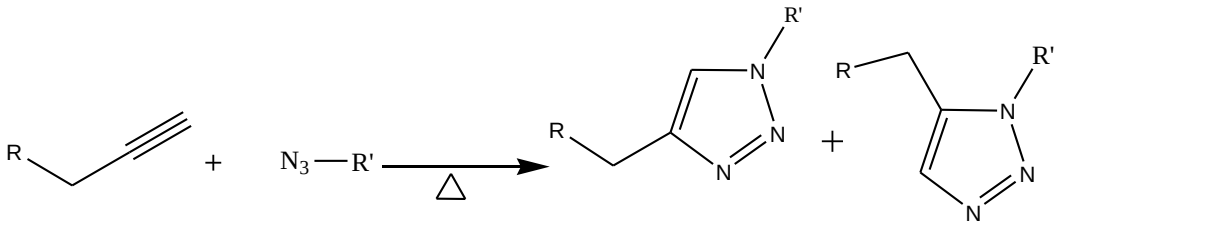

Organic terminal alkyne **Organic azide** **1, 4-disustituted triazole 50%** **1,5-disustituted triazole 50%**

Scheme 1.11: Thermal azide-alkyne Huisgen cycloaddition

Many efforts have made in order to improve the regioselectivity of this reaction. Currently the Cu(I)-catalysed azide-alkyne cycloaddition (CuAAC) (click chemistry) reaction reported by Sharpeless *et al* [51] and Meldal *et al* [52] has proven to be an efficient technique to control regioselectivity in the alkyne-azide cycloaddition reaction. The typical reaction regioselectively yields 1,4-disubstituted 1,2,3-triazoles as shown in Scheme **1.12**.

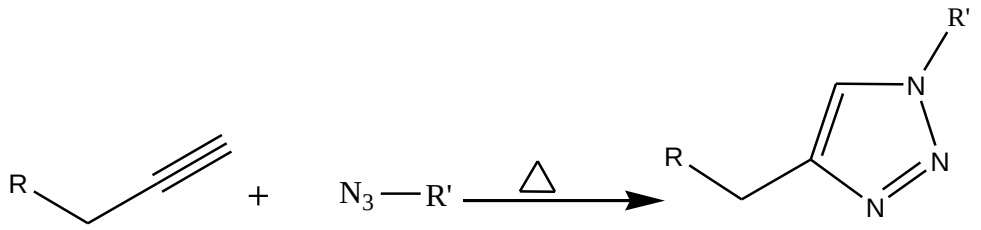

Organic terminal alkyne **Organic azide** **1, 4-disustituted triazole**

Scheme 1.12: Regioselective Cu(I)-catalyzed azide-alkyne cycloaddition (CuAAC)

As examples of click chemistry reactions, the above reactions are characterized by high yields, mild reaction conditions, tolerance of a broad range of functional groups, and regioselectivity. As a hetero-Diel-Alder type reaction the above reaction has proven to be a reliable and powerful tool in heterocyclic organic synthesis,[53] materials science,[54] polymer synthesis [55] and in various biochemical applications such as biomolecular ligation and *in vivo* tagging.[56,57,58]

This versatility originates from the wide variety and accessibility of starting materials as well as insensitivity of both starting materials and the resulting triazole towards side reactions such as oxidation, reduction and hydrolysis.

Cu(I) can be used as a catalyst in aqueous or organic medium. Cu(I)-containing salts such as CuI, CuBr was reported to be excellent source of Cu(I) for the preparation of ligation products, polymeric materials, and in biochemical applications.[59,60,61] In order to increase catalyst solubility in organic solvents as well as its reactivity other Cu(I)-containing salts such as $[Cu(NCMe_3)_4][PF_6]$ and $Cu(OAc)_2$ can be used as Cu(I) source.[62] This type of Cu(I) generation may be performed in the absence of the ligand but the system often requires the use of a nitrogen base such as pyridine, 2,6-lutidine or triethylamine, as well as acetonitrile as co-solvent, to prevent Cu(I) degradation *via* oxidation or disproportionation.

Despite direct generation of Cu(I) from these salts, some drawbacks are associated with this system such as the formation of side-products including bistrazioles, 5-hydroxytriazole and diacetylene. [63]

By using an ultrasound bath, another type of copper catalyst (Cu/C) can be produced from carbon black and $Cu(NO_3)_2.3H_2O$ in water and is activated *via* addition of triethylamine or through microwave heating. This catalyst produces Cu(I) in reaction mixtures and offers advantages over other systems such as easy removal of the catalyst from reaction mixtures, and which can be recovered and reused.[64]

Cu(I) catalyst can also be generated from oxidation of copper metal or from Cu(II) salts *via* reduction or disproportionation of a Cu (II)/Cu^0 couple.[65] This form of Cu(I) generation is widely used in the systems which do not support the use of ascorbic acid and its oxidative products, but its application is limited in some systems such as biological systems.[66]

Based on its easy work-up and the purity of the isolated product, as well as the low price of the catalyst, Cu(II) sulfate pentahydrate ($CuSO_4.5H_2O$) in the presence of a reducing agent such as ascorbate, has often been the preferred source of Cu(I). The presence of a reducing agent prevents the oxidation of the Cu(I) catalyst by oxygen and maintains optimum catalytic conditions for the reaction. Cu(I) generated from the reduction of Cu(II) immediately reacts with alkyne to form an active Cu-acetylide intermediate which interacts with azide to give a copper acetylide azide complex. Subsequent cyclization results in the formation of the triazole ring as shown in the Scheme **1.13**.

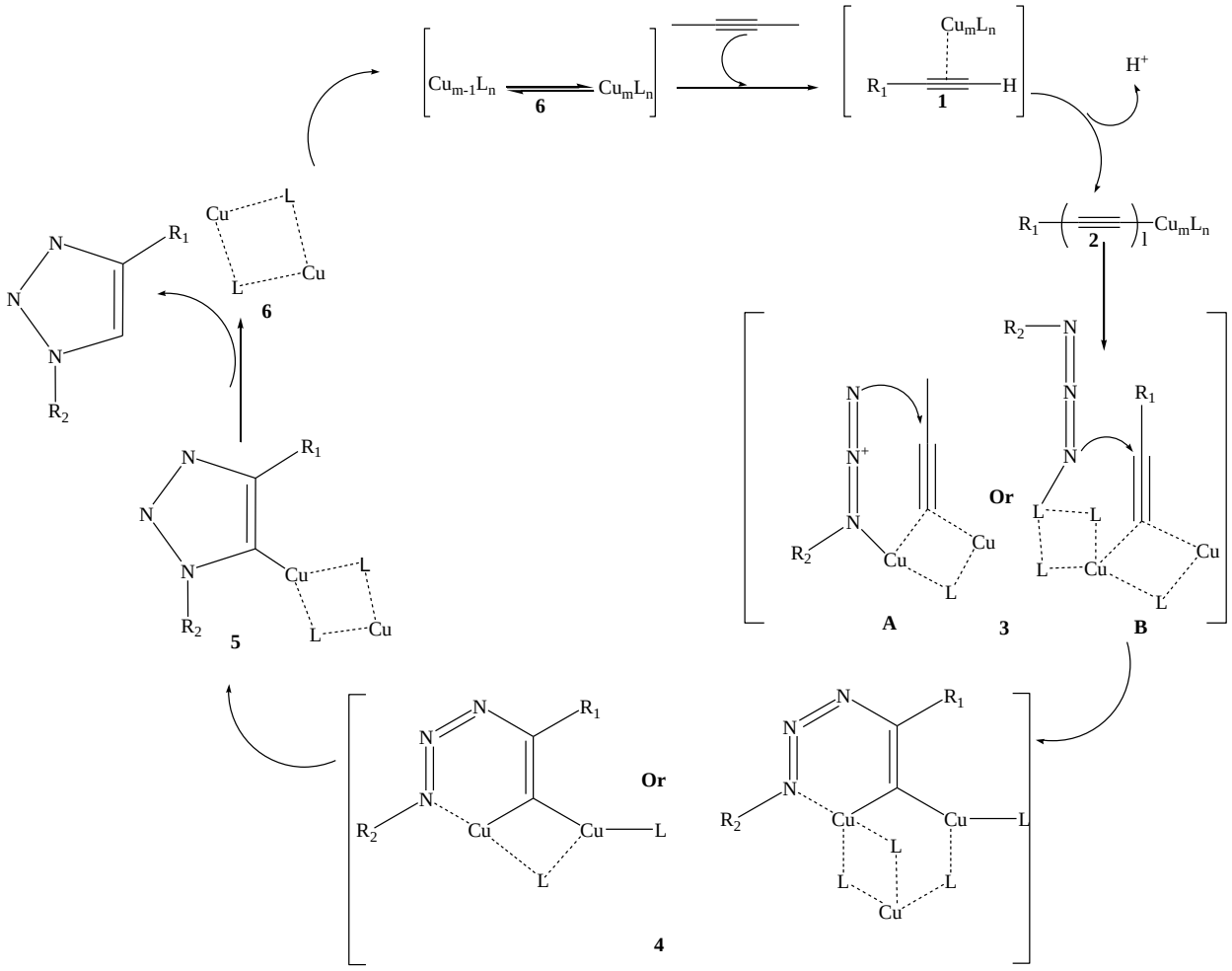

Scheme 1.13: Mechanism of Cu(I) catalysis in the formation of triazoles

Due to the instability associated with Cu(I), the CuAAC reaction may be improved by addition of the ligand which coordinates with the Cu(I) species and reduces possible interactions that may result in Cu(I) destruction and production of side products. The presence of ligand also protects Cu(I) from oxidation by ambient oxygen to Cu(II) which can affect the reaction rate by reducing the concentration of catalytically active complexes. Since the formation of Cu(I) acetylide complex involves deprotonation of the acidic terminal hydrogen of the alkyne, the ligand can also act as a proton acceptor and suppress the use of a base.[67] Nitrogen-containing ligands have proven to be efficient in CuAAC reaction as they form Cu(I) complexes under mild reaction conditions with a range of ligand-dependent structural variations.[68,69] Some ligands that are used in CuAA reactions are shown in Figure **1.4.**

Currently a new approach for click reaction catalysis has been reported. The latter includes a dual click approach “click-click” in which CuAAC has been mediated by two multi-hybridized triazole ligands.[70]

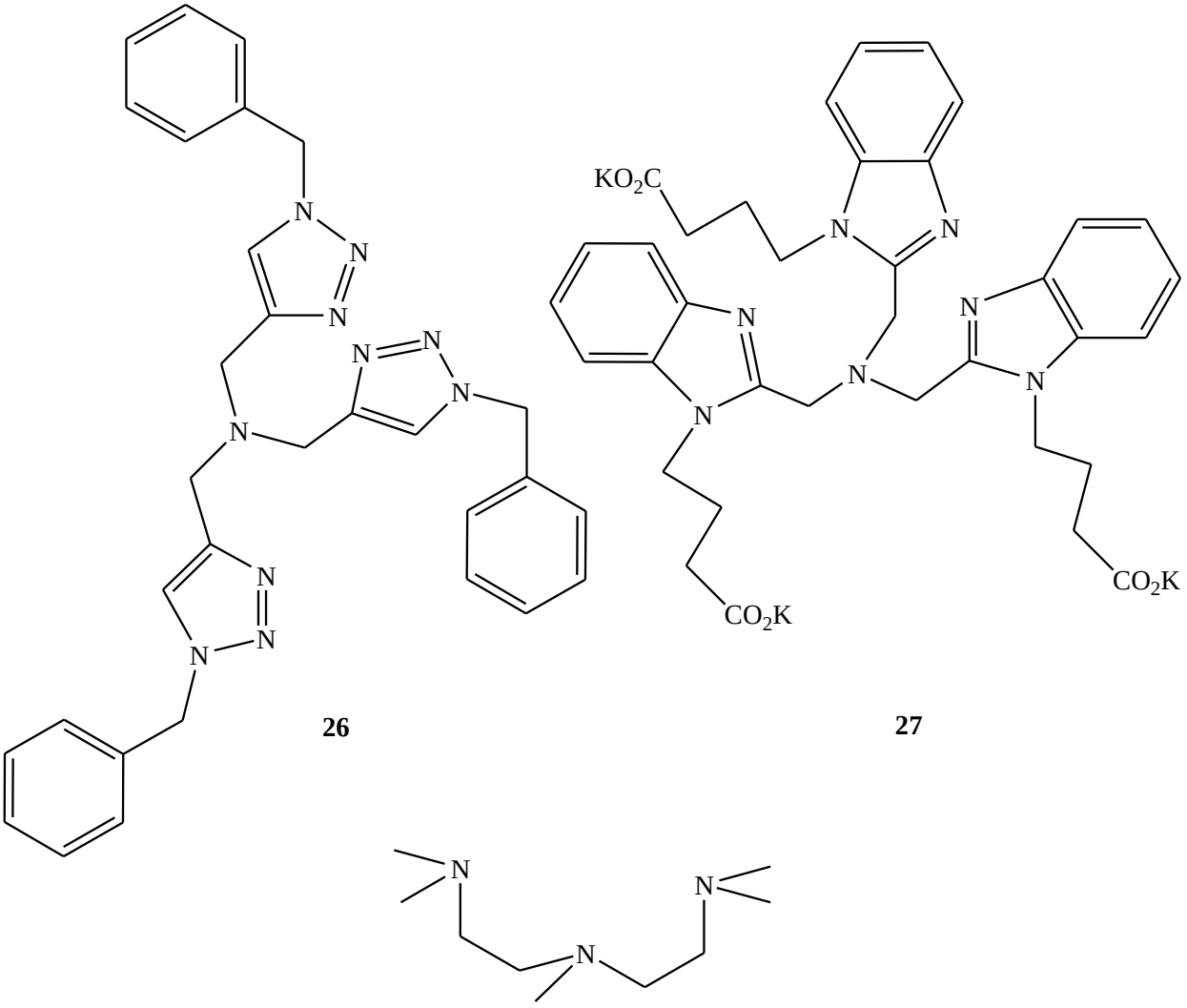

26 **27**

28

Figure 1.4: Examples of the ligand used in CuAAC reaction

Recently a ligated Ag(I) species was developed to promote alkyne-azide cycloaddition. A typical reaction affords exclusively 1,4-substituted triazoles and involves a similar mechanism to the copper catalysed reactions.[71,72]

The CuAAC reaction commonly takes place in either polar aprotic solvents such as THF, DMF, acetonitrile, DMSO or aprotic non-polar solvents such as toluene or in water and water-miscible organic solvent mixtures.[73,74] Based on green chemistry protocols, a few systems that use water as the only solvent have been developed.[75,76,77] The major challenge of these systems is the low solubility associated with organic materials in aqueous medium. The latter has been improved by the use of cyclodextrin-mediated reactions in which water insoluble organic compounds are included in cyclodextrin cavities resulting in enhanced dissolution.[78] In this case the cyclodextrins act as phase transfer catalysts. Recently a CuAAC reaction in water which uses less expensive and widely exploited β-cyclodextrin as the phase transfer catalyst, (Scheme **1.14)** has been reported.[79] The yield was improved up to 99 % through the use of β-cyclodextrin.

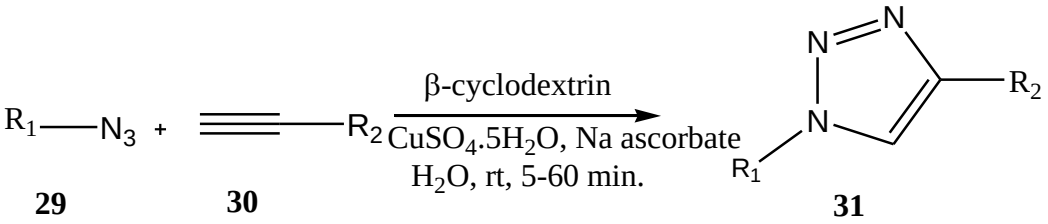

Scheme 1.14: Aqueous CuAAC β-cyclodextrin mediated reaction

1.4. Polymerization processes

Polymer studies should be based on understanding of the procedures or methods from which these compounds are synthesized. As a definition, polymerization is a process in which monomers are joined together *via* a chemical reaction to form linear or three-dimensional networks of polymer chains as shown in Scheme **1.15**.

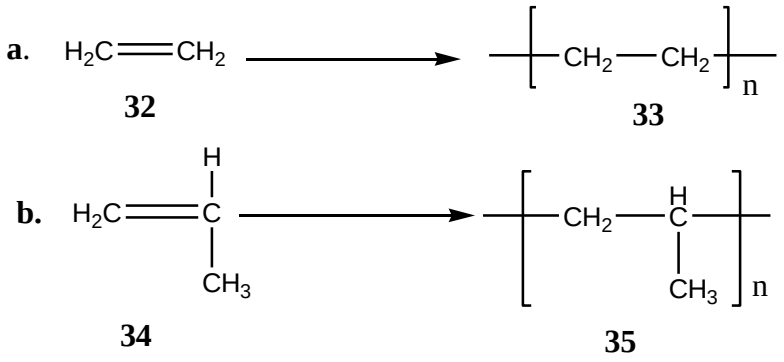

Scheme 1.15: a) Ethylene polymerization b) Propylene polymerization

Due to different functional groups present in the reacting monomers and their inherent steric effects as illustrated by VSEPR theory, polymerization processes can be classified according to various reaction mechanisms. Polymerization processes may be catalytic or non-catalytic. Non-catalytic polymerization includes thermal methods, UV irradiation (photochemical) polymerization, and electrolytic polymerization which takes place at the cathode or anode of an electrolytic cell. Catalytic polymerization includes free radical polymerization in which various radical species may initiate polymerization, ionic polymerization in which either anions or cations are initiators, and highly stereospecific polymerization which uses coordination catalysts. The best known coordination polymerization is Ziegler-Natta polymerization, resulting in highly crystalline polymers.[80] Polymerization reactions can be carried out in solid, liquid or gaseous phases. Depending on the phase and the form of the reaction medium, a polymerization reaction may be classified as homogenous or heterogeneous.

1.4.1. Classification of polymerization reactions

The early studies on polymers and polymerization reactions conducted by Wallace Hume Carothers in 1929 suggested polymerization reactions as condensation and addition processes.[81] Later developments in polymer science introduced another classification of polymerization reactions based on the mechanism and kinetics of the reaction, and classified polymerization into step and chain polymerizations.[82] These two classifications generated confusion, since the terms condensation and step were often used interchangeably as synonym yet were not the same, and the same terminology was applied for addition and chain polymerization. The confusion arises from the fact that not all condensation polymers are generated *via* step polymerization, and also not all addition polymers are generated *via* chain polymerization. Although in the literature the use of condensation and addition terminology to classify polymerization mechanisms continued, the most recent and useful classification has divided polymerization mechanisms into two main classes, step polymerization and chain polymerization.[83]

The main difference between the two types of polymerization mechanisms is the nature of the species that react when polymer molecules are built up. Another difference is that in chain polymerization, monomer molecules are bonded to a growing chain one at a time, while in step polymerization any size species add to one another to form low molecular weight polymer chains which react with one another to form high molecular weight polymer chains.

1.4.2. Chain polymerization

Chain polymerization is a process in which unsaturated monomer molecules bond to each other one at a time in a chain-like way to give linear or 3-D high molecular weight polymers.[84] The typical reaction is characterized by the presence of an active center on the growing polymer chain responsible for its growth. The very first active centers which initiate polymerization are generated from initiator molecules under external factors such as heat or light. Once the active center is formed, monomer molecules add to the active center one by one leaving the active center at the end of the linear growing polymer chain.

The growth of the polymer chain stops either when the active center is destroyed by an appropriate reaction depending on the active center, or when monomer molecules are exhausted leaving the active center at the end of polymer chain. The latter case is observed in living polymerizations.[85]

Since few active centers are present in the reaction mixture and monomers react selectively with the active center at the end of the growing polymer chain one at a time no species of intermediate molecular weight are formed. Depending on the type of reactive species that interacts with monomer, chain polymerization can occur *via* any of the three mechanisms: a free radical mechanism, an ionic mechanism including anionic and cationic, and a coordination catalyst mechanism. All three polymerization mechanisms follow three major steps: initiation, propagation, and termination as shown in Scheme **1.16**.

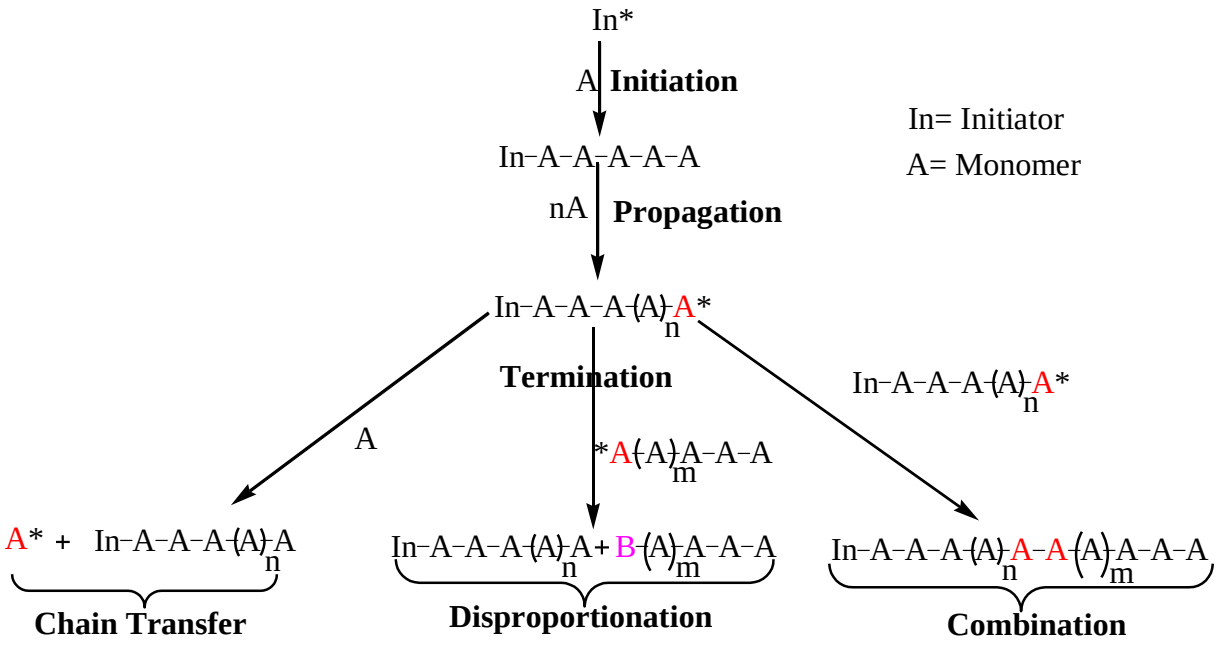

Scheme 1.16: Polymerization steps

1.4.3. Free radical chain polymerization

Free radical polymerization is a chain reaction that uses free radical species to introduce active centers on the growing polymer chain. The driving force for this reaction comes from the fact that a free radical has an unpaired electron and tends to attract an additional electron from an unsaturated monomer. This interaction between free radical species from initiator molecules and unsaturated monomer allows a reactive center which is radical in this case to be transferred to the chain end, followed by successive addition of monomer on the chain. Free radical chain polymerization as a type of chain polymerization occurs *via* three distinct steps; initiation, propagation and termination.

1.4.3.1. Initiation

The initiation step involves the generation of actives species responsible for initiating, the polymerization reaction. This process can be achieved by applying external factors such as heat or light on the monomer-containing medium or by adding initiator species. The initiators commonly used in free radical polymerization are organic compounds containing a bond that can be easily dissociated into free radicals.

The initiation consists of two steps. The first one involves formation of one or two radical species from the initiator molecule, while the second step involves addition of one of these radicals to the monomer molecules. Since the polymerization rate is influenced by the initiator used, the choice of appropriate initiator is a crucial step in free radical polymerization. Thus some features are set for a molecule to function as an initiator. These include commercial availability, thermal stability at room temperature or when refrigerated, and a practical rate of radical generation at a temperature less than 150^{o}C. The methods for free radical generation from appropriate initiators include thermal, photochemical and redox processes.[86]

(a) *Thermal method*

Polymerization initiated by this method is also termed "thermal initiated" or "thermal catalysed polymerization". The process involves homolytic scission of a single bond by heat and is applied for the type of initiators that possess bond dissociation energies in the range of 100-170 KJ mol^{-1}.[83] Compounds with dissociation energies out of the range are excluded, since their dissociation kinetics tend to be too slow or too rapid, which eventually affects polymerization kinetics. Compounds with O-O, S-S, and N-O bonds fall in this range and show potential applications in thermally initiated polymerization.

Due to their availability and relative stability compared to other classes of thermal initiators, organic peroxides has been extensively applied as thermal initiators.[87] Thus various categories of peroxides are widely used as initiator. They include acyl peroxides such as acetyl and benzoyl peroxide, alkyl peroxides such as t-butyl peroxide, hydroxyperoxides such as t-butyl hydroxyperoxide, and perester peroxides such as t-butyl perbenzoate as shown in Scheme **1.17**.

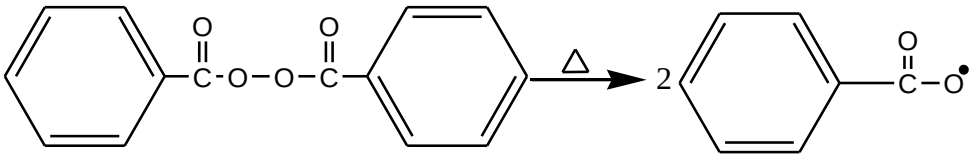

Benzoyl peroxide

36

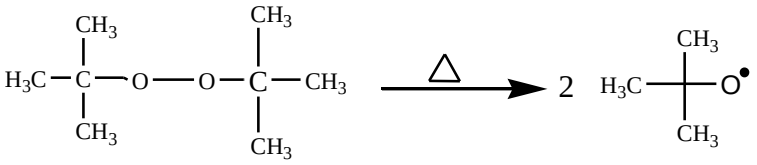

t-butyl peroxide

37

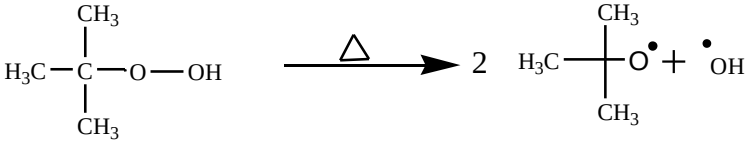

t-butyl hydroperoxide

38

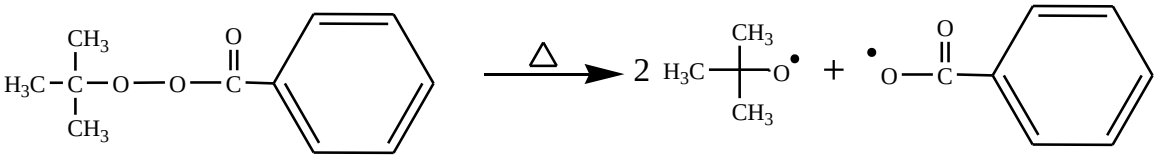

t-butylperbenzoate

39

Scheme 1.17: Thermal free radical generation from peroxide compounds

The azo compounds such as 2,2'-azobisisobutyronitrile (AIBN) also act as good initiators in thermally initiated polymerization. Though the C-N bond dissociation energy is out of the range (~290 KJ mol^{-1}), homolysis is facilitated by the formation of the highly stable nitrogen molecule as shown in Scheme **1.18**.

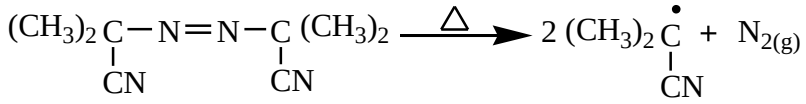

40

Scheme 1.18: 2,2'-azobisisobutyronitrile decomposition

Depending on the initiator's structure and the radical produced in the reaction mixture, different decomposition rate constants (K_d) are observed within a range of 10^{-4}-10^{-9} s^{-1}.[88] The latter is governed by temperature and initiator type, and therefore a specific range of temperature is required to decompose a given initiator.

The examples include azobisisobutyronitrile (AIBN) which is generally used in the range between 50-70 ^{o}C, benzoyl peroxide 80-95 ^{o}C, and di-t-butyl peroxide 120-140 ^{o}C.

(b) *Photoinitiation*

This mode consists of generation of free radicals by exposing a reaction mixture containing an initiator to ultraviolet or visible light. The typical process generally applies light which electronically excites the initiator, with subsequent radical production. This method usually involves metal iodides, metal alkyls and azo-compounds as initiators (Scheme **1.19**).[87] The main advantage of this method is the formation of radicals when the reaction medium is irradiated and which stops as soon as the light source is turned off. Photoinitiation steps may be rapid and controlled. This control can be achieved by combining various factors such as the source of radicals, light intensity and temperature. The major drawback of this mode of initiation is low penetration ability of the light across the wall of reactor.

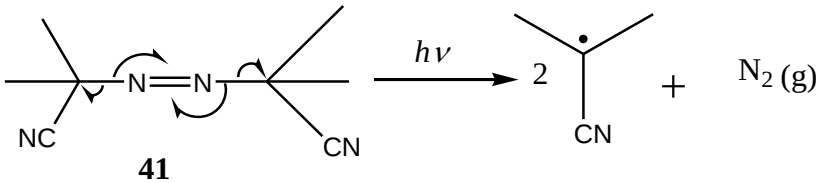

41

Scheme 1.19: Photoinitiation of azoisobutylnitrile

(c) *Redox initiation*

Redox polymerization generally occurs at ambient temperatures and involves generation of radicals *via* transfer of an electron. The process uses redox reactions to initiate polymerization and both organic and inorganic redox reactions are used.[89]

The process may occur *via* two mechanisms, either an electron can be transferred directly from reductant to oxidant or the formation of intermediate reductant-oxidant complex may be involved. In Scheme **1.20** there are the examples for the reduction of hydrogen peroxide, a perester, and alkyl hydroperoxide by Fe(II), resulting in radical production.

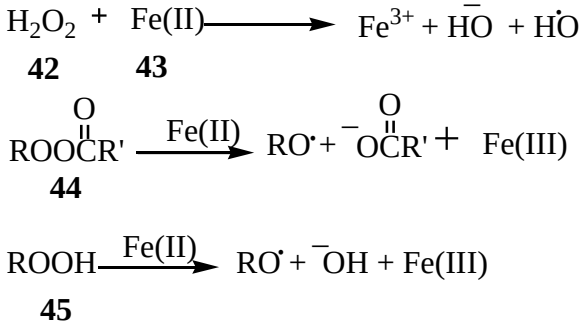

Scheme 1.20: Reduction of hydrogen peroxide and alkyl hydroperoxide by Fe^{2+}

The advantage of this method is that the radicals can be generated over a wide range of temperatures, facilitating the choice of temperature at which thermally initiated redox polymerization occurs best.

d) *Initiation by ionizing radiation*

In this method radicals are produced from the interaction of electromagnetic radiation or accelerated particles with the initiating species.[90] Electromagnetic radiation that is used in this process includes gamma and X-rays, while accelerated particles such as electrons, neutron, and α-particles are also used.

This mechanism involves ejection of an electron by ionizing radiation, followed by dissociation and capture of an electron.[87] Scheme **1.21** illustrates the generation of radicals from a compound by ionizing radiation.

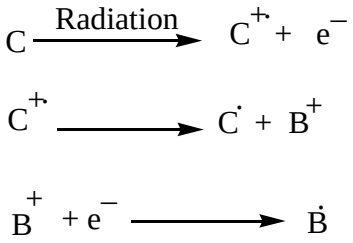

Scheme 1.21: Generation of radicals from a compound (C) by ionizing radiation

(e) *Electrochemical method*

This method has been introduced due to its contribution in initiating polymerization.[91] It involves a reaction mixture containing an electrolyte and monomer compound. When electricity is switched on, the monomer is reduced forming a radical anion at the cathode after gaining an electron, while at the anode the monomer is oxidized to give a radical cation. The produced radical ions may be used to initiate either ionic or free radical polymerization. An interesting example in Scheme **1.22** shows radical ion generation in acetonitrile solution of acrylamide monomer in the presence of tetrabutylammonium perchlorate as an electrolyte.[92]

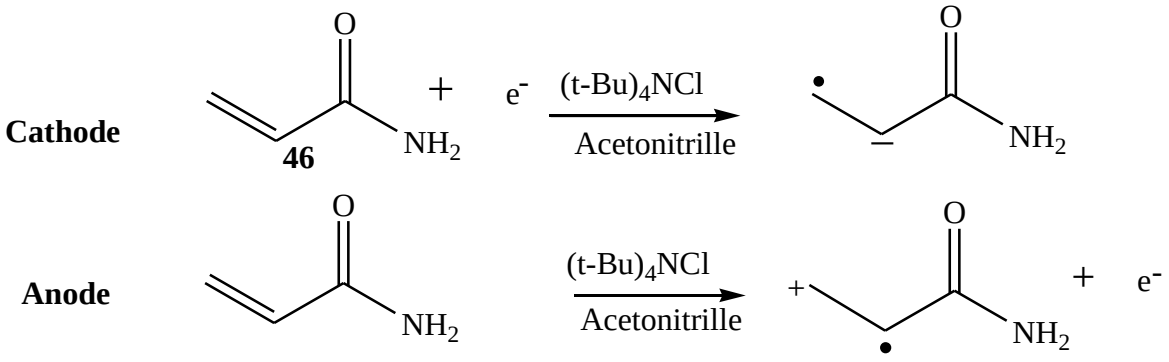

Scheme 1.22: Initiation of acrylamide monomer by electrochemical method

(f) *Plasma method*

This method is very useful in polymerization processes involving different types of organic monomers such as alkenes, alkynes, and alkanes in their gaseous state. A typical process involves placing the gaseous monomer in an electric discharge at low pressure under conditions where ionized gaseous monomer (plasma) can be created.[83] This can be achieved when the system is heated and/or placed in a radiofrequency field.

g) Sonication

In this method the bond breakage leading to the formation of radicals is achieved due to the formation of excited vibrational states from the action of high temperature and pressure. The required conditions are generated *via* a cavitation effect (the formation and collapse of cavities in the liquid) observed when high intensity ultrasound of frequency beyond the range of human hearing is applied to the monomer. The limitation of this method is viscosity effects which can be significant even at low conversion. This limits the cavitation effect and hence radical formation.[93]

h) Ternary initiator

In this method a polymerization reaction is initiated by more than one initiator. An interesting example is the synthesis of poly(methyl methacrylate) using benzoyl peroxide, 3,6-bis(*O*-carboxybenzoyl)-N-isopropylcarbazole, and d-η^5-indenylzirconium dichloride as ternary initiator as shown in Scheme **1.23**.

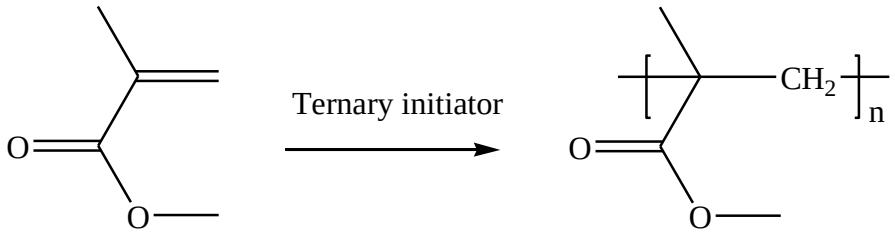

47

Scheme 1.23: Poly(methyl methacrylate) synthesis using a ternary initiator

The three components of a ternary initiator act interdependently to accelerate the polymerization process and result in polymeric material with excellent thermal resistance properties as well as regular microstructure.[94,95]

1.4.3.2. Initiator efficient

Investigations conducted on the initiation step by comparing the amount of initiator that participates in the primary step of initiator decomposition and the amount which initiates polymerization showed that chain initiation efficiency is not 100%. In this case the fraction of radicals produced in the primary step of initiator decomposition and the amount of radicals that are successfully involved in initiating polymerization is used to describe the effective radical concentration. This fraction is termed the initiator efficiency (f) and its highest possible value is 1. However this value is never achieved due to various effects such as side reactions or inefficient generation of the radical species.

1.4.3.3. Propagation

This step is very rapid and even explosive in some case. It encompasses the elongation stage of polymer chains by successive addition of monomer units (M) to the active site located at the end of growing chain. At each monomer addition, the active site is transferred at one chain end as shown below.

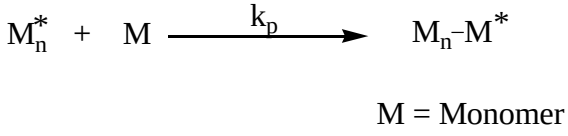

Scheme 1.24: Propagation reaction

In order to increase the probability of an active center reacting with the monomer molecule rather than any other radical species *via* combination or disproportionation, its concentration is lowered to a level where bimolecular radical reactions become negligibly slow. Less than 0.1 wt % monomer is practically acceptable.

Monomer addition to the active site may occur *via* any of the three possible configurations: head-to-tail, tail-to-tail, or head-to-head,[96] as shown below.

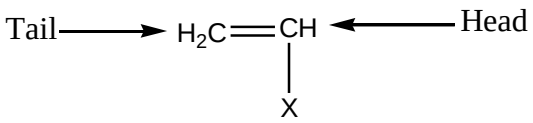

Scheme 1.25: Reactive end of vinyl monomers

1.4.3.4. Termination

This is the last step of chain polymerization. It involves deactivation of the active site at the end of the growing chain which results in a neutral macromolecule. In some cases the ability of the growing polymer chain to be terminated is suppressed and the process is referred to as ‘‘living polymerization’’.[85] The efficiency of the termination step is a function of the monomer, solvent, temperature and viscosity of the medium and may occur *via* various mechanisms.

(a) *Combination*

Combination occurs when two chain ends come into proximity with subsequent coupling of radicals at the end of the chains to form an inert final polymer (Scheme **1.26**). Since this mode of termination results in double the molecular mass of the propagating radical species, its occurrence can be predicted by monitoring the molecular weight of the propagating species.

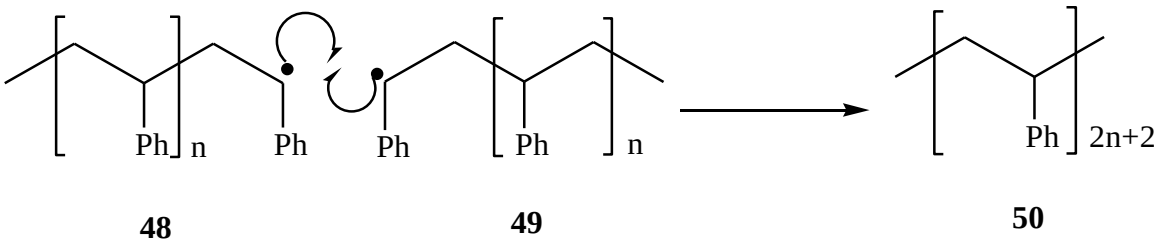

48 **49** **50**

Scheme 1.26: Combination of polystyrene radicals

(b) *Disproportionation*

The mechanism involves hydrogen abstraction from the carbon atom at the β-position to the active center by an activated chain end.[97] This results in two inert polymers in which one exhibits a saturated end while other exhibits an unsaturated end as shown in Scheme **1.27**.

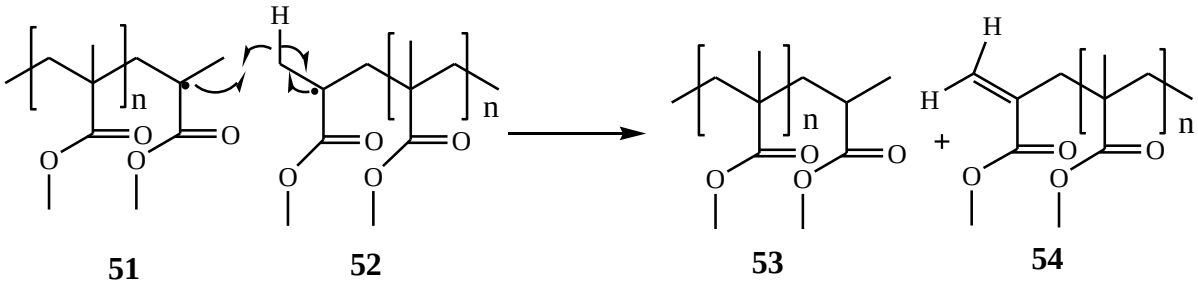

51 **52** **53** **54**

Scheme 1.27: Disproportionation of poly(methyl methacrylate) radical species

(c) *Interaction with impurities or inhibitors*

This results from a reaction between propagating species and a molecule other than the monomer, leading to a less active chain end. An interesting example is styrene polymerization inhibition, which involves the reaction of a growing chain polymer with atmospheric oxygen as shown in Scheme **1.28**. This reaction results in less active peroxides or hydroxyperoxides which terminate the polymerization.

This effect can also cause chain transfer which results in the formation of short polymer chains.[98] Thus many free radical polymerization reactions are carried out in an oxygen-free environment.

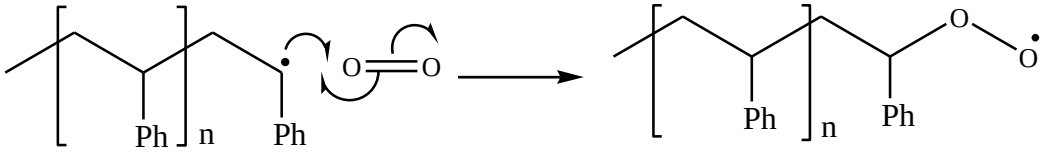

55 **56**

Scheme 1.28: Inhibition of styrene polymerization

(d) Chain transfer

This mechanism involves abstraction of hydrogen as in the case of disproportionation. The difference is that the active center is not destroyed but transferred to other molecules in the medium such as monomer, solvent molecules, an initiator, or another polymer chain.[87]

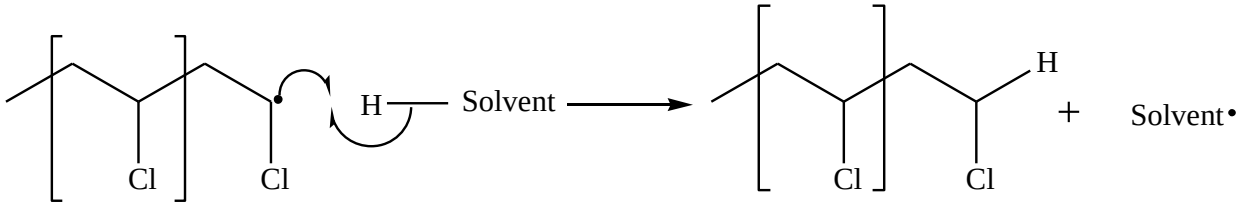

57 **58**

Scheme 1.29: Chain transfer from polyvinyl chloride to solvent

Since one chain is terminated while other is initiated, no net change in radical concentration is observed. In many cases the newly formed radicals are weakly activated to carry on the propagation process. Though chain transfer incorporates side chains in polymer molecules, it is intentionally used to limit the molecular weight of the polymer molecule.

1.5. Controlled ‘‘living’’ free radical polymerization

For many years it was a challenge to synthesize a polymer with well-defined architectural and structural parameters by conventional free radical polymerization. Since the latter involves an initiation step which is a continuous process, and due to the inherent reactivity of free radicals which can facilitate radical couplings or side reactions, molecular weight control *via* this type of polymerization method became a big challenge. This was solved by the development of a new technique referred as Controlled/‘’Living’’ radical polymerization (CRP) based on either reversible deactivation of polymer radical chains, or a degenerative transfer mechanism.

The pioneer of the living polymerization process was Michael Szwarc who in 1956 discovered an ionic living polymerization *via* establishment of a dynamic equilibrium between active and dormant species.[99]

His work offered a considerable contribution in polymer synthesis since well-defined polymers with desired size, topology, composition and functionality were able to be synthesized. The main limitation of his polymerization system arises from the incompatibility between the active sites and certain function groups, which complicate polymerization of various functionalized vinyl monomers. Another limitation resides in reaction handling since the reaction medium requires severe reaction conditions such as chemically ultrapure reagents, and stringent removal of air and humidity.

For many years after its discovery, ionic living polymerization was the only effective method for polymer molecular weight control. This was until the development of CRP by Ostu *et al.* in 1980 from his work which involved initiator-transfer-agent-terminators or iniferters.[100,101] This technique makes use of conventional radical polymerization with reversible termination of the propagating radical in order to control the molecular masses and molecular weight distribution of polymers.

Since controlled/living free radical polymerization relies on the exchange between active species and dormant end-capped chain as shown below, if the life-time of the growing chain propagation is extended to more than hour, it leads to the formation of polymers of different chain topologies.

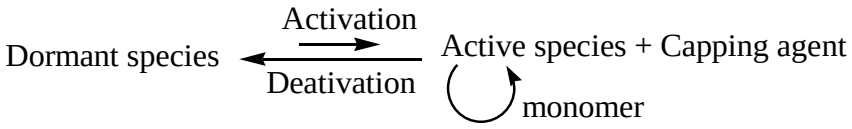

Scheme 1.30: Controlled / living free radical polymerization mechanism

The main advantage of this polymerization process is that it offers efficient control of molecular weight as well as its distribution. In practice this is difficult to achieve so pseudo-living free radical polymerization is often performed where partial control of molecular weight and disperity is observed.

The most popular and successful techniques for controlled/free radical living polymerization include nitroxide mediated polymerization (NMP),[102] atomic transfer radical polymerization (ATRP),[103] and reversible addition-fragmentation chain transfer polymerization (RAFT).[104,105]

1.5.1. Nitroxide Mediated Polymerization (NMP)

In nitroxide mediated polymerization, the living nature of the reaction is based on the persistence radical effect (PRE) [106] as well as an equilibrium established between the growing radical species and nitroxide radicals (Scheme **1.31**), referred to as activation-deactivation ($k = k_d/k_c$).

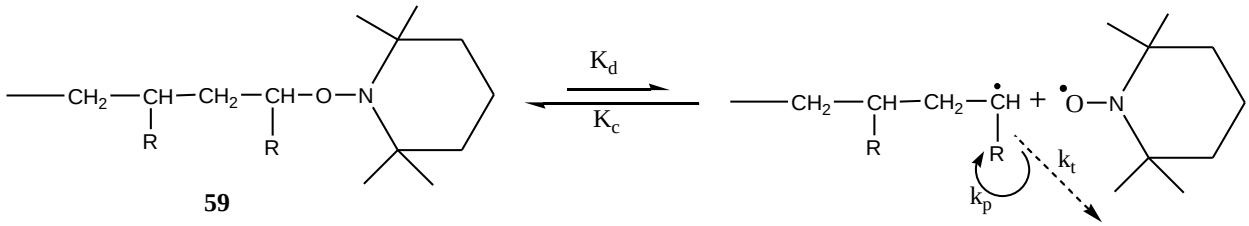

Scheme 1.31: Dynamic equilibrium between growing radical species and nitroxide radical

This occurs in the absence of other reactions, resulting in initiating polymerization *via* reversible capping and de-capping of the growing radical chain by nitroxide radicals acting as the controlling agent. Indeed, the predominant nitroxide radicals bind and unbind to the propagating radical and prevent irreversible coupling of active chains by shifting the equilibrium to the dormant alkoxyamine species.

The latter undergoes homolytic cleavage upon temperature increase to give back the propagating radical and nitroxide. This equilibrium results in a significant reduction of the propagating radical concentration as well as the rate of the polymerization. Consequently polymer chain growth occurs in living fashion and polymers with narrow molecular weight distributions are obtained.

The success of the living nature of Nitroxide Mediated Polymerization is based on the identity of mediated radical ($R^{\cdot}$) which can be generated *via* either a bicomponent pathway or unimolecular pathway.

The bicomponent pathway was the first pathway to initiate nitroxide mediated polymerization after its introduction by Solomon *et al*. in 1986.[107] It involves a conventional thermal initiator such as 2,2'-azobisisobutylnitrile (AIBN) or benzoyl peroxide in the presence of mediating stable free nitroxide such as 2,2,6,6-tetramethylpiperidinyl-1-oxy (TEMPO).

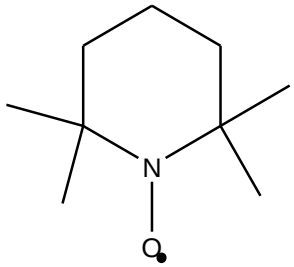

60

Figure 1.5: (2,2,6,6-tetramethylpiperidin-1-yl)oxyl (TEMPO)

The kinetics of this polymerization system depends on the amount of nitroxide present in excess after initiation.[108] The increased amount of free nitroxide causes the equilibrium between propagating radical species and nitroxide radical to shift towards the dormant species and the polymerization rate is then reduced. For this reason fine-tuning of the $[\text{nitroxide}]_0/[\text{initiator}]_0$ ratio is necessary. Recent work has showed that depending on the desired molecular weight, the polymerization rate can be increased by fine optimization of this ratio.[109]

The first limitation of this system is the complication in determining the efficiencies of the initiating radicals generated from the thermal initiator due to effects such as cage effect.[110]

The nature of the initiating groups can also be limiting since most primary radicals react further *via* fragmentation or rearrangement.[111] This leads to poorly reproducible polymerization kinetics and to ill-defined polymer end groups.

Optimum control in nitroxide-mediated polymerization systems was achieved using the unimolecular initiator system introduced by Rizardo[112] in 1986 and Hawker[113] in 1994. This system involves a single compound which decomposes upon heating into a nitroxide radical and an initiating radical in 1:1 ratio as shown in Scheme **1.32**.

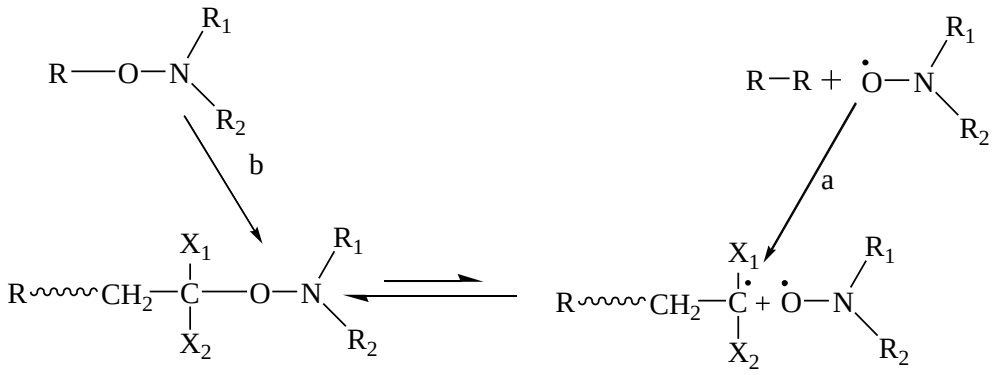

Scheme 1.32: Activation-deactivation equilibrium in Nitroxide-Mediated Polymerization **a**)Bicomponent initiating system **b**) Unimolecular initiating system

1.5.2. Reversible Addition-Fragmentation chain Transfer polymerization (RAFT)

RAFT polymerization technology was first developed at the CSIRO in Australia in 1998.[114] It involves conventional free radical polymerization techniques mediated by a chain transfer agent (CTA) commonly known as a RAFT agent (Scheme **1.33**) to produce polymers with predetermined molecular weights and complex architectures.[115]

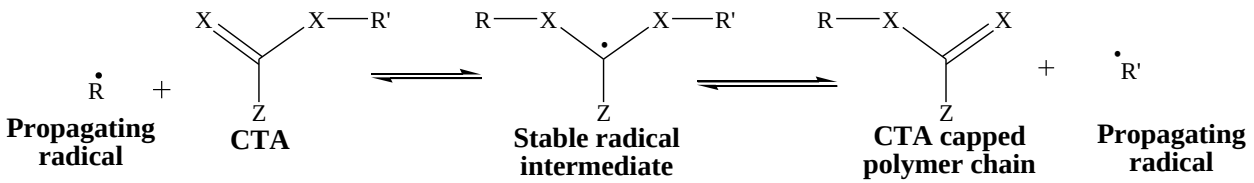

Scheme 1.33: General reaction of reversible addition-fragmentation chain transfer polymerization

The compounds commonly used as RAFT agents in this polymerization technique include thiocarbonylthio compounds such as dithioesters, dithiocarbamates, trithiocarbamates and xanthates.[116]

The living nature of RAFT polymerization is demonstrated by its ability to produce the polymers with narrow molecular weight distribution, its linear molecular weight profile, molecular weight forecast from the ratio of the monomers used up to the transfer agent, and its ability to produce high molecular weight polymers when monomer molecules are added. The molecular weight can be pre-determined using the formula below.

$$\text{Expected molar mass} = ([M]_0/[T]_0)\ C\ M$$

Where $\mathbf{[M]_0}$ and $\mathbf{[T]_0}$ are the initial concentrations of monomer and transfer agent, respectively, **C** is the fractional conversion, and **M** is the molecular weight of the monomer.

Due to its ability to tolerate functionality in the transfer agent as well as in the initiator, and its compatibility with a very wide range of monomers including functional group bearing monomers, RAFT polymerization has proved to be an efficient technique over other living/controlled free radical polymerizations. These properties allow one-step synthesis of polymers containing various functionalities such as styrene, acrylates, methacrylate, and their derivatives without any requirement of protecting and deprotecting processes. RAFT polymerization requires the same conditions as conventional free radical polymerization, except the use of CTA and consequently can be performed in various media including aqueous solutions,[117] organic solutions, emulsions, suspensions, and ionic liquids.[118]

The critical step in RAFT polymerization leading to its success is the selection of reaction medium and the suitable CTA for a particular monomer. The latter has a great impact on polymer length, chemical composition, rate of the reaction, and the number of the side reactions that may occur.[119]

Generally a typical CTA (Figure **1.6)** should have a thiocarbonylthio group (S=C–S) with a substituent R which is released as a free radical, and Z acting as an activator or deactivator of the C=S group reactivity.

Since the reactivity and solubility of CTA is governed by the R and Z groups, several types have been synthesized and grouped according to their effectiveness in mediating different vinyl monomer polymerizations.[120,121]

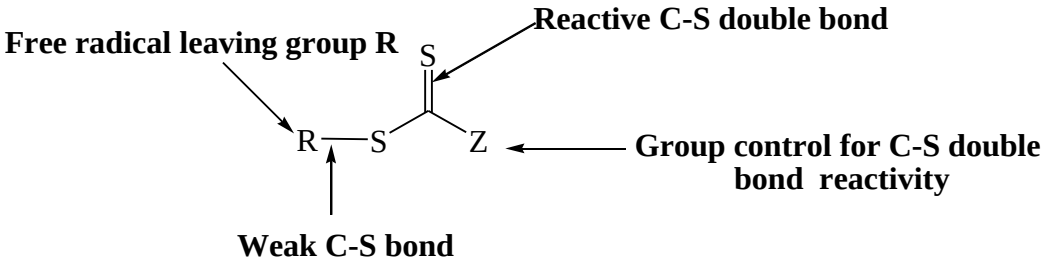

Figure 1.6: General structure of CTA.

The kinetics of the RAFT system differs from those observed in ATRP and NMP processes. It involves a multiple step process encompassing the elementary steps of conventional free radical polymerization such initiation, propagation as well as termination and degenerative chain reactions, resulting in the establishment of two equilibria.

Initially the mechanism begins with a conventional initiation step in which the initiator molecule undergoes homolytic bond cleavage, usually under heating or radiation (γ or UV),[122,123] to generate active free radicals for initiation purpose (Scheme **1.21**). The latter reacts with monomer molecules with transfer of the active centre at the end of the chain to form the propagating radical chain (**$P_m^{\cdot}$**).

The active end on the propagating radical chain attacks reactive C=S bonds of CTA (**1**) to yield stable carbon-centred intermediate radicals (**2**); this step is referred to as pre-equilibrium. The resulting radical species may undergo two different reversible β-cleavage reactions leading either to the original propagating radical chain $\mathbf{P_m^{\cdot}}$ or to the formation of a dithioester capped polymer chain (**3**) and a new radical ($R^{\cdot}$) which can reinitiate polymerization. For a polymerization to be successful the dithioester capped polymer chain which is considered as dormant must exhibit the same general structure and functionality as the original CTA.

When the entire initiator is consumed and all the leaving groups (R) are released as free radicals to initiate new chains, a rapid equilibrium known as the main equilibrium between propagating radical chains and dormant species is established. The latter keeps most chains in a dithioester end-capped state. At this point the living nature of the reaction is achieved as all chain growths occur at the same rate and termination reactions are minimized.

When polymerization is completed the chains in their capped state can re-initiate and more complex molecules are formed.

Though RAFT polymerization exhibits complex mechanisms the molecular weight of the synthesized polymer can be easily estimated by multiplying the ratio of the monomer consumed to the concentration of CTA used, by the molecular weight of the monomer.

Initiation

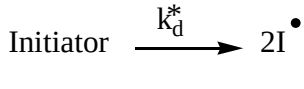

Preequilibrium involving the initial RAFT agent

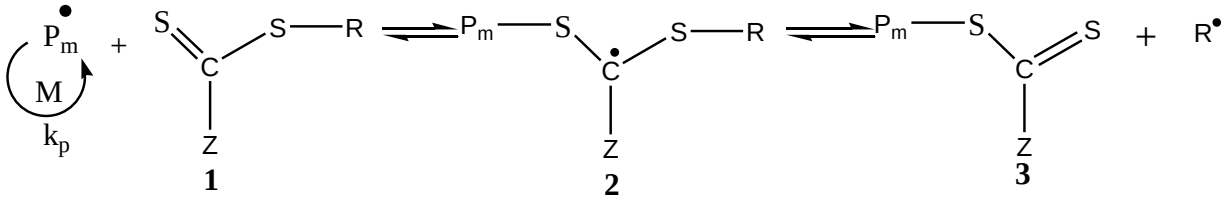

Reinitiation

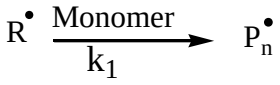

Addition-fragmentation equilibrium

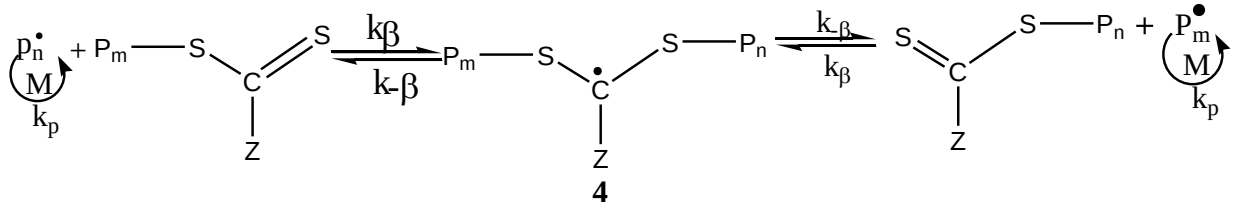

Termination

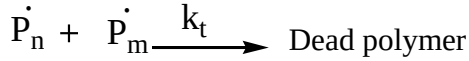

Scheme 1.34: RAFT polymerization mechanism reported by Rizzardo *et al*. [124]

1.5.3. Atom Transfer Radical Polymerization (ATRP)

Atom transfer radical polymerization is one of the most known techniques of controlled radical polymerization which has been applied mainly to the synthesis of polymers with precisely controlled functionalities, topologies, and compositions.[125] Based on its promising characteristics such as simple experimental set-up, tolerance of various functional groups, and use of commercially available catalysts and initiators, a wide range of vinyl monomers have been polymerized *via* ATRP and various functionalities have been introduced into polymer structures.

It was simultaneously discovered by Sawamoto *et al*. [126] and Matyjaszewski *et al*. in 1995,[127] based on the catalytic system used for atomic transfer radical addition reactions (ATRA). Sawamoto reported on ruthenium-mediated polymerization while Matyjaszewski reported on a well-known copper-catalysed version of ATRP.

The key reaction linked to this discovery is the Kharasch addition reaction **(**Scheme **1.35)** which involves carbon-carbon bond formation between a halogenated alkane and alkenes, resulting in 1:1 addition product of alkyl halide and alkene.[128]

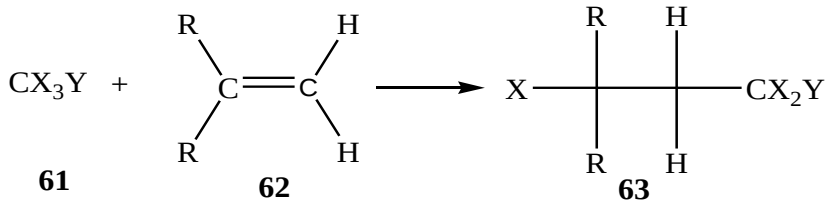

Scheme 1.35: Kharasch reaction

This addition reaction can be photochemically or catalytically initiated. The latter is the basis of the ATRA reaction, in which transition metal complexes are used to activate organic radicals *via* atom transfer from organic halide to the metal complex, followed by a rapid deactivation due to the reverse transfer of an atom from the metal complex to organic halide.[129]

In ATRP the alkyl radical (R$^{\bullet}$) generated from the alkyl halide reacts with the unsaturated species (monomer) and results in a reactive and stable propagating radical chain as shown in Scheme **1.36**.

The control in this type of polymerization is obtained from establishment of a dynamic equilibrium due to rapid reaction between the growing radical intermediates and the metal complex in its higher oxidation state (deactivator). This results in a predominantly halide-capped dormant chain and metal complex in its reduced state (activator), ready to reinitiate a new process.

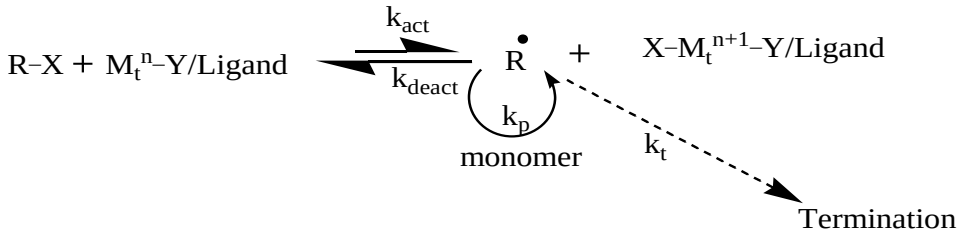

Scheme 1.36: General mechanism of ATRP reported by Matyjaszewski et al.[130]

In general, the active radicals form with a rate constant k_{act}, propagate with rate constant $k_{p,}$ and terminate with a rate constant k_t. As the reaction proceeds k_t is minimized and living growth of the chain is achieved. This is due to increased chain length, viscosity, and persistent radical effect which cause the equilibrium to shift towards the halide-capped dormant polymer chain ($k_{act} << k_{deact}$).[131]

Various transition metals including iron, copper, cobalt, ruthenium and nickel have been used in ATPR along with different nitrogen and phosphine complexing ligands.[132] The ligands act as solubilizing agents for metal ions and also adjust the redox potential around the metal centre which eventually affects both reactivity and the equilibrium dynamics of atom transfer processes. Among those transition metals which are used as salts of halides, copper is widely used in ATPR polymerization processes due to its low cost and versatility.

The kinetic of ATRP can be greatly affected by various factors including temperature,[133] pressure,[134] the nature of the initiator (alkyl halide) and the catalyst.[135] The average molecular weight (M_n) of polymers produced *via* ATRP is proportional to the molecular weight of the monomer (M_w), initial concentration ratio of the monomer ($[M]_0$) to the initiator $[RX]_0$ as well as the monomer conversion as shown below.

$$M_n = ([M]_0/[RX]_0) \times \text{Conversion} \times M_w$$

1.6. Quinoline complexes

Many living organisms directly depend on various metal ions which are involved in a number of physiological mechanisms taking place in their systems. Example include Fe(II) which is involved in oxygen transportation and Zn(II) ion which is involved in various cellular processes such as gene expression and signal transduction.[136] Beside the physiological activities, metal ions may be involved in several chemical processes where they can act as catalysts. However, some metal ions are environmental pollutants and their effects in the human body may be observed even at low concentrations. Examples includes mercury which affects kidneys,[137] and Cd^{2+} which results in tissue destruction. For these reasons monitoring and quantitative determination of these ions are necessary.

Initially, detection of these ions was carried out *via* classical techniques including titration and electrochemical methods. But the latter are limited in many cases, including *in vivo* detection of metal ions. This limitation was overcome by the development of chemosensors which interact with metal ions and result in significant changes in their photophysical properties.

Due to their preferred features such as simplicity, high sensitivity and real time *in situ* imaging, fluorescence sensors which result in an emission signal which shifts when bound to metal ions, were widely used for *in vivo* detection of metal ions. Recently, various fluorescence sensors have been developed. However, most of them exhibit serious drawbacks such as low Stokes shifts, and high excitation energies which can lead to tissue destruction when used for *in vivo* detection of metal ions. There is clearly much scope for designing fluorescence sensors with improved properties.

Due to the greater selectivities and lower excitation energies observed for some of their derivatives, quinoline-based sensors have become a focus for many researchers. The design and functionalization of these sensors usually relies on three mechanisms, including photoinduced electron transfer (PET),[138] intermolecular charge transfer (ICT),[139] and fluorescence resonance energy transfer (FRET).[140]

1.6.1. Photoinduced electron transfer (PET)

This involves a fluorescent group and a receptor with a high energy non-bonding electron pair which are linked with a less than three atoms spacer. The "off" state for this mechanism (Scheme **1.37a**) consists of fluorescence quenching of the excited fluorophore group by electron transfer from the receptor. The fluorescence "on" state (Scheme **1.37b**) is achieved by attaching species with unfavourable thermodynamics for PET at the receptor site.[141] Examples of turn-on species include metal ions as shown below.

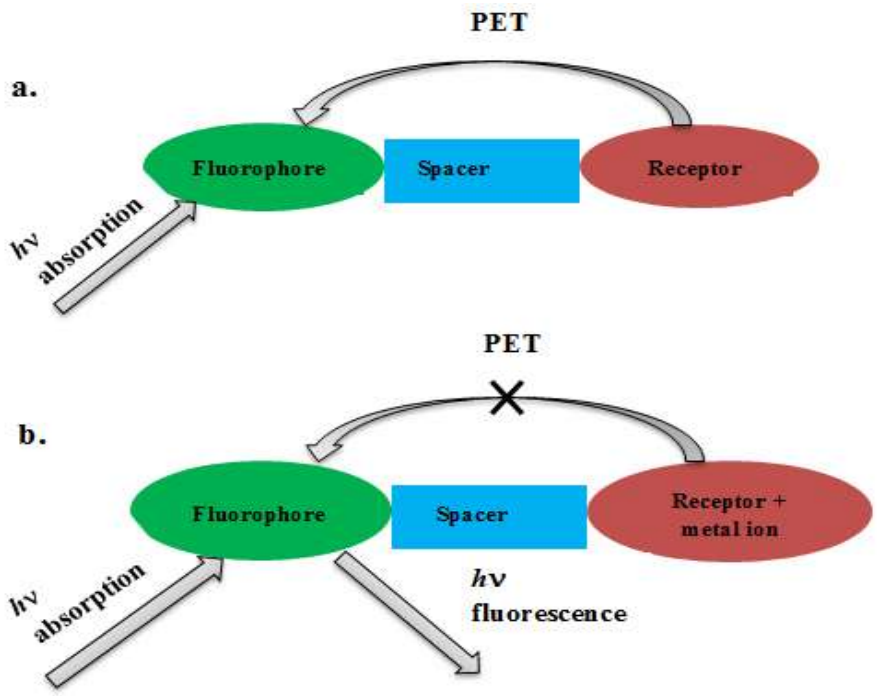

Scheme 1.37: PET mechanism

Though most of quinoline-based fluorescence "turn-on" sensors function by this mechanism, they result in low Stokes shifts (<25 nm) which complicates quantitative measurement and bioimaging.

1.6.2. Intermolecular charge transfer (ICT)

ICT has found application in the design of ratiometric fluorescence sensors. It involves electron rich and electron deficient terminals linked by new conjugation systems resulting from the interaction of the *p*-electrons of the receptor (usually amino) and an adjacent conjugated system (fluorophore) (Scheme **1.38**).

Upon excitation this results in charge transfer enhancement from the electron donor to the electron acceptor. The incorporation of metal ions *via* coordination affects the electronic properties of the receptor which can act either as an electron donor or electron receptor, either by minimizing its electron donating ability or enhancing the electron push-pull effect. This will result either in a blue shift when a metal ion is coordinated with an electron-donating receptor (Scheme **1.38a**) or red shift when coordinated to an electron-pulling receptor (Scheme **1.38b**).

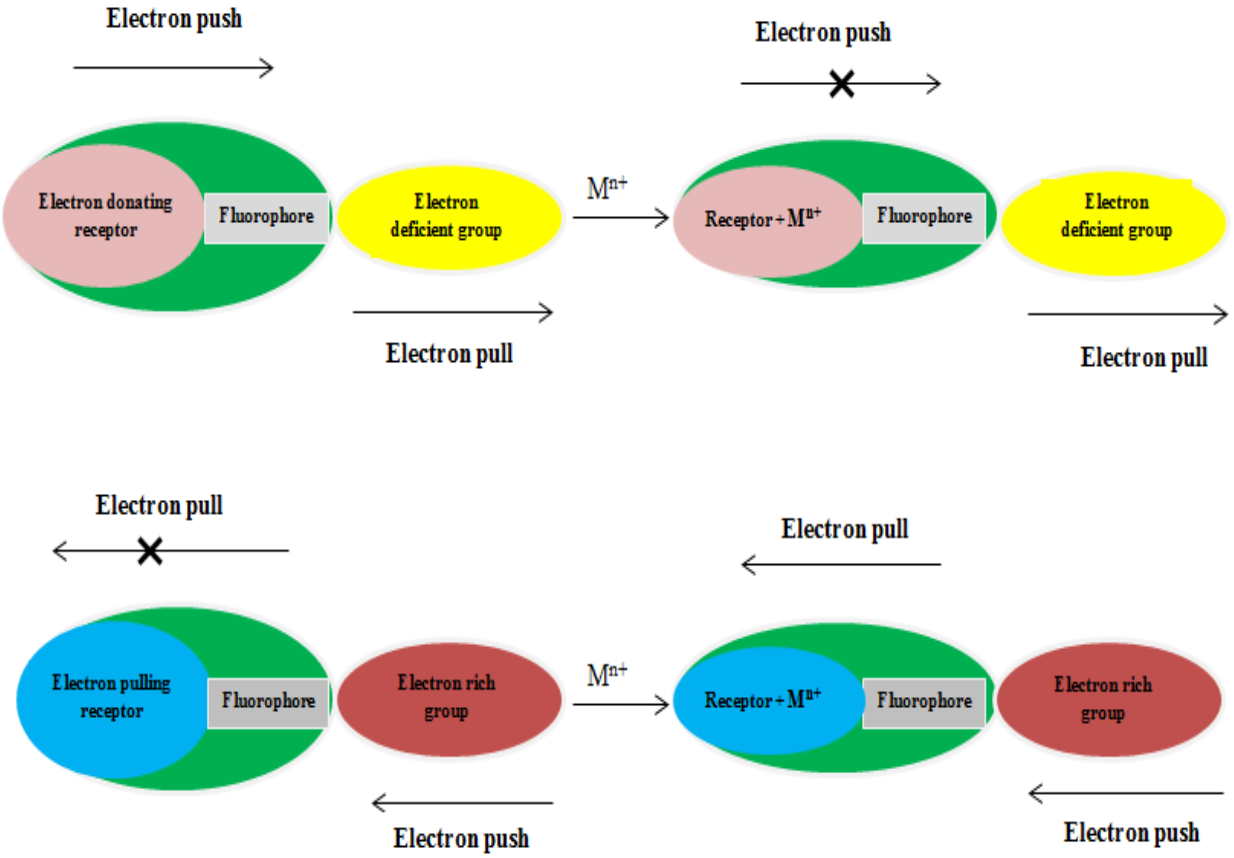

Scheme 1.38: ICT mechanism

1.6.3. Fluorescence resonance energy transfer

This process is also known as a spectroscopic/molecular ruler due to its contribution in measuring distance and change in distance between two active sites both *in vivo* and *in vitro*. This mechanism usually involves two fluorophore groups linked to one another with a spacer *via* a covalent bond. One group acts as an energy donor and absorbs the excitation energy from incident radiation and transfers the energy to a ground-state acceptor at a distance less than 10 nm *via* dipole-dipole interactions (Figure **1.7)**. This transfer is verified by the quenching of the donor fluorescence and an increase in the acceptor fluorescence intensity.

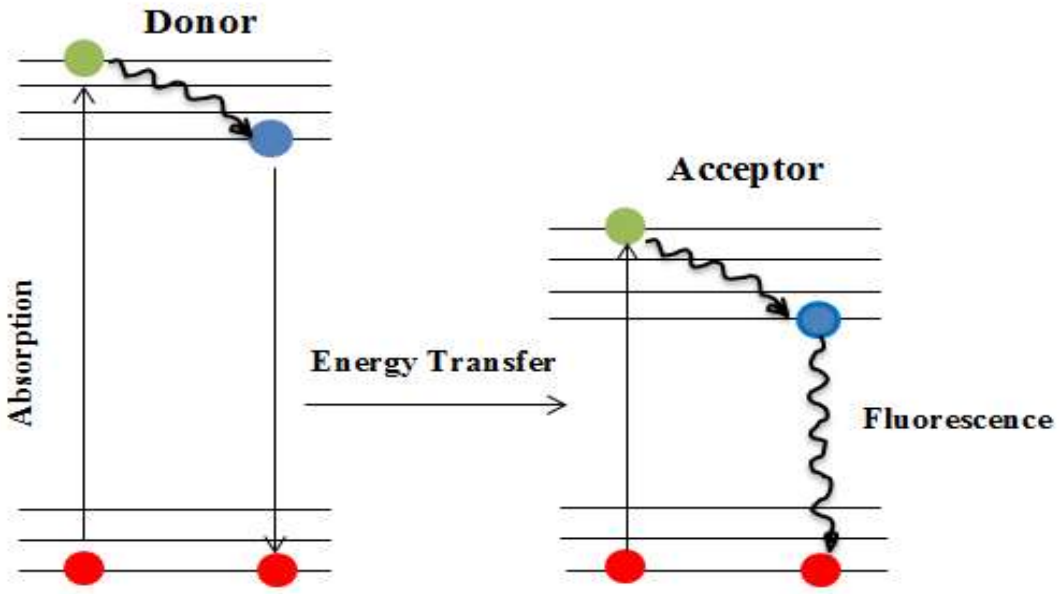

Figure 1.7: Illustration of FRET by a Jablonski diagram.

FRET efficiency is governed by some internal and external factors including the donor emission spectrum which must overlap the absorption spectrum of the acceptor for energy transfer to occur (Figure **1.8).** Other factors such as donor-acceptor distance (<10 nm), dipole orientations (approximately parallel), and sufficient fluorescence lifetime of the donor, are also important.

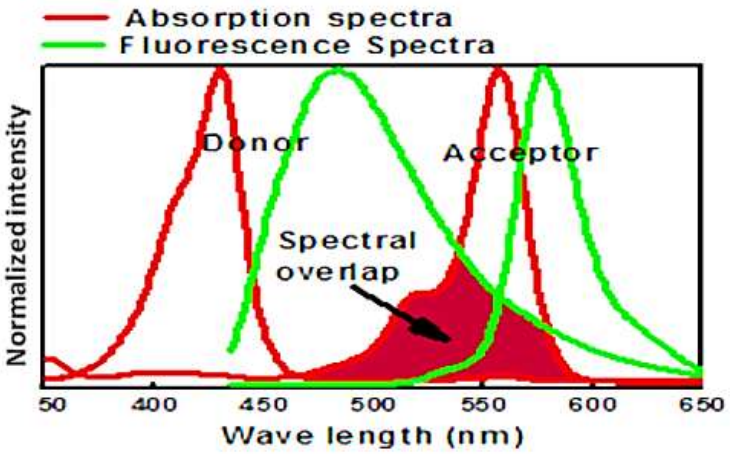

Figure 1.8: Absorption spectra of a donor-acceptor pair and spectral overlap between fluorescence of donor and absorption spectrum of the acceptor.

The efficiency of the FRET mechanism (E_{FRET}) is directly proportional to the inverse sixth power of the distance between the donor and acceptor (r), as derived by Förster.[142]

$$E_{FRET} = R_o^6 / R_o^6 + r^6$$

Where R is the Förster radius

Recently, a number of quinoline-based sensors for various metals ion have been designed by changing the receptor group at positions 2 and 8 of the quinoline scaffold, and incorporation of electron-donating or withdrawing groups at positions 4 and 6. Those include the highly-selective water-soluble and ratiometric chemosensor for Zn^{2+} ions reported by Zhang *et al*. in 2008.[143] The latter exhibits an 8-fold enhancement of the fluorescence quantum yield and 75 nm red shift in its fluorescence emission.

Another selective and ratiometric (under visible light) quinoline-based sensor for Zn^{2+} ions was developed recently by Zhou *et al*.[144] It is characterized by enhanced chelating ability to Zn^{2+} ions

leading to an approximately 14-fold increase in fluorescence response in the presence of Zn^{2+} ions, and more than 7-fold increase in quantum yield.

Based on the ICT mechanism, Xue *et al*. managed to synthesize a highly sensitive and selective sensor for detection of Cd^{2+}, from 4-isobutoxy-6-(dimethylamino)-8-methoxyquinaldine.[145] Ratiometric measurements showed a large blue shift emission and up to 15-fold change in emission intensity.

Other quinoline-based sensors for metal ion detection including Cu(II),[146] Ag(I),[147] Hg(II), [148] Cr(III),[149] Fe(III),[150] and In(III)[151] were designed, but most of them showed limited application in biological systems due to their high UV excitation energies which can cause tissue damage.

Though this field involves many single molecules as chemosensors, some polymers were proven to be efficient in metal ion detection. Examples include the triazole containing fluorescent polymers for Hg^{2+} ion detection.[152] Our study will focus on the investigation of the coordination ability of triazole-quinoline based polymers in which the electron rich-triazole ring is attached at position 6 of the quinoline scaffold, and this unit forms a pendant group of a polymer skeleton. The aromatic amine of quinoline and heterocyclic triazole provide the binding site for metal ions.

1. 7. Research aims and objectives

The general aims of this project were to synthesize fluorescent polymers with triazole-quinoline pendant groups using reversible addition-fragmentation chain transfer polymerization (RAFT). The main objectives of the project can be divided as follows:

1. Synthesis of fluorescent triazole-quinoline vinyl monomer starting with *p*-nitroaniline and using Click chemistry;

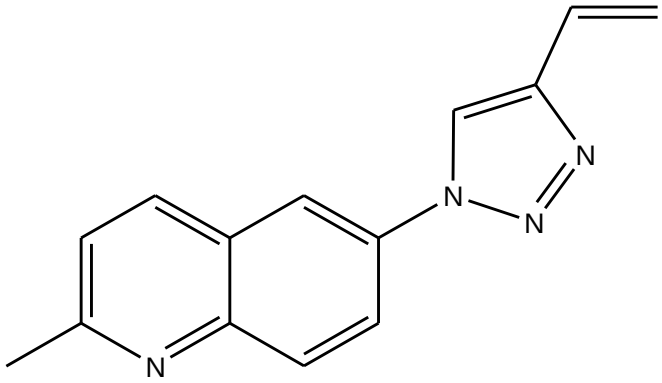

64

Figure 1.9: Vinyl monomer structure

2. Synthesis of fluorescent polymers with pendant quinoline-triazole units using RAFT-mediated polymerization;
3. Comparison of the spectral absorption and emission properties of polymers;
4. Investigation of the chelating ability of the polymers to some metal ions and their impact on the fluorescent properties of the polymers.

Chapter 2

Results and Discussion

2.1. Synthesis of fluorescent 4-vinyl-1,2,3-triazole based quinoline monomer(64)

Due to their enhanced electronic and photonic properties as well as thermal stabilities, quinoline-containing materials and polymers are being intensively studied in academia and industry.[153,154] In order to improve their properties, a number of chemical modifications on the quinoline scaffold which leads to the formation of different types of molecular units can carried out. Some of these include functional groups which can allow them to be polymerized into various polymers with improved properties and higher processability ability compared to the smaller molecules.

Since the properties of quinoline-based polymers are influenced by the spatial arrangement of quinoline chromophores in the chain, many quinoline-based polymers, including linear and non-linear, have been reported. In this study, polymers with triazole-quinoline units on the side chains will be synthesized.

The synthesis of fluorescent 4-vinyl-1,2,3-triazole-quinoline based monomer (**64**) involved multiple steps from commercially available 4-nitroaniline and crotonaldehyde as shown in Scheme **2.1**. Reactions including metal-mediated reduction of the nitro group to amine, diazotization-azidation of the amino group to azide, and Cu(I)-catalyzed Huisgen's 1,3-dipolar cycloaddition of terminal alkynes with azide ("Click" reaction) were used to introduce various substituents into the quinoline backbone. The resulting monomer was polymerized to form a non-linear quinoline-based polymer in which quinoline chromophores are incorporated in pendant chains (Scheme **2.2**).

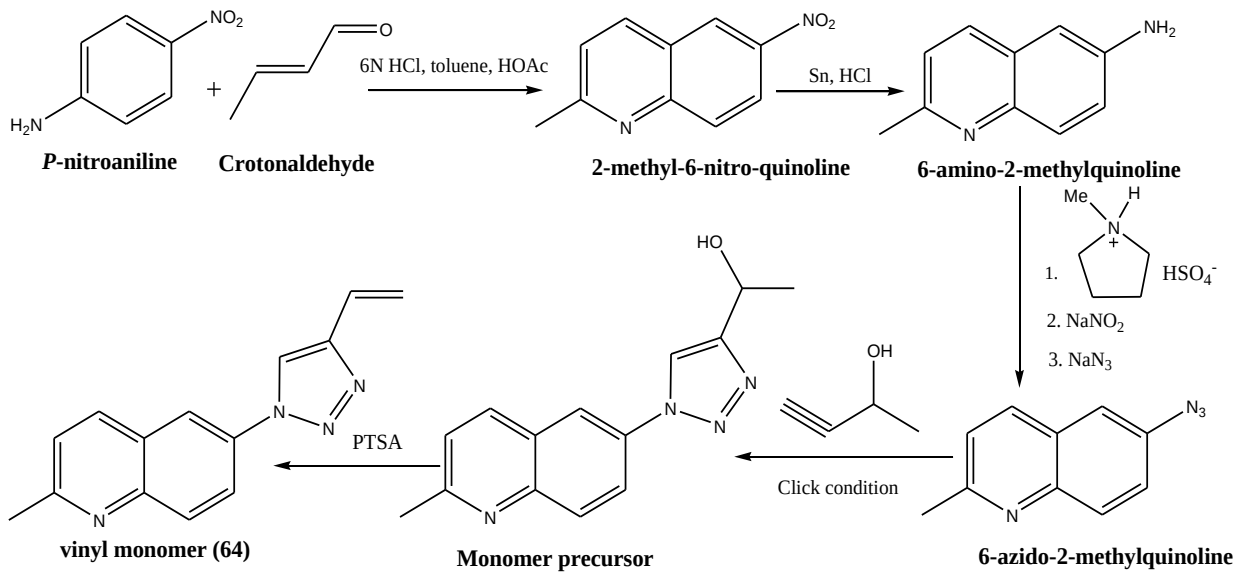

Scheme 2.1: Overall synthesis of novel vinyl monomer (**64**)

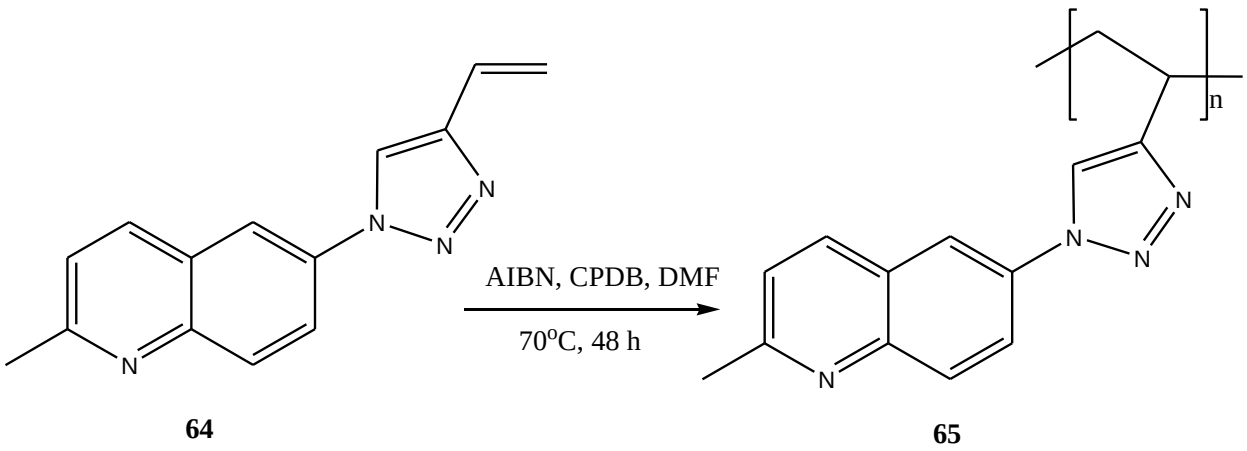

Scheme 2.2: Polymerization of vinyl monomer (**64**)

2. 1. 1. Synthesis of 2-methyl-6-nitroquinoline (68)

The synthesis of the quinoline-based monomer started with the preparation of the nitro-functionalized quinoline skeleton. This was successfully achieved *via* a Skraup-Doebner-Von Miller quinolines synthesis.[155]

The starting materials for this reaction were *p*-nitroaniline and crotonaldehyde which were heated to reflux in concentrated hydrochloric acid for 0.5 hours at 100 ^{o}C in the presence of acetic acid as shown in Scheme **2.3**. A catalytic amount of potassium iodide and some toluene were added resulting in the formation of a heterogeneous mixture. Then crotonaldehyde in toluene was added drop-wise over a period of 1h. The mixture was heated to reflux further for 6 h and after cooling to room temperature, the reaction was quenched with concentrated ammonia/sodium hydroxide solution to afford crude 2-methyl-6-nitroquinoline. The latter was purified by column chromatography using 30% ethyl acetate in hexane to afford a pure product as a light yellow solid, in 60% yield.

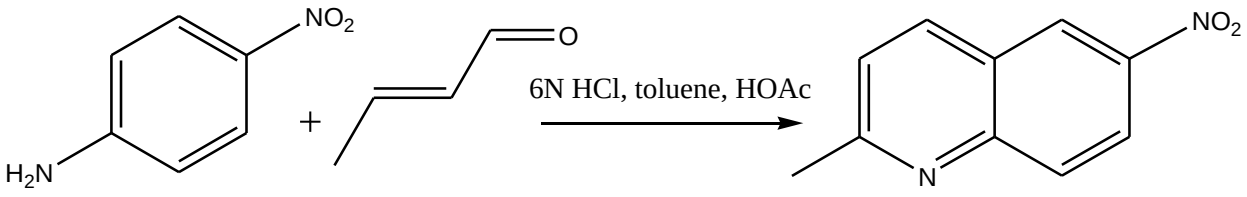

66 **67** **68**

Scheme 2.3: 2-Methyl-6-nitroquinoline synthesis

The pure product was characterized by NMR and FT-IR spectroscopy. Figure **2.1** gives the assignment of the proton signals in the ^{1}H-NMR spectrum of 2-methyl-6-nitroquinoline. The methyl protons were assigned to the signal at 2.75 ppm integrating for three protons. The aromatic quinoline protons were evident between 7.38 ppm and 8.67 ppm. A singlet at 8.67 ppm integrating for one proton was assigned to H-5. Four doublet signals integrating for one proton each were observed at 7.38 ppm, 8.06 ppm, 8.16 ppm and 8.37 ppm.

The higher field doublet signal at 7.38 ppm was assigned to H-3 due to the shielding effect of the methyl group.

The doublet at 8.06 ppm was assigned to H-8 due to the dual effects of the electron-withdrawing nitro group and highly electronegative N-atom, which caused a downfield shift of this proton compared to the previous one. The doublet at 8.16 ppm was assigned to H-4 due to the combination of the weakly shielding effect of the electron donating groups (alkyl and nitrogen) and the electron withdrawing effect of nitro group-bearing aromatic ring. The lower field doublet at 8.37 ppm was assigned to H-7 owing to the deshielding effect of the nitro group at position 6.

The above structure was confirmed by the ^{13}C NMR spectrum (Figure **2.2**) which showed all 10 carbon atom in the range 24.66-162.27 ppm. The highest field signal observed at 24.66 ppm was assigned to the sp^3 hybridized methyl carbon C-11.

The nine aromatic quinoline carbon signals were observed in the range 122.01-162.27 ppm. The highest field resonance in this range at 122.01 ppm was assigned to C-3 due to shielding effect of neighbouring groups. The next signal observed at 122.93 ppm was assigned to C-7 due to the *ortho*-deshielding effect of the nitro group. The signal at 123.3 ppm was assigned to C-5 due to enhanced ortho-dieshielding effect from resonance. The signal at 124 ppm was assigned to C-10 due to the additional deshielding effect from neighbouring groups to the deshielding effects of electron-withdrawing nitro group. The signal at 136 ppm was assigned to C-8 due to dual deshielding effects of the nitro group and heterocyclic quinoline ring. The signal at 137 ppm was assigned to C-4 due to the deshielding effect of the nitro group *via* conjugation. The signal at 144 ppm was assigned to C-6 experiencing enhanced dieshielding effect from the nitro group. The signal at 149.9 was assigned to C-9 due to enhanced inductive effect of the quinoline nitrogen atom and the influence of the nitro group. The lowest field was observed at 164 ppm and was assigned to 2-C which experiences two enhanced inductive effect from neighbouring methyl and quinoline nitrogen atom resulting in considerable deshielded carbon atom.

The functional group in the product were confirmed by FT-IR spectrum (**Figure 2.3**) showing the nitro group stretching at 1529 cm^{-1} and 1336 cm^{-1} and aromatic C=C bonds stretching at 1608 cm^{-1}. The absence of any -NH_2 stretch in the range 3500-3300 cm^{-1} which was present in the starting 4-nitroaniline FT-IR spectrum (**Figure 2.4**) confirmed the utilization of this functional group during the quinoline skeleton formation.

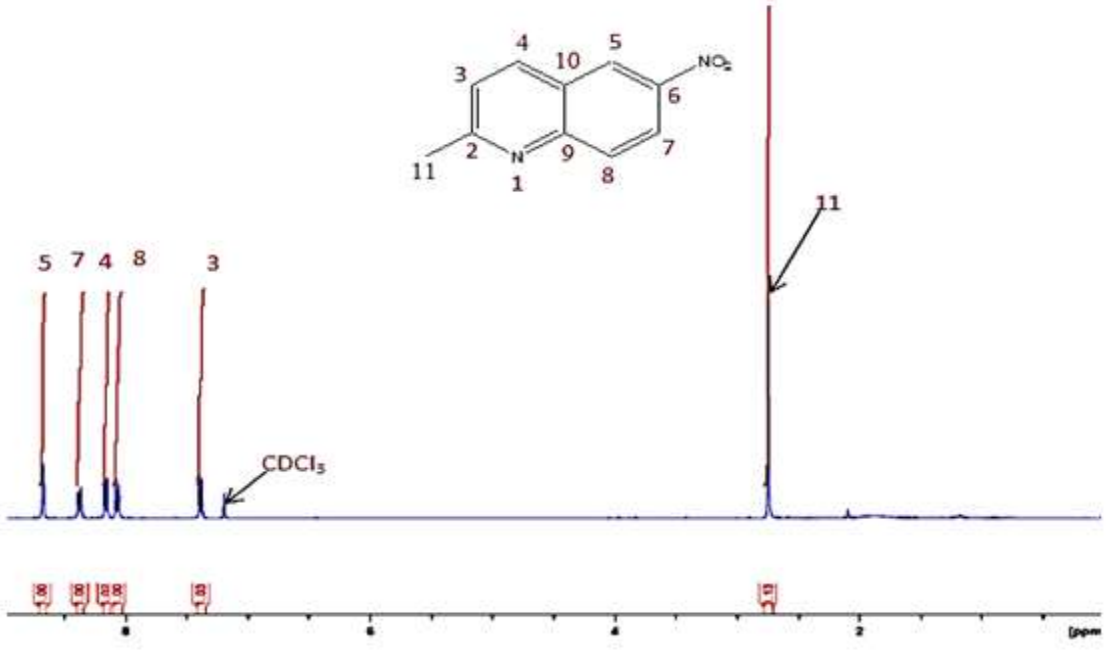

Figure 2.1: ^{1}H-NMR spectrum of 2-methyl-6-nitroquinoline **(68)** in $CDCl_3$

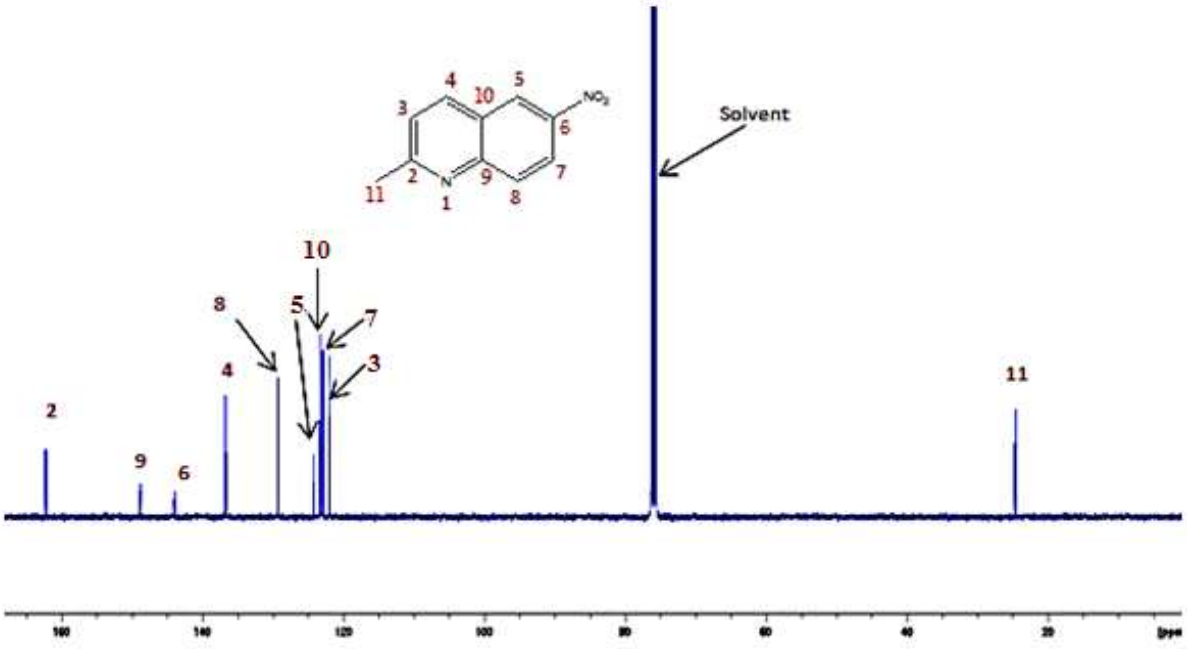

Figure 2.2: ^{13}C NMR spectrum of 2-methyl-6-nitroquinoline (**68)** in $CDCl_3$

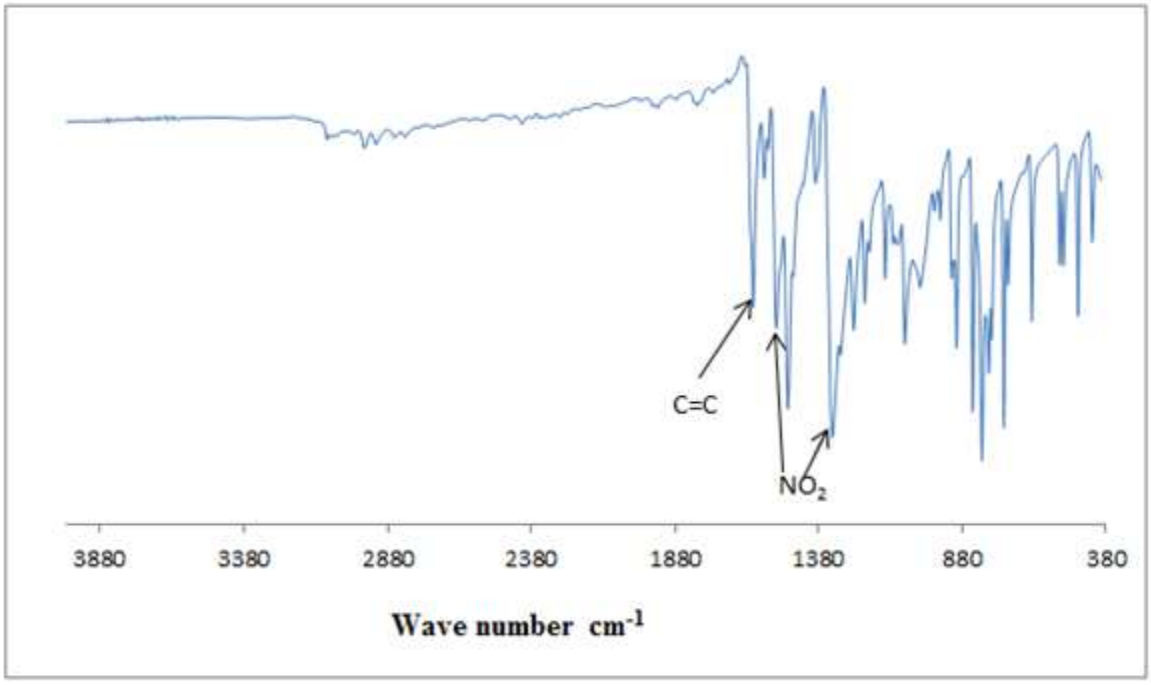

Figure 2.3: FT-IR spectrum of 2-methyl-6-nitroquinoline (**68**)

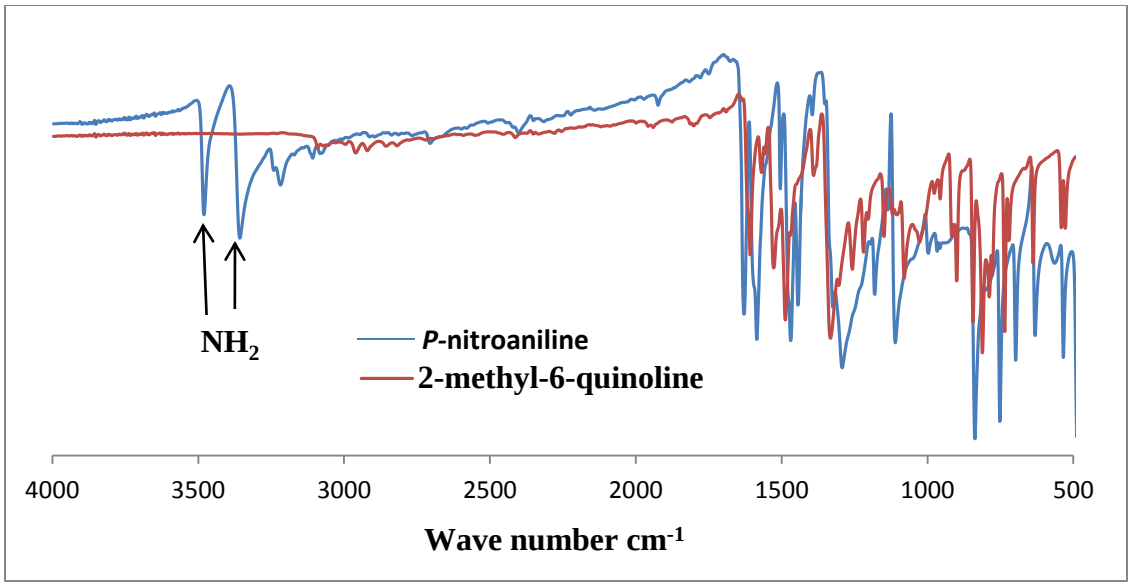

Figure 2.4: FT-IR spectra of *p*-nitroaniline and 2-methyl-6-nitroquinoline (**68**)

2. 1. 2. Synthesis of 6-amino-2-methylquinoline (69)

The chemical modification of the quinoline nucleus leading to the formation of required monomer started with the reduction of the nitro group of the quinoline derivative synthesized in the first stage. This reduction was achieved using tin in concentrated hydrochloric acid (Scheme **2.4)** to afford a pure product as a white solid in 65 % yield.

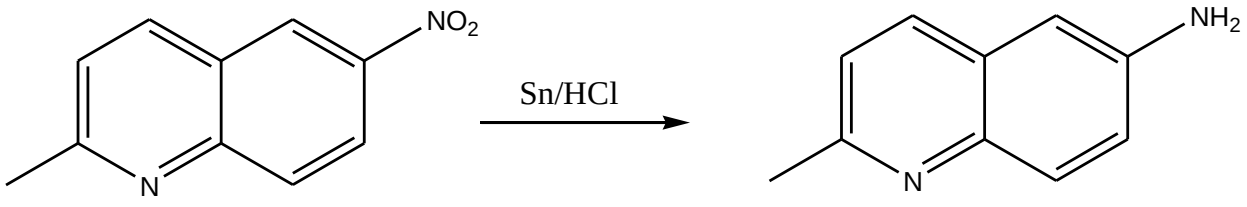

68 **69**

Scheme 2.4: 6-Amino-2-methylquinoline (**69**)

Attempts were made to improve the reaction yield by carrying out the reaction at different temperatures below 50^{o}C but no significant change in yield was observed.

We investigated the possible use of alternative reducing agents for the nitro group, but all of those shown in Table **2.1** were unsuccessful. The reducing agents included the transition metals salts of iron, zinc and tin ($SnCl_{2.}2H_20$). The iron mediated reduction reaction was carried out in acetic acid at 50^{o}C and resulted in a reddish product after all the iron was consumed. The red colour suggested the formation of an iron-quinoline complex rather than effecting the expected conversion. The zinc reaction was performed in an aqueous/ether mixture at 70^{o}C, but no product was isolated after 8 h of reflux. A similar result was obtained after 1h refluxing 6-amino-2-methylquinoline and $SnCl_{2.}2H_20$ in ethanol.

Reagents	**Condition**	**Results**
$SnCl_2.2H_2O$	EtOH, Reflux	No reaction
Fe	HOAc, 50 ^{o}C	No reaction
3.0-3.5 eq. Zinc	Ether/water mixture, 70^{o}C, 8h	No reaction
$HCO^{-}_2NH^{+}_4$/ Pd-C	CH_3OH, rt	No reaction

Table 2.1: Attempted reaction for 6-amino-2-methylquinoline reduction

Another attempt was carried out at room temperature using ammonium formate with Pd/C as a catalytic hydrogen transfer agent in dry methanol. After refluxing for 1h under nitrogen only unreacted starting material was recovered.

The isolated pure product was characterized by NMR and FT-IR spectroscopy. The ^{1}H-NMR spectrum (Figure **2.5**) showed a new broad peak integrating for two protons at 3.81 ppm which was assigned to the amino group protons, which confirmed the formation of product. This was further confirmed by a significant up-field shift in the aromatic quinoline protons close to the amino group emphasizing the substitution of the strongly electron-withdrawing nitro group by the positively mesomeric amino group.

The singlet previously observed for H-5 at 8.67 ppm in 2-methyl-6-nitroquinoline shifted to 6.8 ppm in the amino product, while the doublet due to H-7 shifted from 8.37 to 7.05 ppm.

This was further confirmed by ^{13}C NMR (Figure **2.6**) which showed an up-field shift for C-5 from 123.3 ppm to 107.73 ppm due to mesomeric effect from nitrogen lone pair of electron on amino group and down field shift of 7-C from 122.93 ppm to 127.8 ppm due to inductive effect of nitrogen of the amino group.

The presence of the amino functionality was further confirmed using FT-IR spectroscopy which showed the absence of the nitro group absorptions at 1338 and 1529 cm^{-1} and appearance of two N-H absorptions in the range between 3500 and 3100 cm^{-1} (Figure **2.7)**.

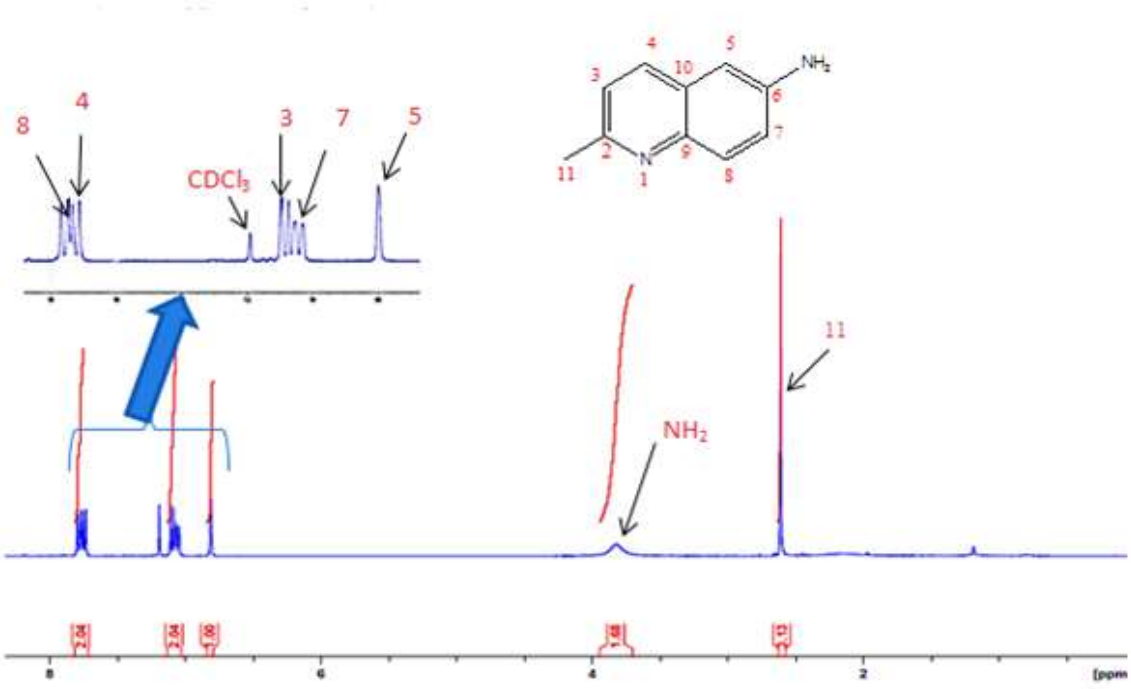

Figure 2.5: ^{1}H-NMR of 6-amino-3-methylquinoline (**69**) in $CDCl_3$

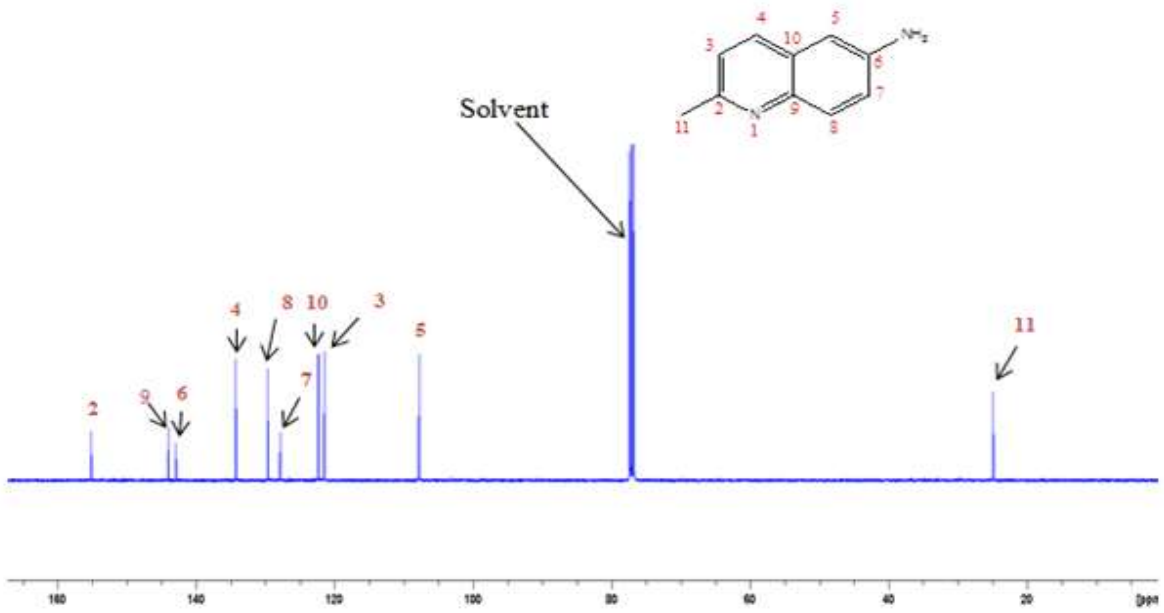

Figure 2.6: ^{13}CNMR spectrum of 6-amino-2-methylquinoline (**69**) in $CDCl_3$

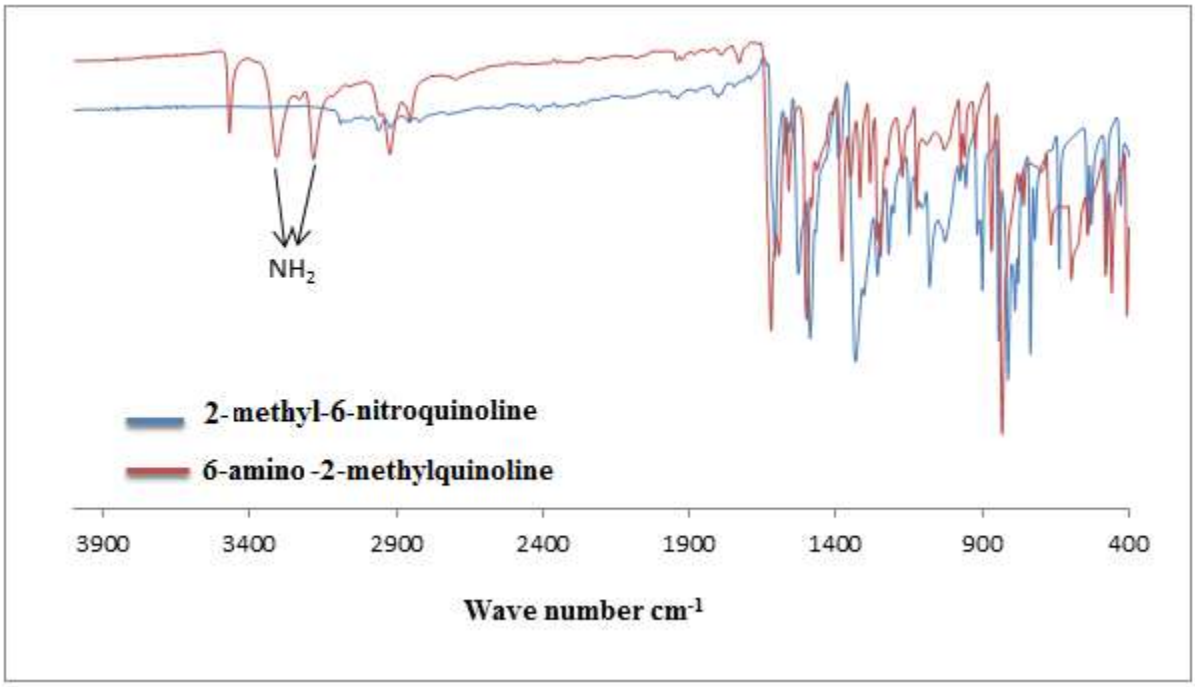

Figure 2.7: FT-IR spectra of 6-amino-2-methylquinoline (**68**) and 2-methyl-6-nitroquinoline (**69**)

2. 1. 3. Synthesis of 6-azido-2-methylquinoline (70)

The next chemical modification on the quinoline moiety was carried out on the amino group of the previously synthesized compound, leading to the formation of the azide functionalized quinoline product, which allows application of Click chemistry. This was successfully achieved at room temperature using a well-documented diazotization-azidation method in which acidic ionic liquid *N*-methyl-2-pyrrolidinium bisulfate ($[H\text{-}NMP]^+$ HSO_4^-) was used as a proton source.[156]

The reaction was accomplished in a 1:1 mixture of water and tetrahydrofuran in order to dissolve both the quinoline derivative and ($[H\text{-}NMP]^+$ HSO_4^-). The highly reactive quinoline-based diazonium salt formed after addition of $NaNO_2$ was converted to the azide by addition of sodium azide as shown in Scheme **2.6**. After work up, the crude product was purified by column chromatography using 10% ethyl acetate in hexane to afford a pure product as a brown oil in 40% yield.

This low yield was attributed to reaction between the nitrogen atom in the quinoline skeleton with the proton released from ($[H\text{-}NMP]^+HSO_4^-$), leading to the formation of an ammonium ion with significant reduction in the proton concentration in the reaction mixture. The attempt to use higher concentration of ($[H\text{-}NMP]^+HSO_4^-$) complicated the work up process, as the product associates strongly with the acidic ionic liquid residues. The use of hydrochloric acid failed to give the desired product, with only starting material being recovered.

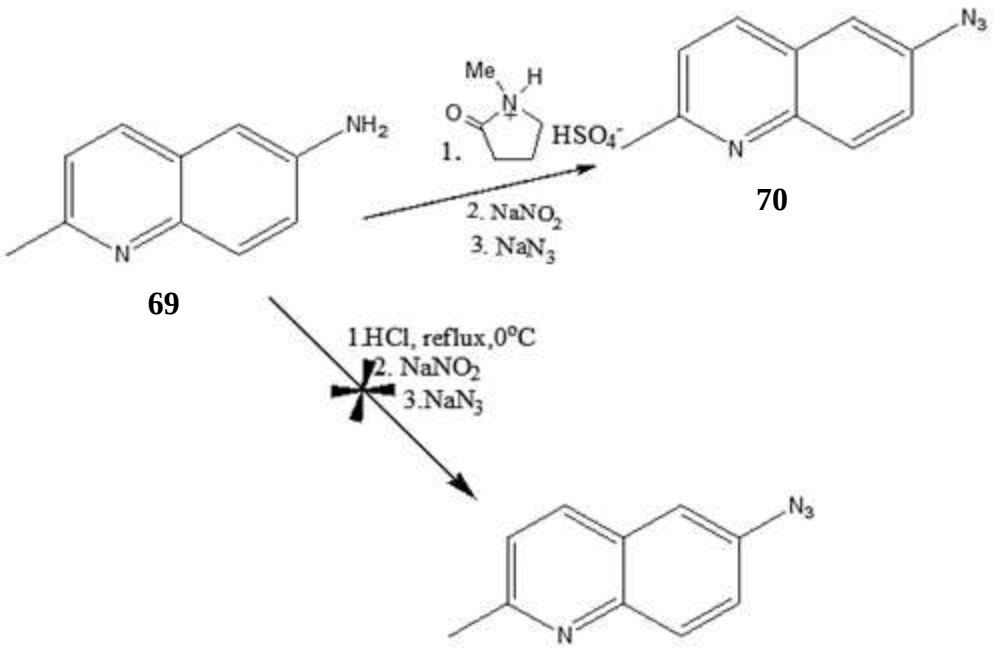

Scheme 2.6: Synthesis of 6-azido-2-methylquinoline (**70**)

The acidic ionic liquid ($[H\text{-}NMP]^+HSO_4^-$) used in this reaction was synthetized at room temperature from *N*-methyl-2-pyrrolidone and concentrated sulphuric acid as shown in Scheme **2.7.** The reaction was accomplished in dichloromethane in which dissolved *N*-methyl-2-pyrrolidone was converted into ($[H\text{-}NMP]^+HSO_4^-$) through drop-wise addition of concentrated sulphuric acid, followed by stirring at RT for 4h. After solvent removal, the product was obtained as colourless oil, in good yield.

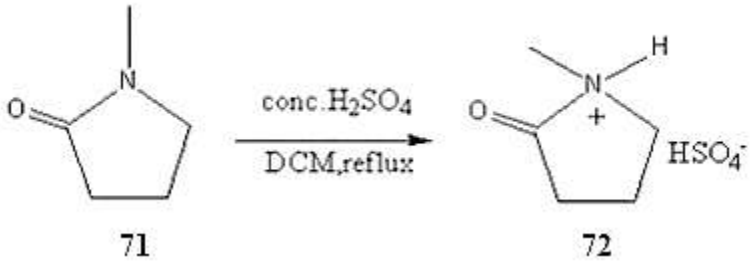

Scheme 2.7: Synthesis of acidic ionic liquid ($[H\text{-}NMP]^+ HSO_4^-$)

The synthesized acidic ionic liquid ([H-NMP]$^{+}$HSO$_4^{-}$) was characterized by ^{1}H-NMR and FT-IR spectroscopy as shown in Figures **2.8** and **2.9** below. The N-H signal appeared as a singlet at 2.5 ppm in the ^{1}H-NMR spectrum and the pyrrolidone ring protons were observed between 1.88 and 3.47 ppm. The existence of the ammonium salt was confirmed from the broad peaks between 2000 and 3200 cm^{-1} in its FT-IR spectrum.

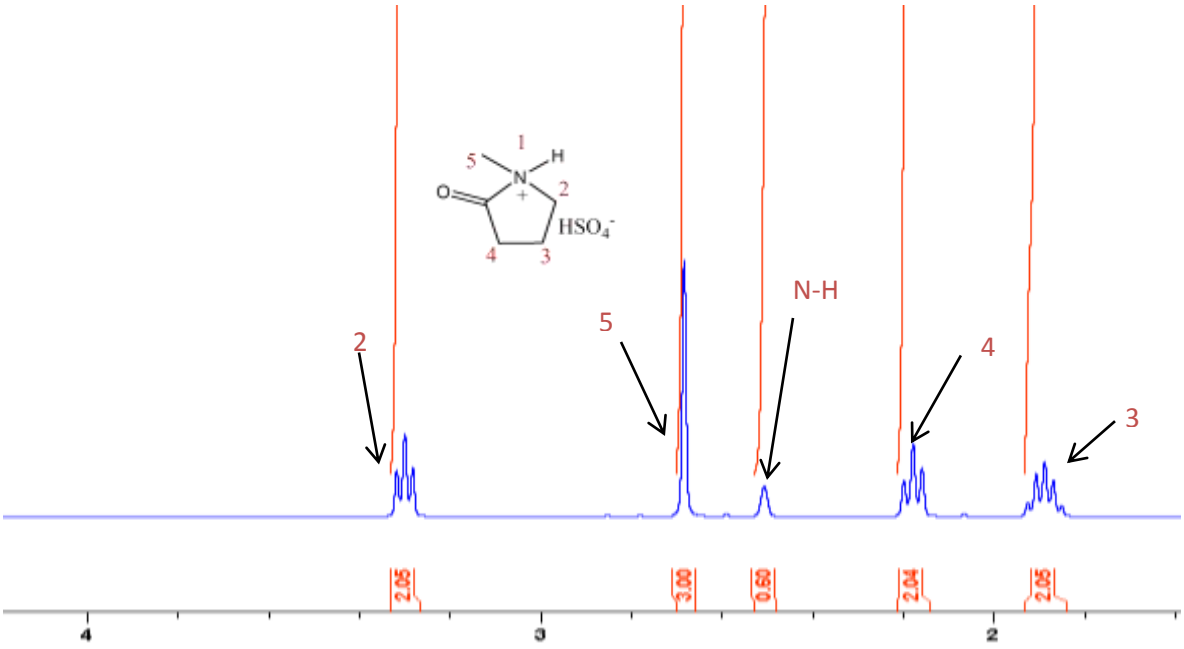

Figure 2.8: ^{1}H-NMR spectrum of the acidic ionic liquid ([H-NMP]$^{+}$HSO$_4^{-}$) in CDCl$_3$

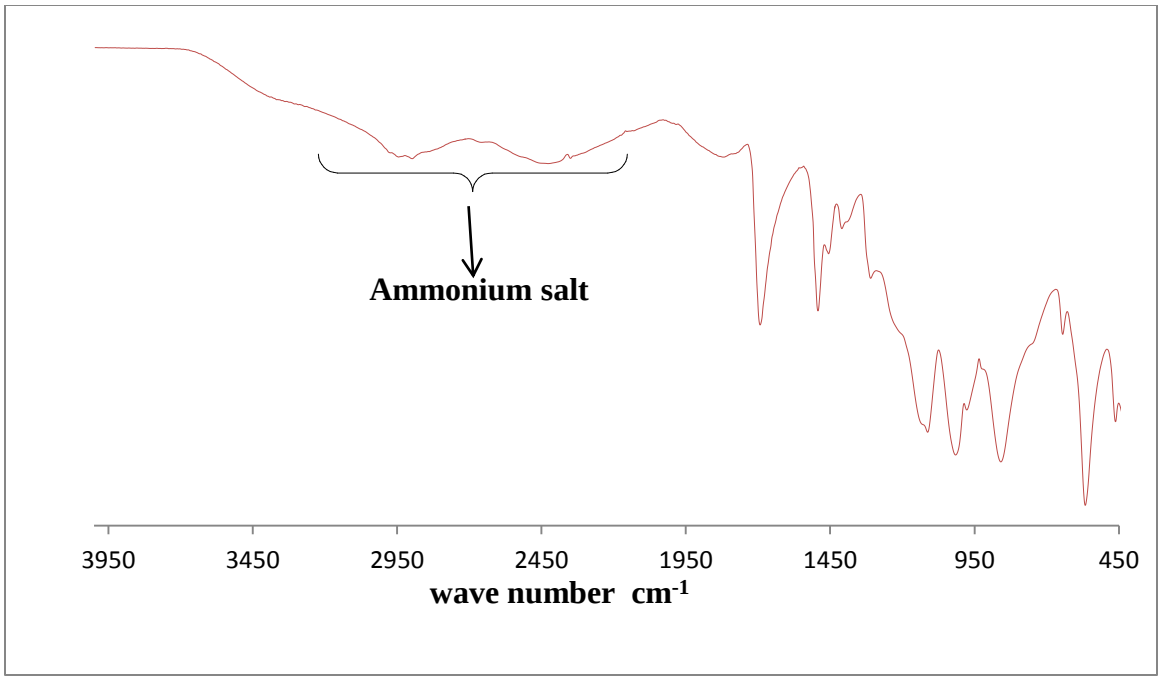

Figure 2.9: FT- IR spectrum of the acidic ionic liquid ($[H\text{-}NMP]^+ HSO_4^-$)

The structure of 6-azido-2-methylquinoline (**70**) was confirmed by ^{1}H-NMR spectroscopy. The four doublets integrating for one proton each at 7.2 ppm, 7.28 ppm, 7.9 and 7.95 in the ^{1}H NMR spectrum shown in Figure **2.10** were assigned to aromatic protons H-3, H-7, H-5, H-4, and H-8, respectively. The methyl signal occurs at 2.67 ppm. The disappearance of the primary amine (NH_2) signal previously observed at 3.81 ppm in the ^{1}H-NMR spectrum of the starting amino quinoline (Figure **2.5**) and the down-field shift of 5-H proton signal due to introduction of the less electron-donating azide group compared to the amino group confirmed the success of this synthesis.

This was further confirmed by ^{13}C-NMR (Figure **2.11**) which showed ten carbon signals and a shifting of the signals of the carbons close to azide group. The 5-C and 7-C shifted down-field from 107.73 ppm and 127.8 ppm to 126.6 ppm and 134.46 ppm, respectively due to the electron withdrawing effect associated with the azide group. The 6-C showed an upfield shift due to the resonance in azide group which cause a shielding at position 6.

The structure was further confirmed by its FT-IR spectrum **(**Figure **2.12)** which exhibited absorption for the azide group at 2100 cm^{-1} and the absence of two N-H absorptions previously detected in the range between 3500 and 3100 cm^{-1}.

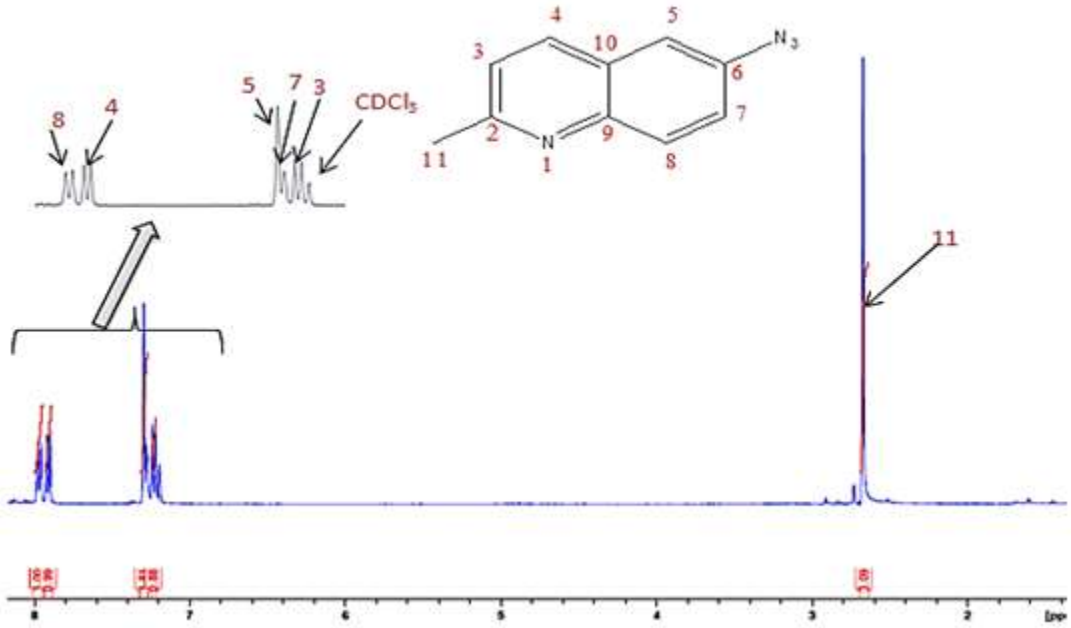

Figure 2.10: ^{1}H-NMR spectrum of 6-azido-2-methylquinoline (**70**)

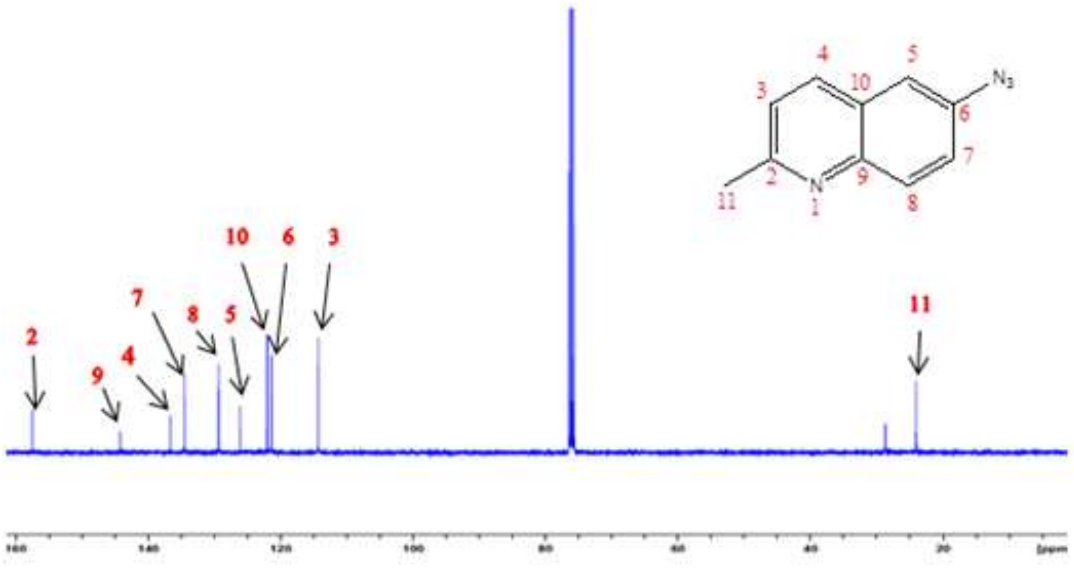

Figure 2.11: ^{13}C-NMR spectrum of 6-azido-2-methylquinoline (**70**)

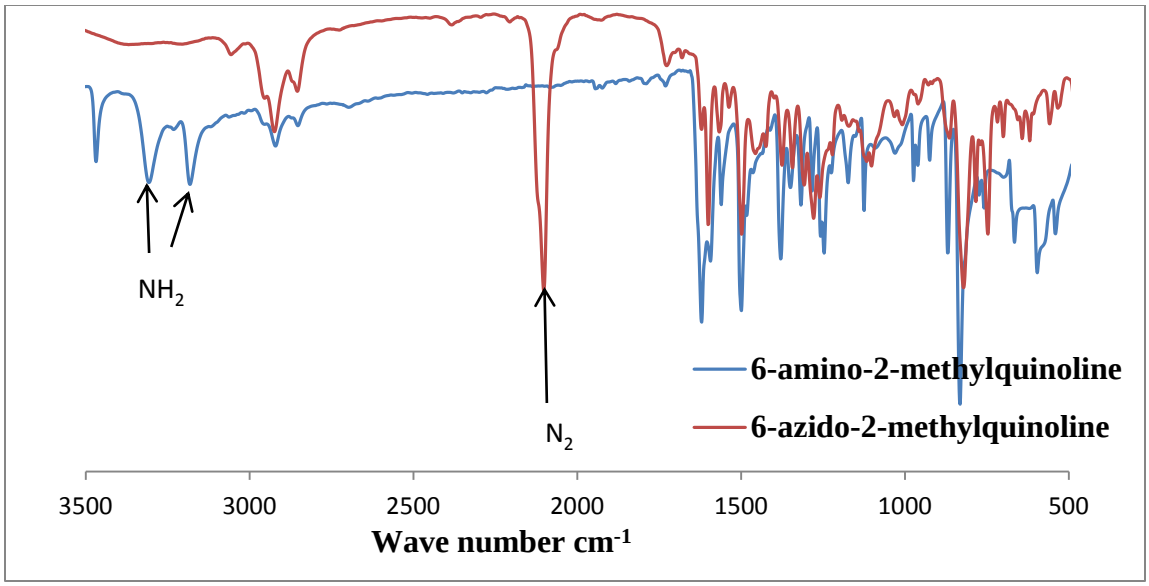

Figure 2.12: FT-IR spectra of 6-azido-2-methylquinoline (**70**) and 6-amino-2-methylquinoline (**69**)

2. 1. 4. Synthesis of 1-(1-(2-methylquinolin-6-yl)-1H-1,2,3-triazol-4-yl)ethanol

Incorporation of the triazole ring in chemical structures to afford 4-vinyl-1,2,3- triazole monomer has been previously accomplished *via in situ* generation of 2-vinyl acetylene from the direct reaction of trimethylsilyl (TMS)-protected vinyl acetylene and the appropriate organic azide under Click conditions. Due to the cost associated with this approach and other disadvantages such as a complicated synthesis and handling of the TMS-derivatives, alternative synthetic approaches were developed to overcome those problems. Since Click reactions are tolerant of a wide range of functional groups, allowing early triazole ring incorporation rather than in the last step of the synthesis, two well-known synthetic procedures (elimination and Wittig reaction) which generate the vinyl monomer in the last step have been introduced.[18]

Due to its low cost and availability, 3-butyn-1-ol and its isomer 3-butyn-2-ol have been widely used in $3\pi + 2\pi$ cycloaddition reactions of alkynes and organic azides, leading to the formation of triazole-bearing molecules which undergo dehydration to give the desired 4-vinyl-1,2,3-triazole monomers.

Since dehydration reactions on secondary alcohols occurs more readily than for primary alcohols, 3-butyn-2-ol proved to be the preferred starting material for the $3\pi + 2\pi$ cycloaddition reaction.

In our study, the triazole unit was incorporated using the well-documented high-yielding and regioselective Cu(I) catalysed azide-alkyne cycloaddition reaction developed by Sharpless *et al.*[51] The reaction as shown in Scheme **2.8** was accomplished in THF in which 2-methyl-6-azidoquinoline, 3-butyn-2-ol in the presence of the Cu(I) source, $CuSO_4$/NaAsc, and the Cu(II) stabilizing ligand PMDETA, were stirred at room temperature for 24 h. THF was removed under reduced pressure and the residues were treated with water which was then extracted with chloroform. After concentration, the crude product was purified by column chromatography using 70% ethyl acetate in hexane to afford a pure product as a white solid in 50% yield. The low yield was attributed to complex formation between the Cu(I) and quinoline, resulting in a lower Cu-acetylide complex concentration which in turn reduced the yield of product.

The use of excess of Cu(II) was unsuccessful, suggesting inhibition of formation of the appropriate Cu-acetylide complex species.

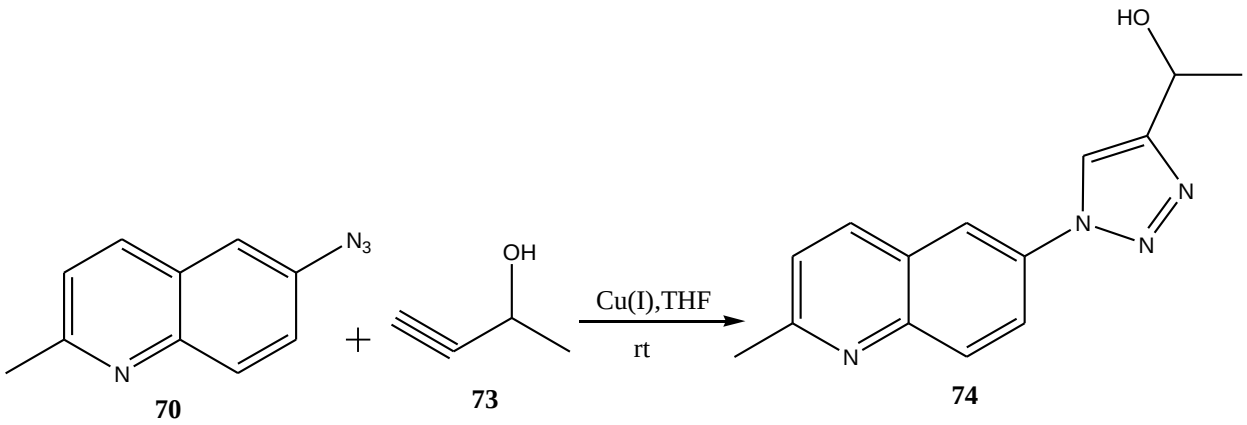

70 **73** **74**

Scheme 2.8: Synthesis of monomer precursor (**74**)

The structure of the monomer precursor was confirmed by its ^{1}H-NMR spectrum shown in Figure **2.13**. The doublet signal integrating for three protons at 1.71 ppm was assigned to the methyl group in the alkanol side chain.

The broad signal integrating for one proton at 2.55 ppm was assigned to the hydroxyl group which was also evident from a stretch absorption at 3328 cm^{-1} in the FT-IR spectrum. The quartet at 5.25 ppm is due to resonance of the methine proton of the alkyl group of the side chain.

The triazole ring -CH proton was assigned to the peak at 8.17 ppm; its integral was affected by overlapping quinoline ring proton signals. The presence of aromatic quinoline proton signals in the range 7.4 -8.19 ppm as well as the methyl signal at 2.80 ppm confirmed the successful incorporation of the triazole ring without affecting the quinoline moiety.

The monomer precursor structure was also confirmed by ^{13}C-NMR, DEPT (135) and 2D-Homonuclear (H,H)-Correlated NMR Spectroscopy (H,H-COSY).

The ^{13}C-NMR spectrum showed all fourteen carbon signals expected for the monomer precursor as shown in Figure **2.14**. The signals of the two triazole carbons (C-1', C-2') and those from carbons at the α and β positions to the triazole ring (C-3', C-4') were assigned to 118.58 ppm, 153.27 ppm, 63.28 and 23.28 ppm, respectively.

The ten carbon signals observed in the aromatic region were assigned to the aromatic quinoline carbons. A DEPT(135) spectrum showed nine methine/methyl signals (Figure **2.15**) which is consistent with the proposed structure.

The three spin systems in the structure was confirmed by a H,H-COSY NMR spectrum which showed three different coupled proton signals as shown in Figure **2.16**. The first coupling is the side chain methine protons and the methyl protons as illustrated by the blue rectangle. This results in the doublet at 1.71 ppm and quartet at 5.25 ppm. The second coupling interaction was observed between 3-H and 4-H of the quinoline ring system as shown by the red rectangle and resulted in the pair of doublets at 7.33 ppm and 8.09 ppm, respectively. The third spin system was assigned to coupling between 7-H and 8-H as shown by the black rectangle and produced another pair of doublets at 7.99 ppm and 8.12 ppm, respectively. The presence of these spin systems confirmed the structure of product.

The structure of the product was also confirmed with its FT-IR spectrum. Figure **2.17** showed the disappearance of the azide peaks previously observed in the starting azido-quinoline moiety at 2100 cm^{-1}. The OH group stretch frequence was observed at 3317 cm^{-1} and triazole ring formation was confirmed by the N=N stretch frequence at 1402 cm^{-1} (Figure **2.18)**.

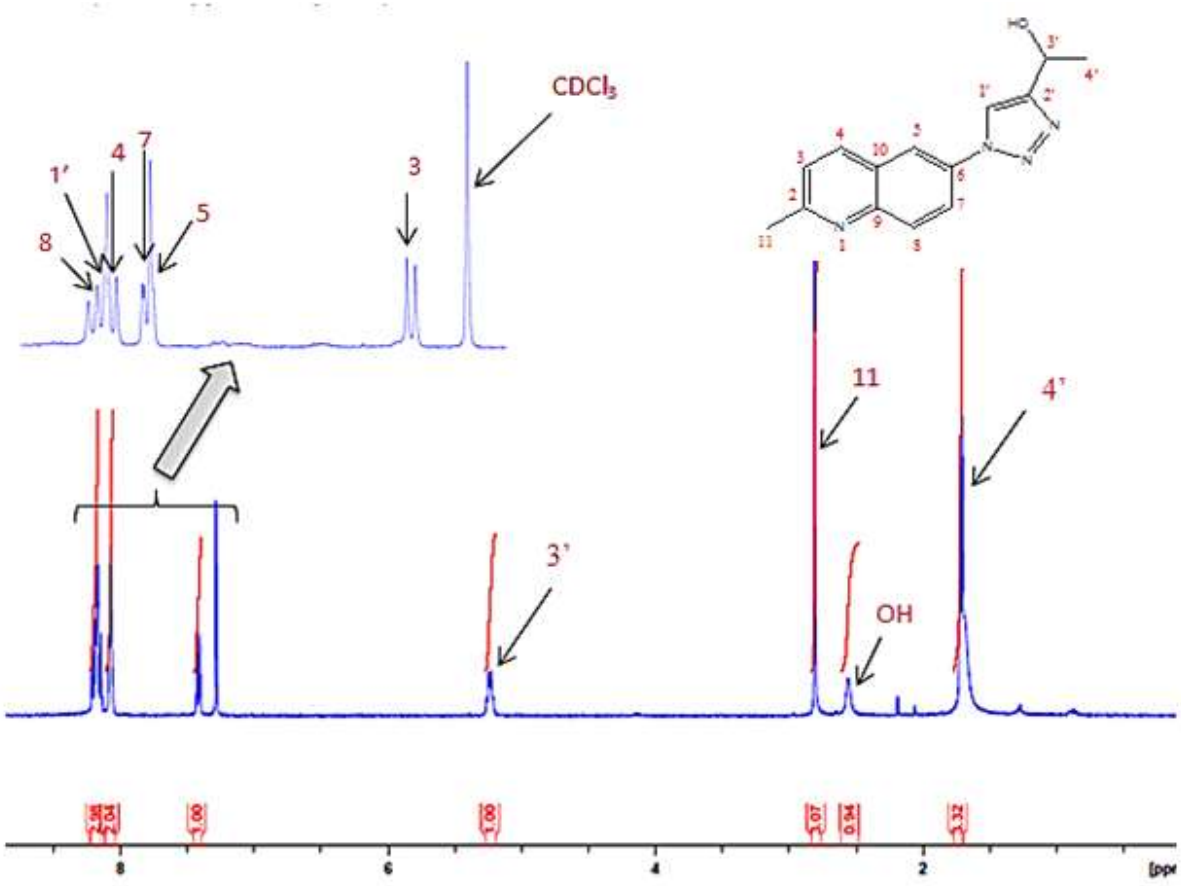

Figure 2.13: ^{1}H-NMR spectrum of 1-(1-(2-methylquinolin-6-yl)-1H-1,2,3-triazol-4-yl)ethanol in $CDCl_3$

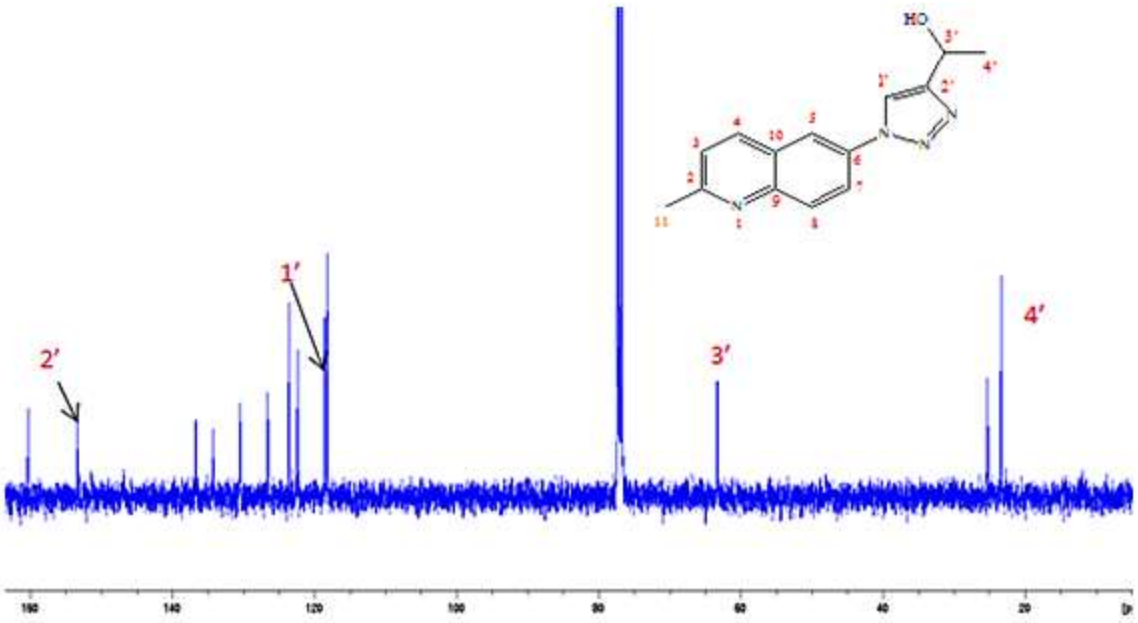

Figure 2.14: ^{13}C-NMR spectrum of 1-(1-(2-methylquinolin-6-yl)-1H-1,2,3-triazol-4-yl)ethanol in $CDCl_3$

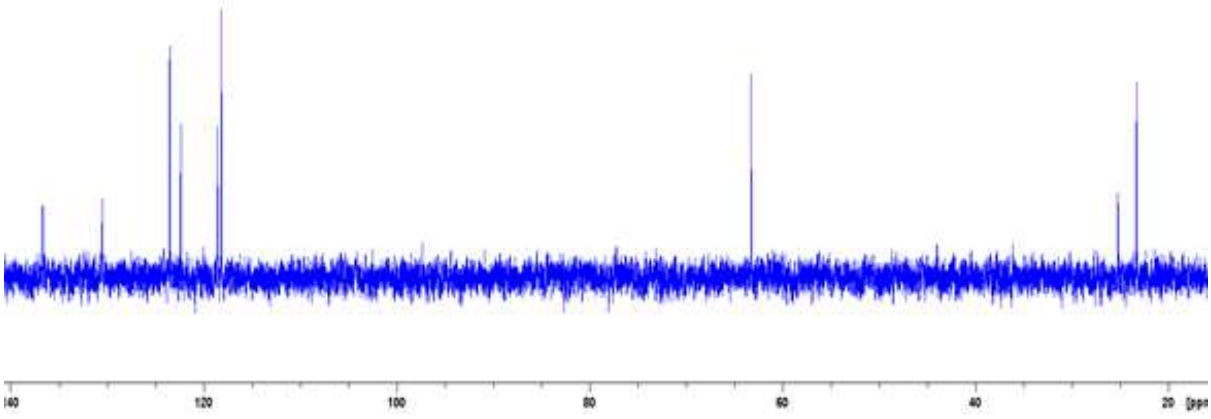

Figure 2.15: DEPT(135) -NMR spectrum of 1-(1-(2-methylquinolin-6-yl)-1H-1,2,3-triazol-4-yl)ethanol in $CDCl_3$

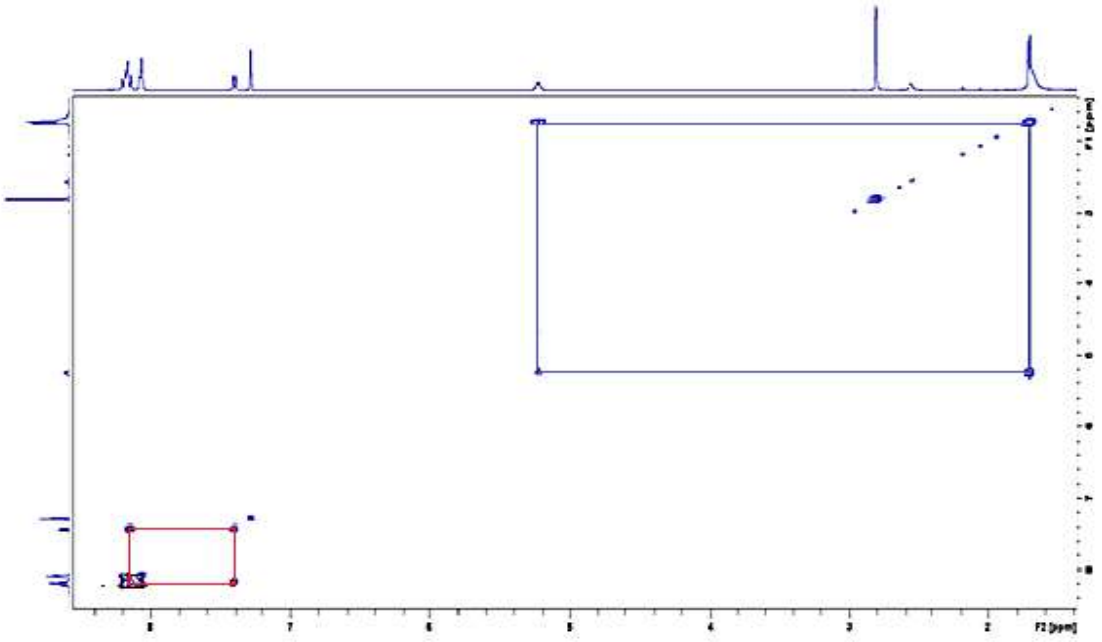

Figure 2.16: H,H-COSY NMR spectrum of 1-(1-(2-methylquinolin-6-yl)-1H-1,2,3-triazol-4-yl)ethanol in $CDCl_3$

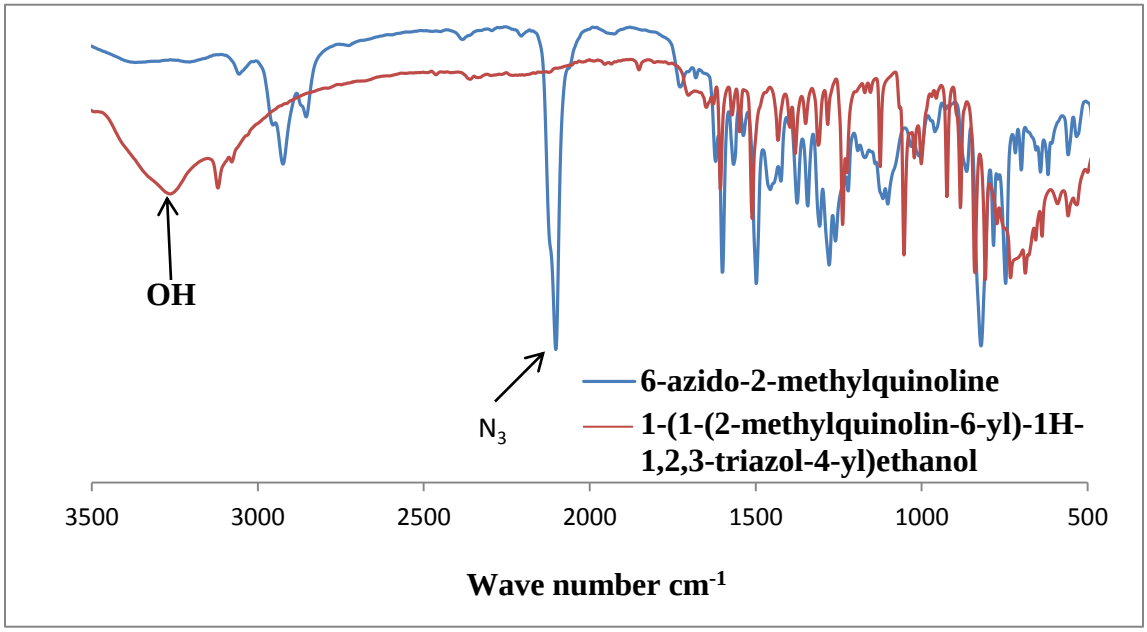

Figure 2.17: FT-IR spectrum of 1-(1-(2-methylquinolin-6-yl)-1H-1,2,3-triazol-4-yl)ethanol and 6-azido-2-methylquinoline

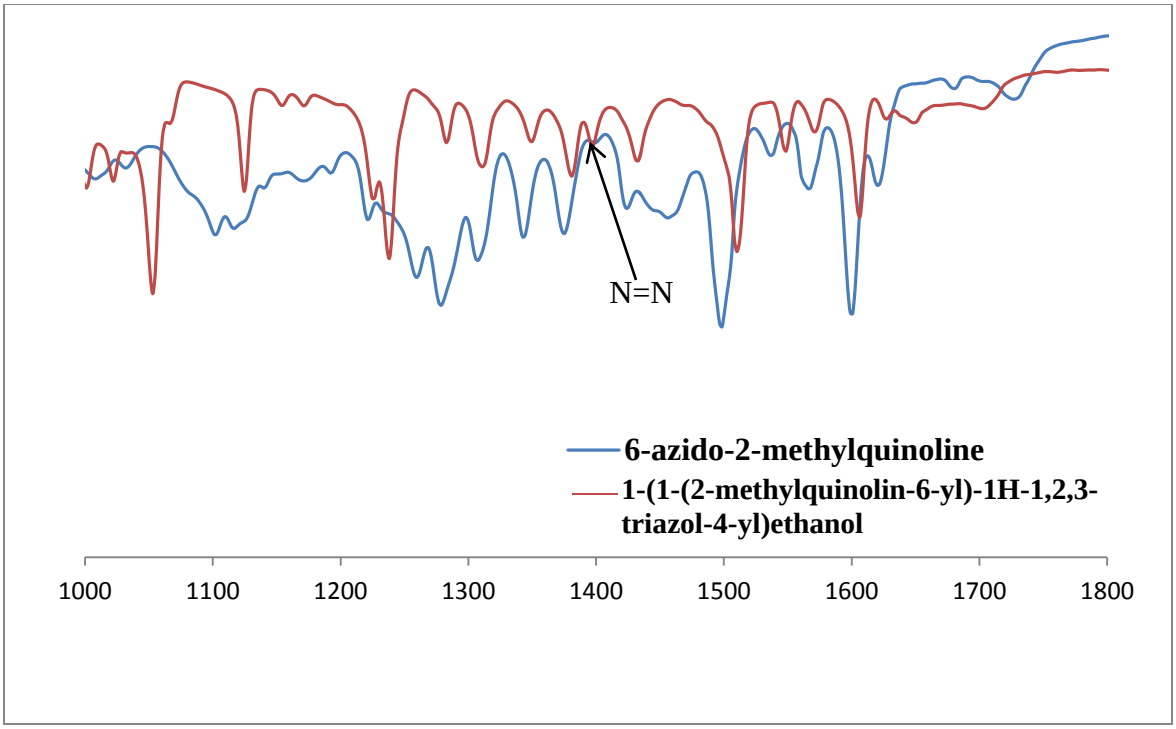

Figure 2.18: The expanded FT-IR spectrum of the 1-(1-(2-methylquinolin-6-yl)-1H-1,2,3-triazol-4-yl)ethanol and 6-azido-2-methylquinoline (**70**)

An X-ray single crystal structure was obtained for the alcohol (Figure **2.19)** showing the quinoline ring system with its nitrogen atom (N1), the triazole ring with its three nitrogens atoms (N2, N3, N4) and the alcohol functionality attached to C14. The crystal structure also showed that methyl and hydroxyl groups attached to the triazole ring lie in different geometrical planes intersecting the triazole-quinoline plane. The crystal structure differs from the preferred conformation as determined from molecular orbital calculations at the semi-empirical (PM3) level as shown in Figure **2.20**.

A similar result was obtained at the DFT level (B3LYP/6-31G*) (Figure **2.21)**. The hydroxyl group which was in a plane intersecting the triazole-quinoline plane in the crystal structure of the product was shown to be coplanar with triazole-quinoline ring system. The reason for this difference could be that the experimental results were obtained from solid state of the compound while the DFT calculation was obtained for the gaseous phase.

The solid state involves intermolecular interactions such as hydrogen bonding between molecules which can cause the crystal structure to differ from the theoretically computed structure where the molecule was treated as isolated.

Differences between the structures determined through computation at the DFT (B3LYP/6-31G*) and semi-empirical (PM3) levels is predictably, since the DFT approach offers greater precision.

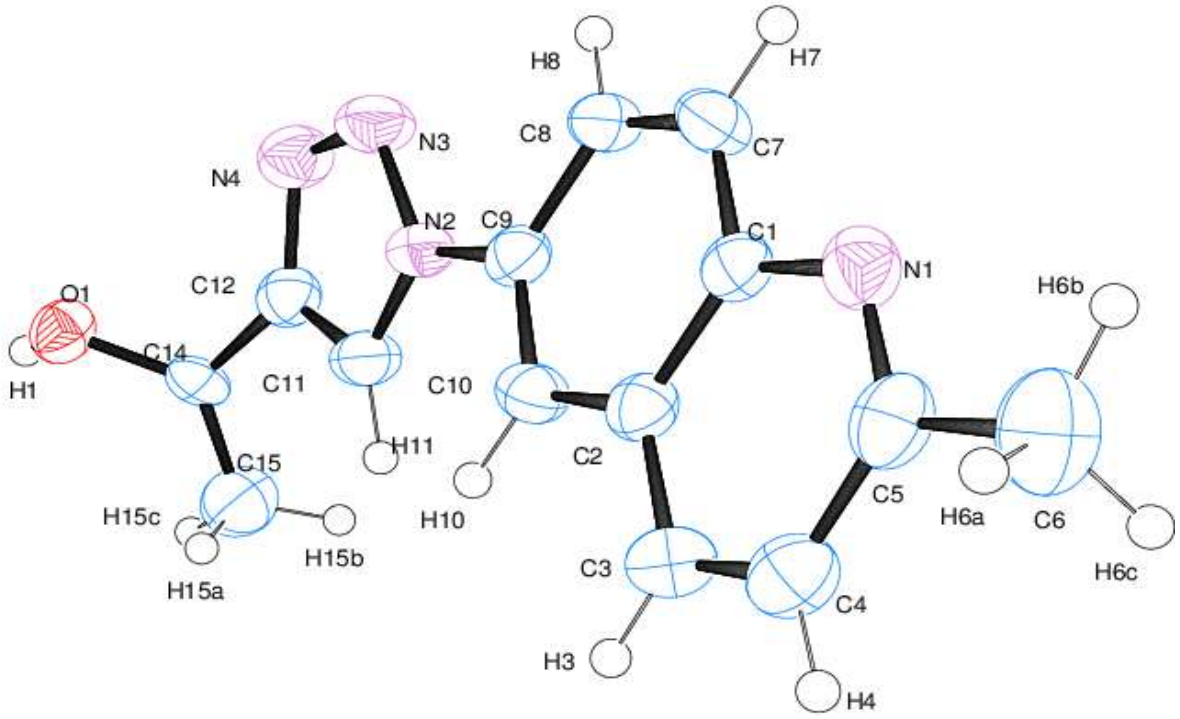

Figure 2.19: Single crystal X-ray structure of 1-(1-(2-methylquinolin-6-yl)-1H-1,2,3-triazol-4-yl)ethanol **(74)**

Figure 2.20: Computed structure of 1-(1-(2-methylquinolin-6-yl)-1H-1,2,3-triazol-4-yl)ethanol at the semi-empirical PM3 level

Figure 2.21: Computed structure of the 1-(1-(2-methylquinolin-6-yl)-1H-1,2,3-triazol-4-yl)ethanol at the DFT (B3LYP/6-31G*) level

The desired quinoline monomer was obtained by dehydrating the alcohol (**74**). This was successfully accomplished by refluxing in toluene in the presence of *p*-toluene sulfonic acid (PTSA) as the dehydrating agent (Scheme **2.9)**.

Initially this reaction was performed using a 1:10 ratio of PTSA to substrate. After work-up and purification by column chromatography, the pure product was obtained as a light yellow solid in 10% yield. The low yield was suspected to be due to the basic nitrogen atom on the quinoline ring scavenging the acid necessary to catalyse the dehydration.

Increasing the amount of PTSA to 1:5 (PTSA: substrate), the yield was improved to 20 %. When the amount of PTSA was further increased to 1:2 (PTSA: substrate) thin layer chromatography showed a complete reaction within 4 h. After work up and purification, a light yellow solid product was isolated in 50% yield.

The use of higher temperature was unsuccessful since thermal polymerization of the formed monomer (**64**) probably occurred.

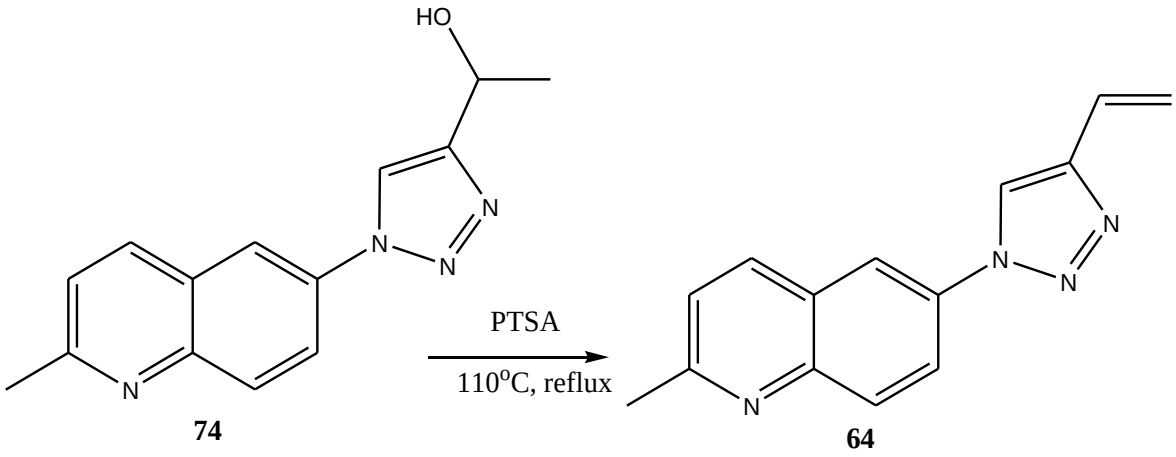

74 **64**

Scheme 2.9: Synthesis of 4-vinyl-1,2,3-triazole-quinoline (**64**)

The structure of the monomer (**64**) was confirmed by NMR and FT-IR spectroscopy. A ^{1}H-NMR spectrum (Figure **2. 22)** showed the disappearance of the broad signal at 2.55 ppm, the doublet at 1.71 ppm, and the quartet at 5.22 ppm previously assigned to the OH proton, H-4' and H-3', respectively, as well as the appearance of a pair of doublets integrating for two protons at 5.38 ppm and at 5.97 ppm, and a doublet of doublets integrating for one proton at 6.72 ppm. The pair of doublets was assigned to the two terminal geminal hydrogens H_a and H_b of the newly formed double bond, while the doublet of doublets signal was assigned to the proton attached to the sp^2 hybridized carbon adjacent to the triazole ring (3'-C).

The triazole ring proton signal was observed at 8.15 ppm while the quinoline ring proton signals appeared in the range 7.33-8.15 ppm and the methyl protons at 2.7 ppm.

The structure of the vinyl quinoline monomer (**64**) was further confirmed by ^{13}C-NMR and DEPT (135)-NMR as shown in Figures **2.23** and **2.24**, respectively. The ^{13}C-NMR spectrum showed fourteen carbon signals reflecting the number of carbon atoms in the molecule. The down-field shift of 3'-C and 4'-C upon dehydration to the alkene confirmed the success of the reaction.

The DEPT (135)-NMR spectrum (Figure **2.24)** showed one methylene group and seven methine and one methyl carbons in the molecule.

The coupling patterns of the vinyl quinoline monomer were confirmed by a H,H-COSY NMR spectrum which revealed the spin system due to the three vinylic protons, as well as the four quinoline ring protons as shown in the (Figure **2.25**)**.** The two geminal 4'-hydrogens (H_a, H_b) spin system is illustrated by the red rectangle. Both the vinylic methylene protons couple with H-3' and *vice versa* as illustrated by the blue rectangle for the Ha and H-3' coupling, and green rectangle for the H_b and H-3' coupling.

These interactions resulted in two doublets at 5.38 and 5.97 ppm as well as a doublet of doublets at 6.72 ppm. Two reciprocal nuclear interactions of the quinoline ring protons (3-H and 4-H, 7-H and 8-H) were illustrated by rose and black rectangles, respectively, and resulted in four doublets at 7.33, 7.99, 8.09, 8.12 ppm. These observations matched the expected coupling patterns of this structure.

The success of the dehydration was further confirmed by an FT-IR spectrum (Figure **2.26)** which showed the disappearance of the broad peak at 3328 cm^{-1} previously assigned to hydroxyl group in the monomer precursor.

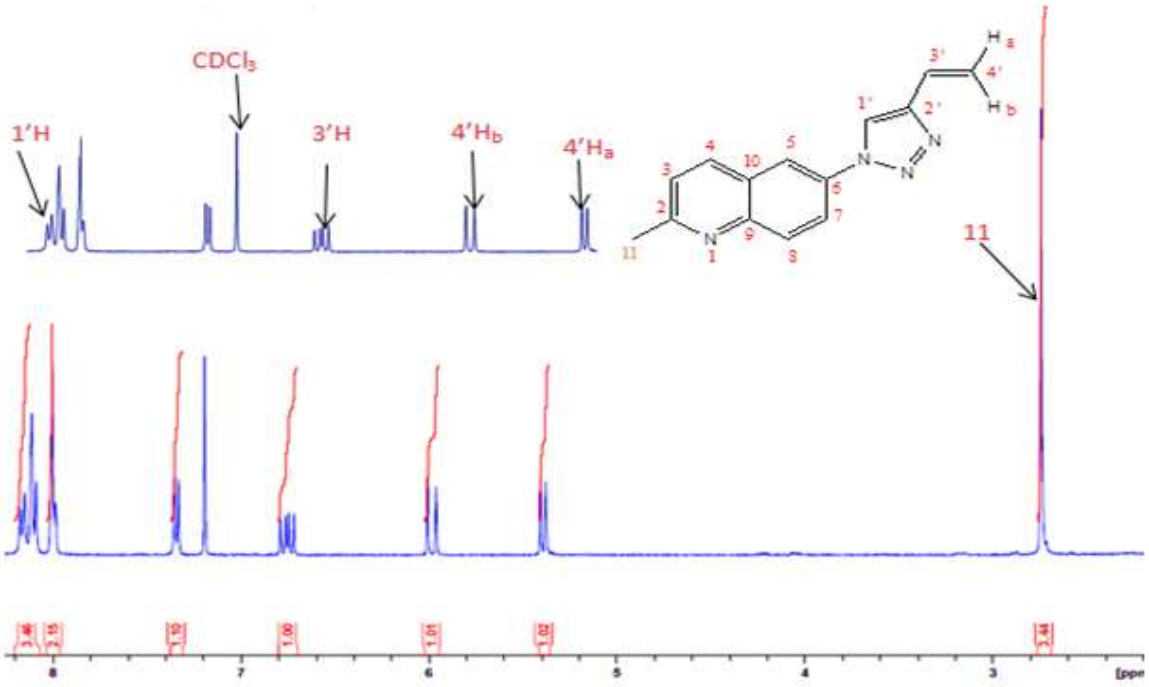

Figure 2.22: ^{1}H-NMR spectrum of 2-methyl-6-(4-vinyl-1H-1,2,3-triazol-1-yl)quinoline (**64**) in $CDCl_3$

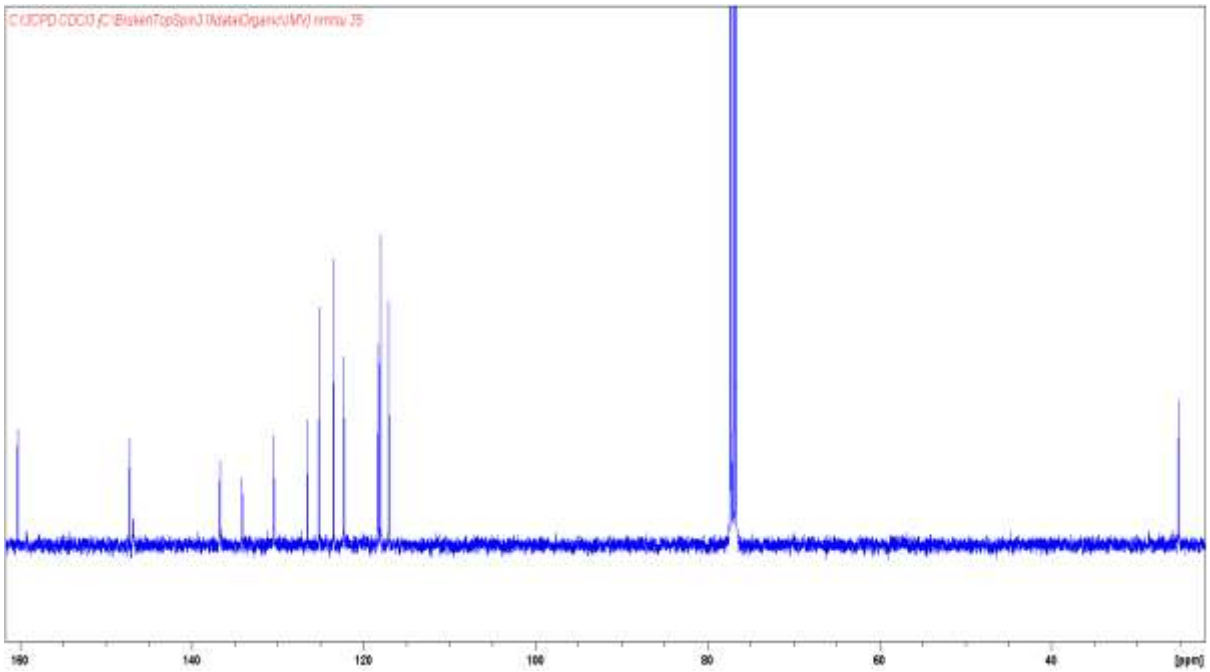

Figure 2.23: ^{13}C-NMR spectrum of 2-methyl-6-(4-vinyl-1H-1,2,3-triazol-1-yl)quinoline (**64**) in $CDCl_3$

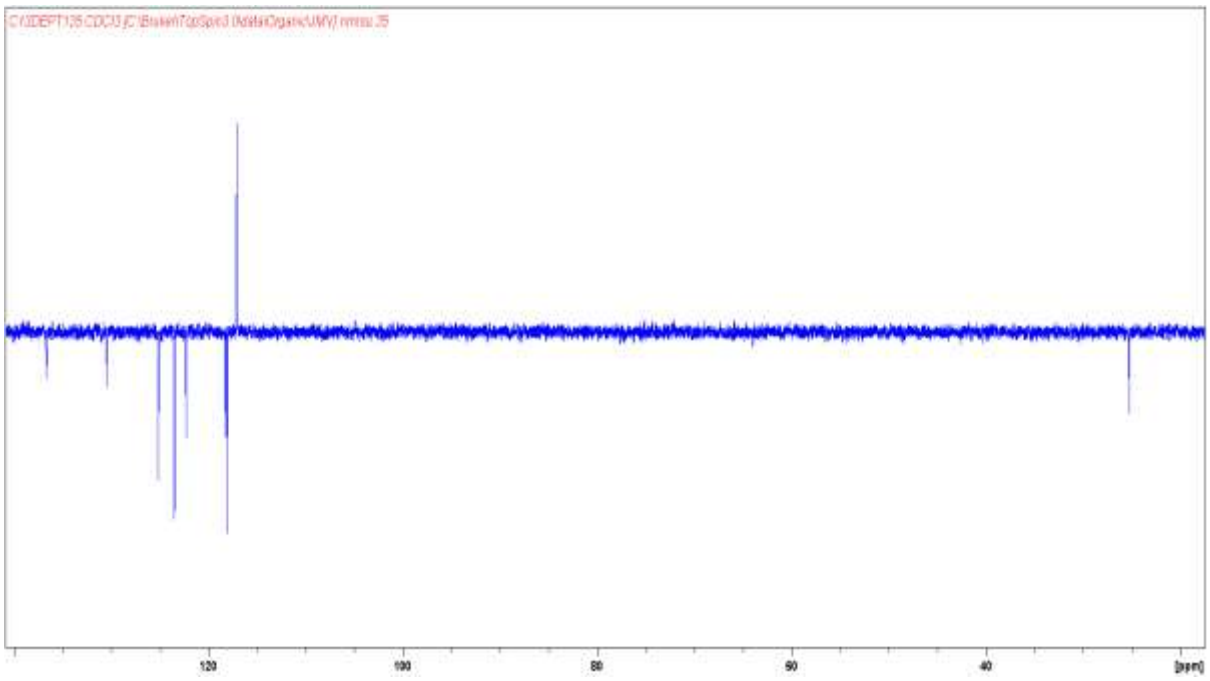

Figure 2.24: DEPT(135)-NMR spectrum 2-methyl-6-(4-vinyl-1H-1,2,3-triazol-1-yl)quinoline (**64**) in $CDCl_3$

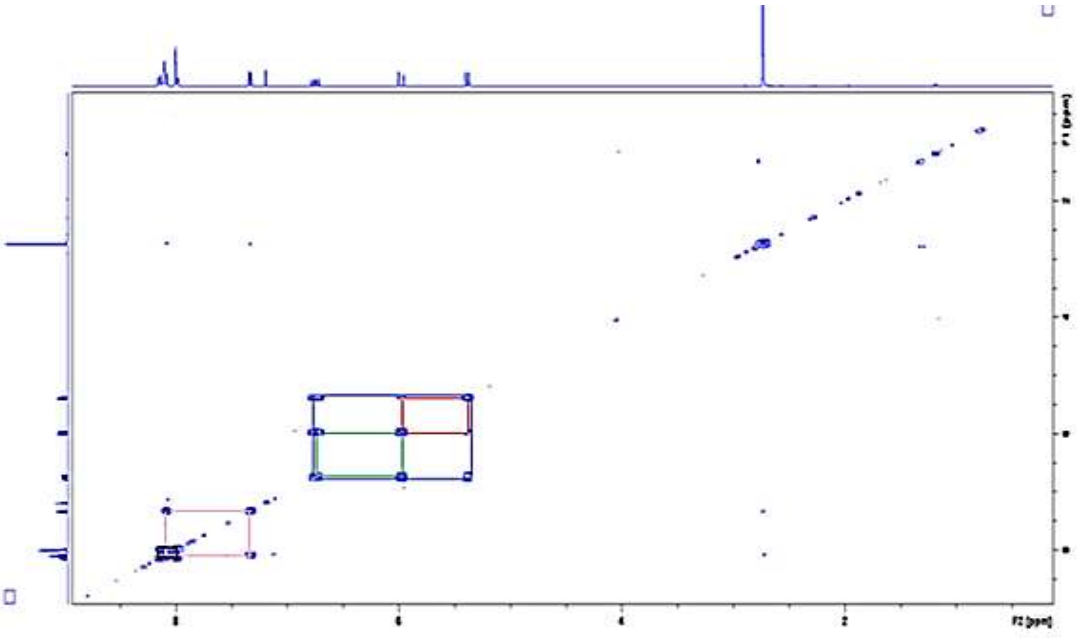

Figure 2.25: H,H-COSY NMR spectrum of 2-methyl-6-(4-vinyl-1H-1,2,3-triazol-1-yl)quinoline (**64**) in $CDCl_3$

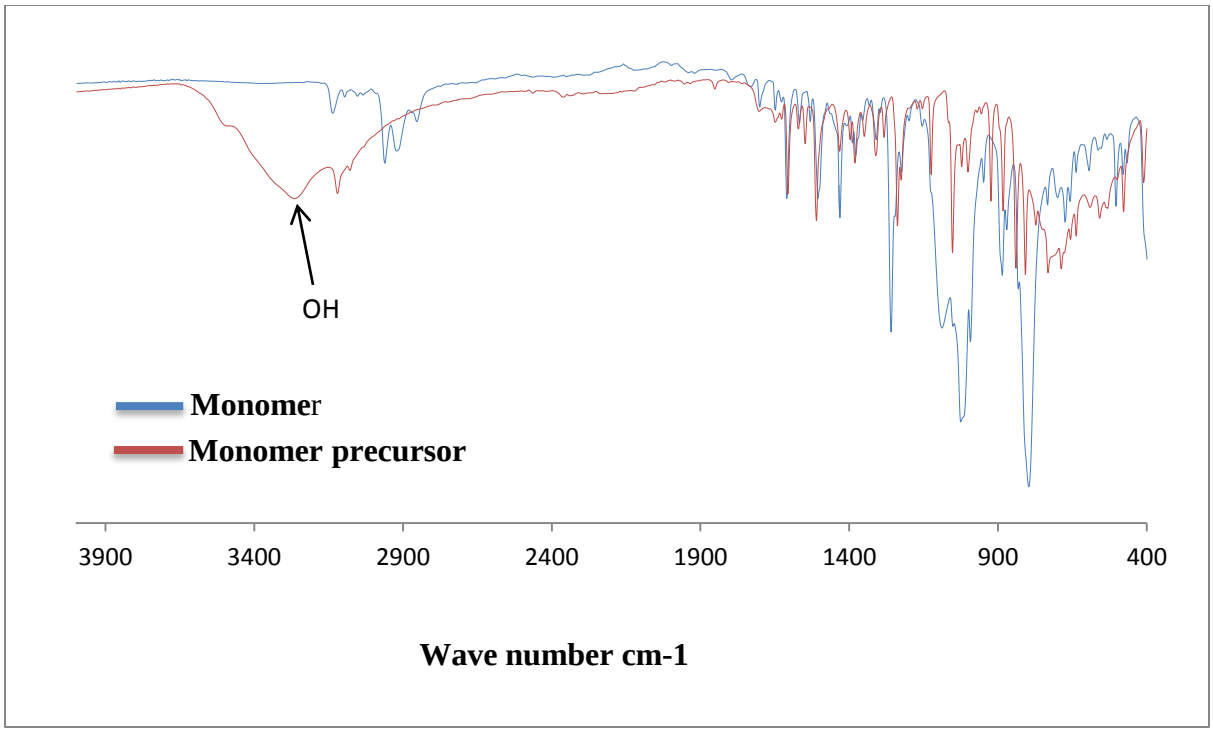

Figure 2.26: IR spectrum of monomer precursor (**74**) and monomer (**64**)

Repeated recrystallization of the monomer unfortunately failed to give crystals suitable for X-ray crystallography. A geometrically optimized structure for the monomer was determined through computation at the DFT level (B3LYP/6-31G*) as shown in the Figure **2.27** below. The computed structure showed all the constituents of the monomer lying in the same plane except for the protons of methyl group attached to the quinoline ring. This would be expected in such an extensively conjugated system.

Figure 2.27: Computed structure of the 2-methyl-6-(4-vinyl-1H-1,2,3-triazol-1-yl)quinoline (**64**) at the DFT (B3LYP/6-31G*) level

Chapter 3

Conventional free radical vinyl polymerization of 2-methyl-6-(4-vinyl-1H-1,2,3-triazol-1-yl)quinoline (64)

In order to allow chain-building to begin during polymerization, an initiator such as heat or a suitable chemical species depending on the type of the active functionality in the repeating unity is required. Due to the relatively non-specific nature of intermolecular free radical reactions, free radical polymerization has become a popular technique for a wide range of vinyl monomers. Radical polymerization can also be applied in the copolymerization reactions in which the structures of the polymers depend on monomer reactivity ratios or polarity. Monomers with the same bond polarities result in random polymers while monomers with different polarities lead to alternating polymers.

Due to its poor molecular weight control, and molecular weight distribution as well as difficulty in the preparation of polymers with predetermined functionality, free radical polymerization has shifted to a new approach known as controlled free radical polymerization. Among recently developed controlled free radical polymerization techniques, RAFT (Reversible Addition Fragmentation chain Transfer) polymerization has proven to be versatile. It offers a facile method for the synthesis of polymers with predetermined molecular weight, and low molecular weight distribution in both homogeneous and heterogeneous environments.

3.1. Conventional free radical vinyl polymerization of 2-methyl-6-(4-vinyl-1H-1,2,3-triazol-1-yl)quinoline (64)

In order to confirm that the synthesized monomer was reactive, uncontrolled free radical polymerization was initially carried out. The initiator used for the polymerization of our novel quinoline-based monomer (**64**) was azobisisobutyronitrille (AIBN) owing to its ready solubility in organic solvents, relatively low decomposition temperature, and its half-life at the optimum

temperature. The latter extends the duration of radical production and consequently the polymerization is kept active for a longer period.

This process was accomplished at 70 ^{o}C in dimethylformamide (DMF) over a period of 48 hours as shown in Scheme **3.1**. The system was degassed using a four-cycle freeze-thaw method to remove dissolved oxygen gas which traps the initiating radical, and hence significantly affects the rate of propagation. The polymers were precipitated in methanol and purified by washing with hexane.

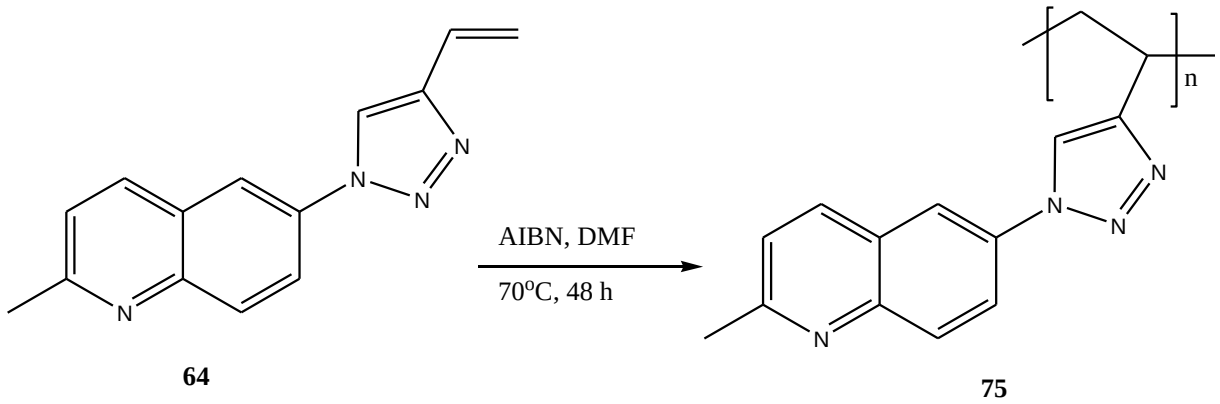

64 **75**

Scheme 3.1: Homopolymerization reaction of 2-methyl-6-(4-vinyl-1H-1,2,3-triazol-1-yl)quinoline (**64**)

The same procedure and technique were applied in the polymerization of styrene monomer to form polystyrene (Scheme **3.2**) which was synthesized as a reference polymer for photophysical studies on triazole-quinoline polymers.

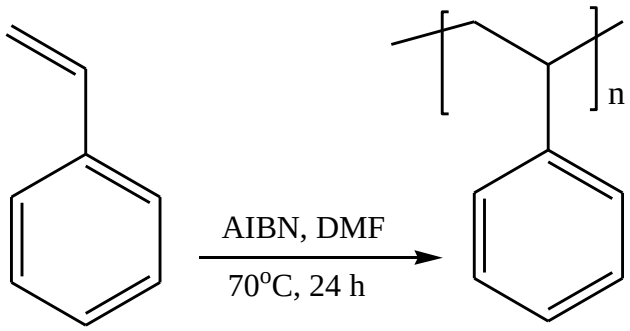

76 **77**

Scheme 3.2: Polymerization of styrene monomer

Polystyrene was characterized by ^{1}H-NMR and FT-IR spectroscopy. The broad signal between 6.4 ppm and 7.3 ppm in the ^{1}H NMR spectrum (Figure **3.1**) and the disappearance of the vinyl proton signals in the range 5-6.5 ppm confirmed the success of the polymerization reaction. The broad peaks were assigned to benzylic proton signals which overlap owing to the slightly different chemical environments they experience in the polymer.

The FT-IR spectrum (Figure **3.2**) of the polymer showed the disappearance of the vinyl protons stretch frequency of the monomer at 3089 cm^{-1}, and the appearance of methylene and methine stretch frequencies at 2935 cm^{-1} and 2890 cm^{-1}, as a result of carbon-carbon double bond destruction during polymer formation.

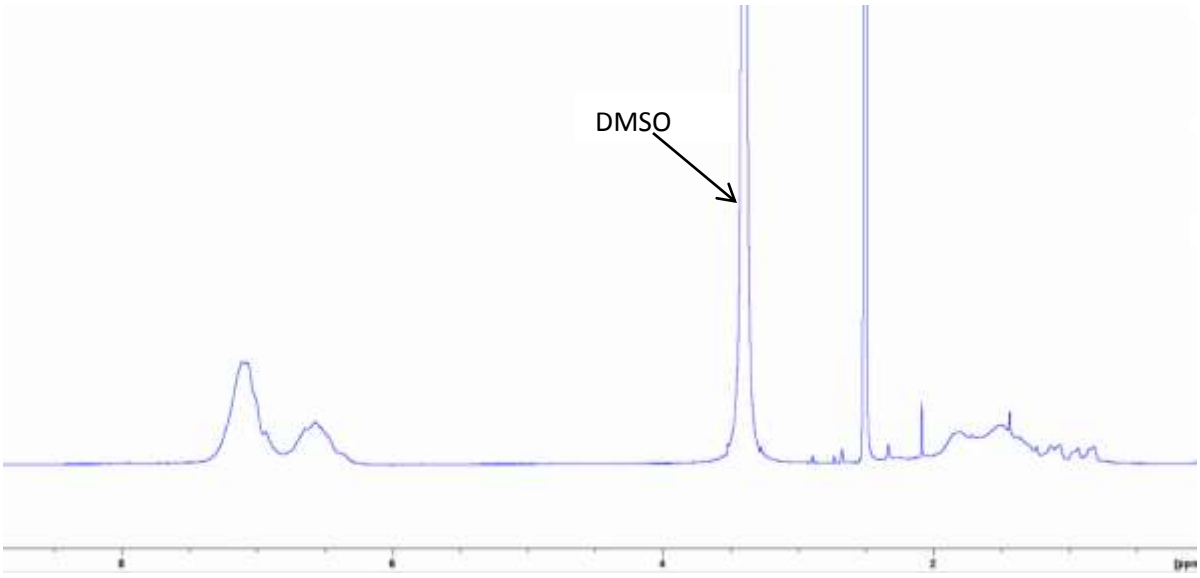

Figure 3.1: ^{1}H-NMR spectrum of polystyrene in DMSO

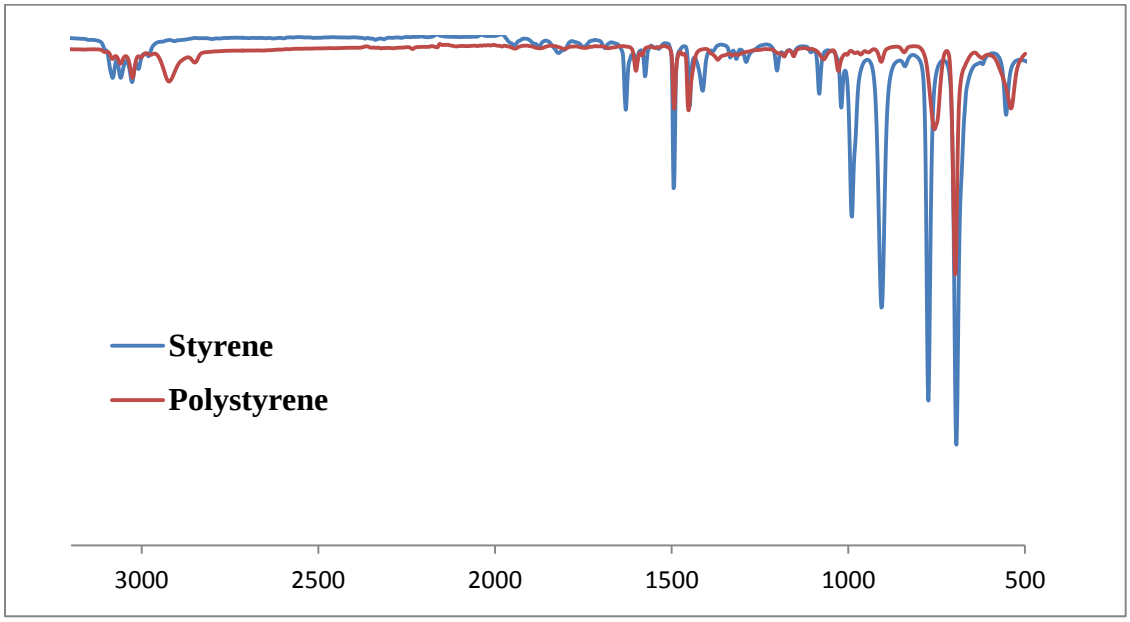

Figure 3.2: FT-IR spectrum of styrene and polystyrene

3.2. Copolymerization of 2-methyl-6-(4-vinyl-1H-1,2,3-triazol-1-yl)quinoline (64) with styrene

The quinoline-containing materials are known to have significant electron mobility, excellent thermal and oxidative stabilities, and significant photoluminescence efficiencies.

Various chemical processes or reactions such as polymerization can be utilized to incorporate these important properties into materials which are inert towards electron or energy transfer. In our studies the fluorescence properties of polystyrene were improved by the incorporation of quinoline units *via* a copolymerization process. This was achieved through the copolymerization of 2-methyl-6-(4-vinyl-1H-1,2,3-triazol-1-yl)quinoline and styrene in a 50:50 mole feeding ratio (Scheme **3.3**). The reaction was accomplished in DMF in the presence of AIBN as initiator. The system containing both the monomer and the initiator was degassed as described for the previous polymerization, and then heated for 48 h at 70^{o}C. The copolymer was precipitated with methanol and then washed with hexane to yield the desired copolymer as a brown solid.

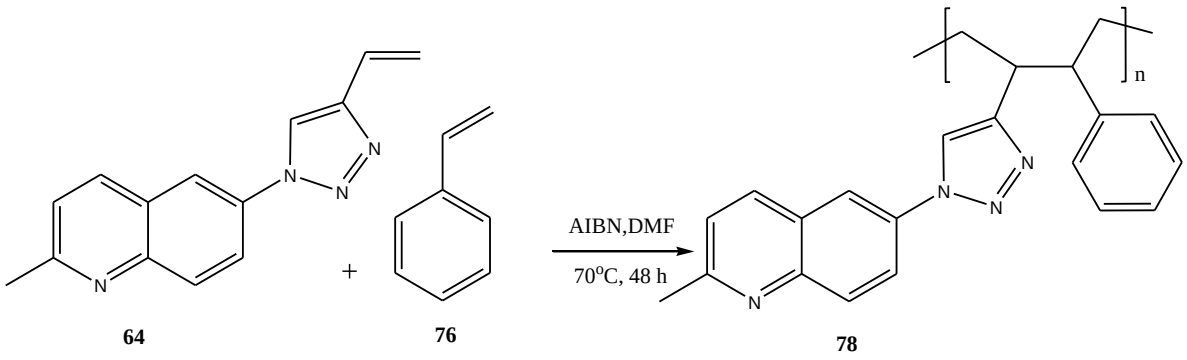

64 **76** **78**

Scheme 3.3: Free radical copolymerization of quinoline-based monomer **64** with styrene monomer

The copolymer was characterized by ^{1}H-NMR and FT-IR spectroscopy. The partial ^{1}H-NMR spectrum shown in Figure **3.4**, confirmed the successiful incorporation of both the quinoline and styrene moieties in the polymer structure.

The aromatic quinoline and triazole protons signals in the polymer were observed as broad signals in the range 7.4-8.5 ppm while the aromatic proton signals from styrene was observed in the range 6.3-7.4 ppm.

The above results were further confirmed by the FT-IR spectrum (Figure **3.5**) which showed the disapearance of the stretch frequency at 3147 cm^{-1} assigned to the vinyl C-H protons of the quinoline-based monomer.

The expanded FT-IR spectrum (Figure **3.6**) also comfirmed the success of the copolymerization reaction of the quinoline-based monomer and styrene. The C=N and aromatic C-N bond stretchings of quinoline ring system were observed at 1577 cm^{-1} and 1270 cm^{-1}, while the N=N and C-N group of the triazole ring were observed at 1438 $cm^{-1}$and 1514 cm^{-1} respectively. Comparison of the FT-IR spectrum of the copolymer with that of the polystyrene also comfirmed the presence of both monomers by matching all the stretch frequncies in the polystyrene FT-IR spectrum.

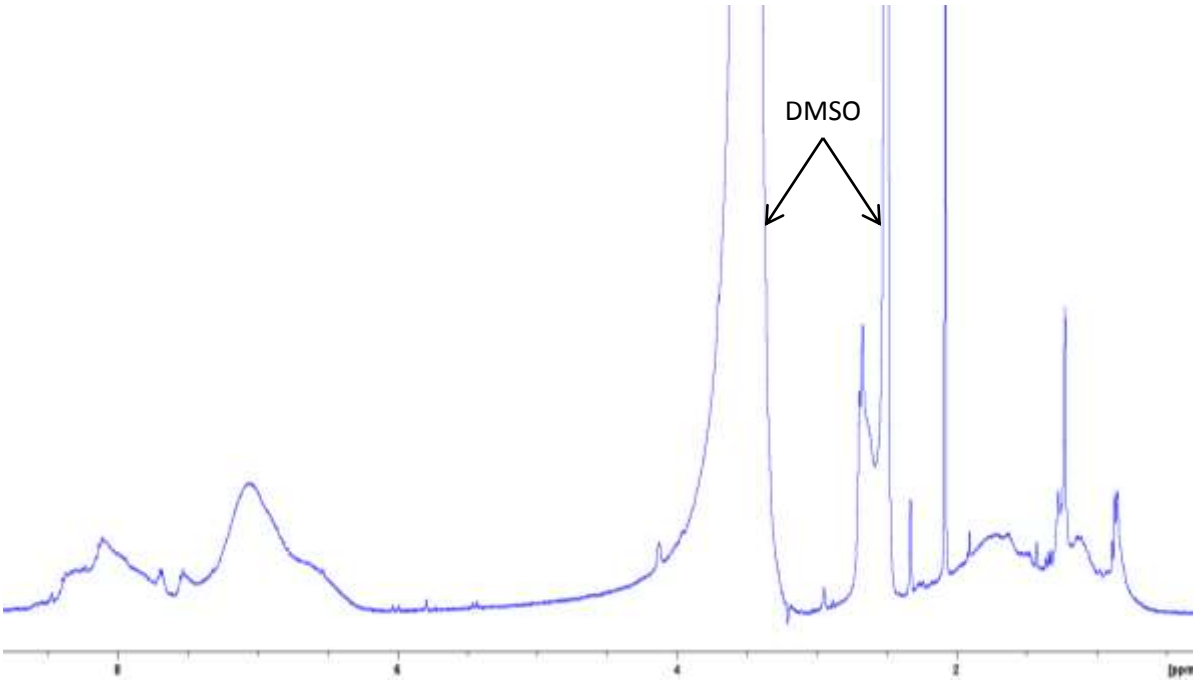

Figure 3.3: ^{1}HNMR spectrum of copolymer (**78**) in DMSO

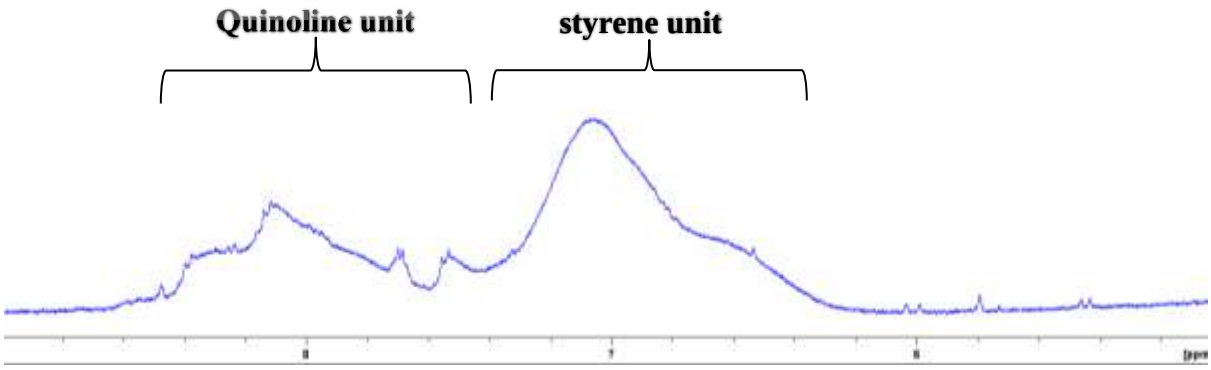

Figure 3.4: ^{1}H-NMR spectrum of copolymer (**78**) in DMSO

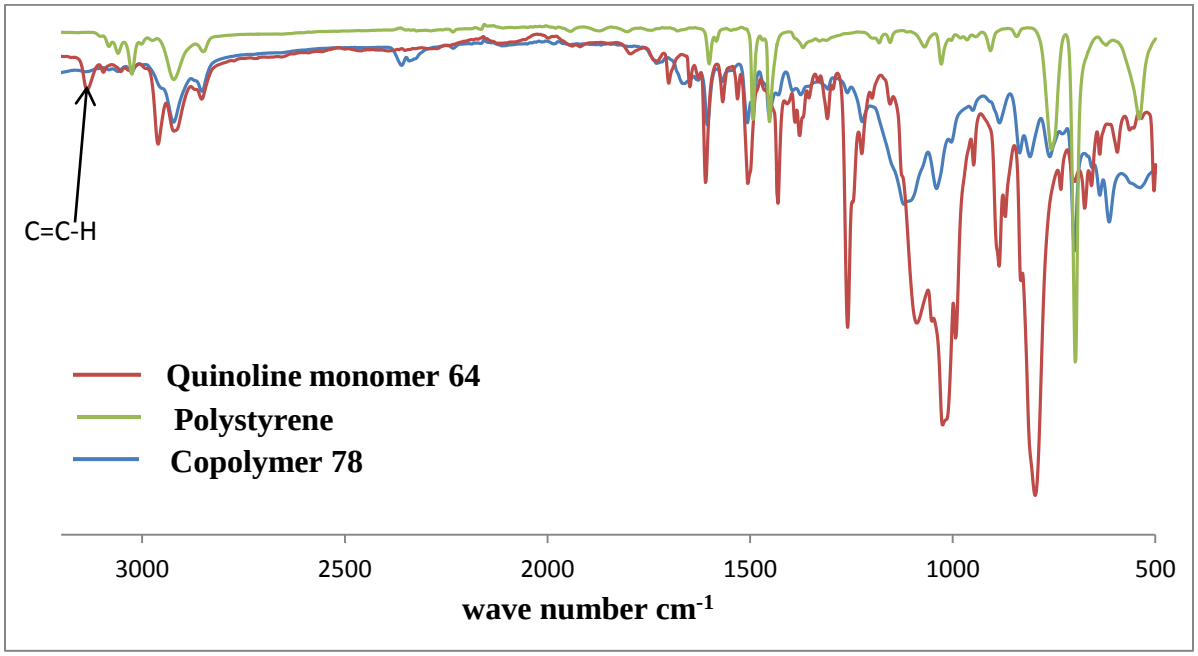

Figure 3.5: FT-IR spectrum of copolymer (**78**), polystyrene and quinoline-based monomer (**64**)

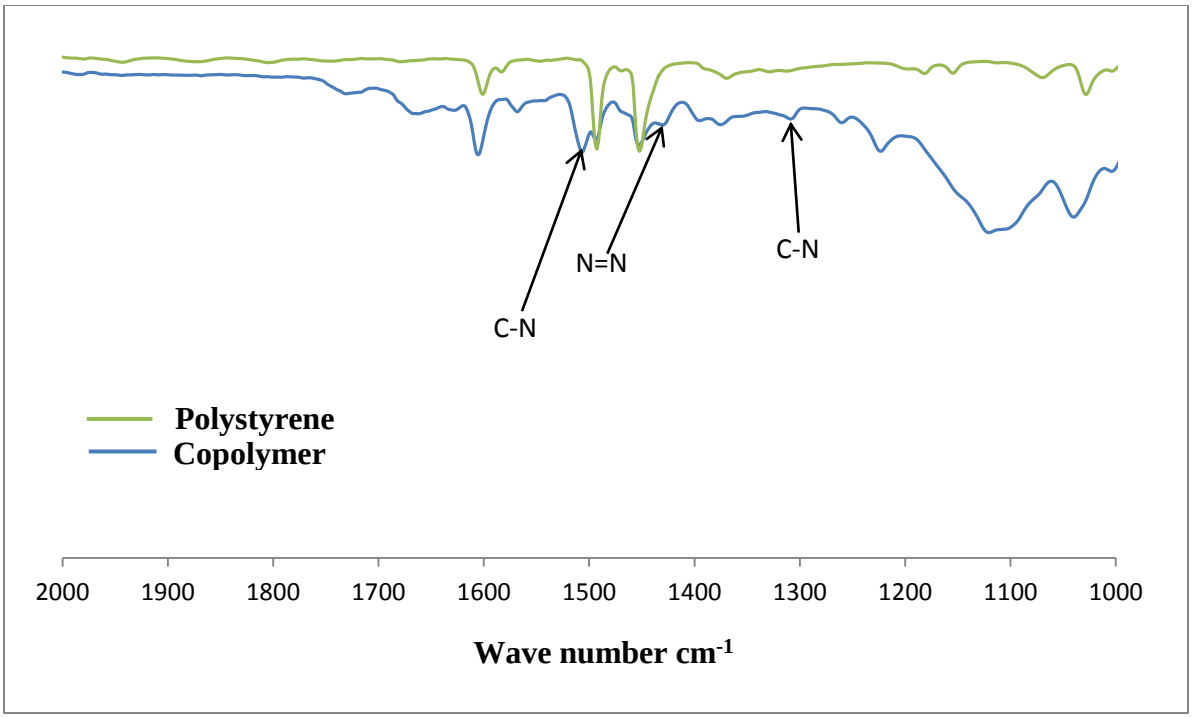

Figure 3.6: Expanded FT-IR spectrum of copolymer (**78**) and polystyrene (**76**)

Though the polymer structure characterization confirmed the success of this synthesis, the determination of the number of quinoline-based monomer units in the copolymer was hampered as its ^{1}H-NMR spectrum showed overlapping signals.

3.3. Controlled Free radical vinyl polymerization of 2-methyl-6-(4-vinyl-1H-1,2,3-triazol-1-yl)quinoline (64)

This polymerization technique relies on either reversible deactivation of the growing radical chain or a degenerative transfer process. It requires pure reaction conditions so that no premature chain termination can occur. It stops when all the monomers have been consumed or intentionally terminated. It can also be restarted by the addition of more monomers.

This type of polymerization offers molecular weight control for a wide range of monomers, using different chemical species and chemical environments.

In the first part of our report, different types of controlled free radical polymerization were discussed and among them only RAFT polymerization has been applied to our monomer along with 2-(2-cyanopropyl)-dithiobenzoate (CPDB) as the RAFT agent.

3.3.1 Synthesis of 2-(2-cyanopropyl)-dithiobenzoate (CPDB)

The success of the RAFT polymerization process is highly amplified by the choice of the appropriate RAFT agent, which is usually a thiocarbonylthio compound. As dithioester chain transfer agents have proven to be efficient for this purpose, they have been widely applied to the polymerization of different types of vinyl monomers.

In our study the dithioester used for RAFT polymerization along with AIBN was 2-(2-cyanopropyl)-dithiobenzoate (CPDB) (**82**). The latter was successfully synthesized in two steps from bromobenzene.

The first step was carried out using a well-documented procedure which involved a Grignard reaction of phenyl magnesium bromide with CS_2 as shown in Scheme **3.4**.[157] The resulting dithiobenzoic acid salt was then treated with *p*-tosyl chloride in THF to produce di-(thiobenzoyl) disulfide as red-purple crystals.

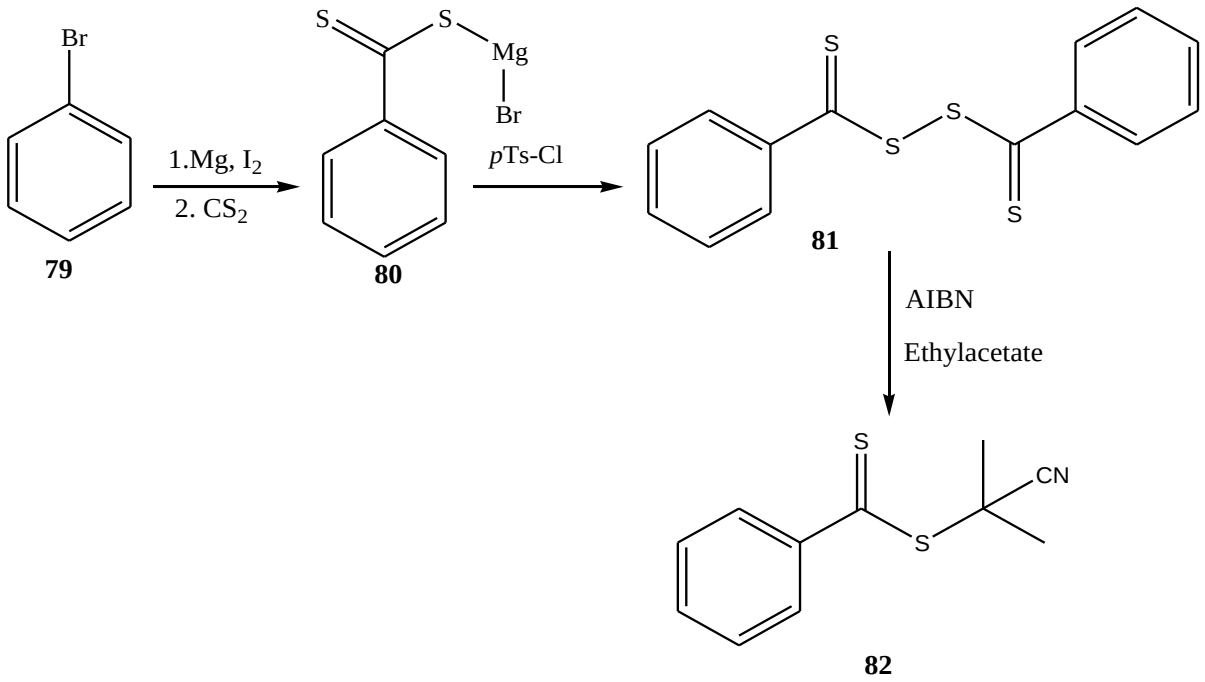

Scheme 3.4: Synthesis of 2-(2-cyanopropyl)-dithiobenzoate (CPDB)

In the second step the di-(thiobenzoyl) disulfide obtained in the previous step was heated to reflux for 18 h in the presence of azobisisobutyronitrile (AIBN) in ethyl acetate. After solvent removal under reduced pressure the crude product was purified by column chromatography to afford the pure product (**82**) as a purple solid in 80% yield.

The structure of 2-(2-cyanopropyl)-dithiobenzoate (CPDB) (**82**) was confirmed with both ^{1}H-NMR and ^{13}C-NMR spectroscopy. The ^{1}H-NMR spectrum (Figure **3.7**) showed five aromatic protons which were divided in three sets due to the molecular symmetry.

Triplets integrating for two and one proton, respectively, at 7.3 ppm and 7.48 ppm were assigned to the *meta*- and *para*-protons of the benzene ring while the *ortho* protons were assigned to the doublet at 7.87 ppm. The six methyl protons were assigned to the singlet at 1.85 ppm.

The product structure was further confirmed by ^{13}C-NMR (Figure **3.8**) which showed the methyl carbons (C-7,7') at 26.47 ppm, C-6 at 41.76 ppm and the cyanide carbon at 119.97 ppm. The aromatic carbon signals were observed in the range 120-135 ppm.

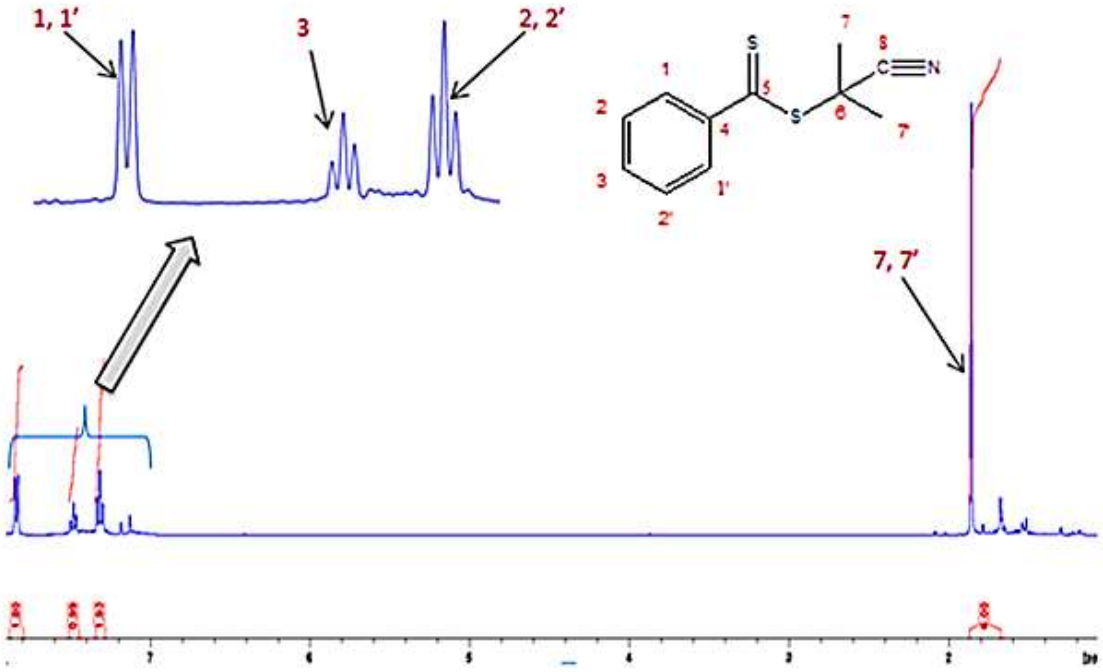

Figure 3.7: 1H-NMR spectrum of CPDB (**82**) in $CDCl_3$

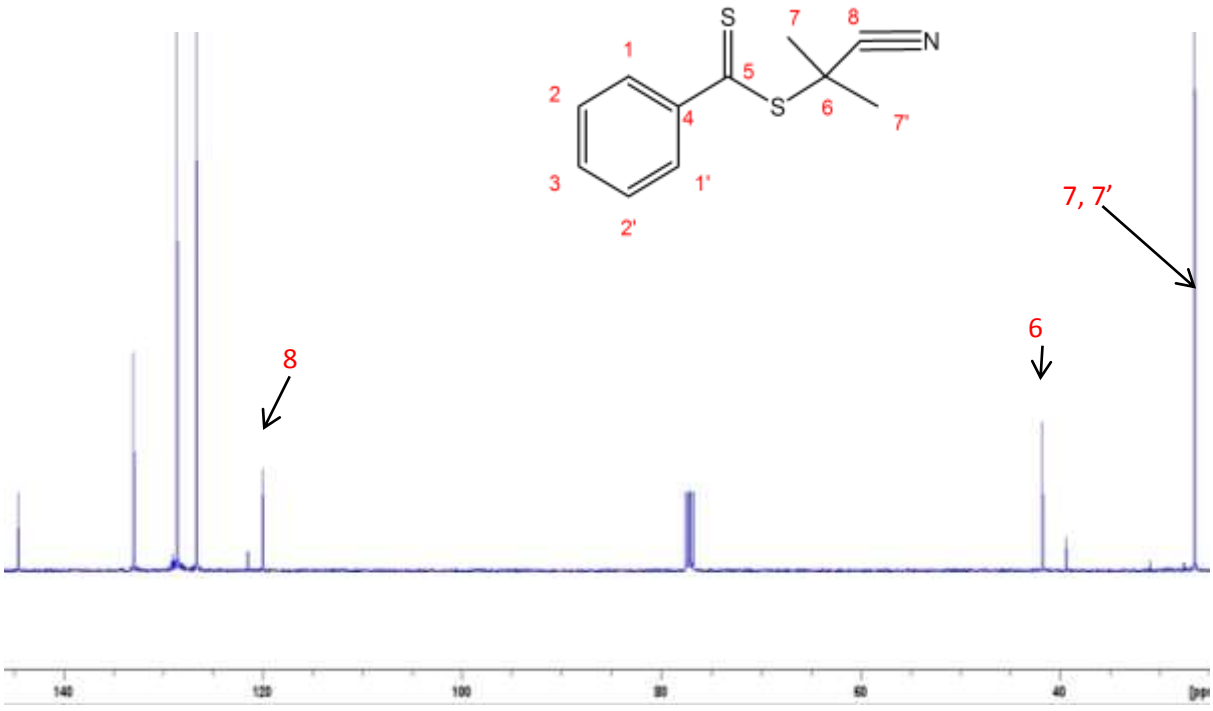

Figure 3.8: ^{13}C-NMR spectrum of CPDB in $CDCl_3$

3.3.2. RAFT polymerization

For our system RAFT polymerization was accomplished at 70 ^{o}C in DMF in the presence of the azobisisobutyronitrile (AIBN) (Scheme **3.5**). In order to avoid retardation of the polymerization process, the system was degassed by the freeze-thaw method which was repeated four times to remove all oxygen. The latter can trap the active radicals at the early stage of the polymerization. This polymerization reaction was completed within 48 h.

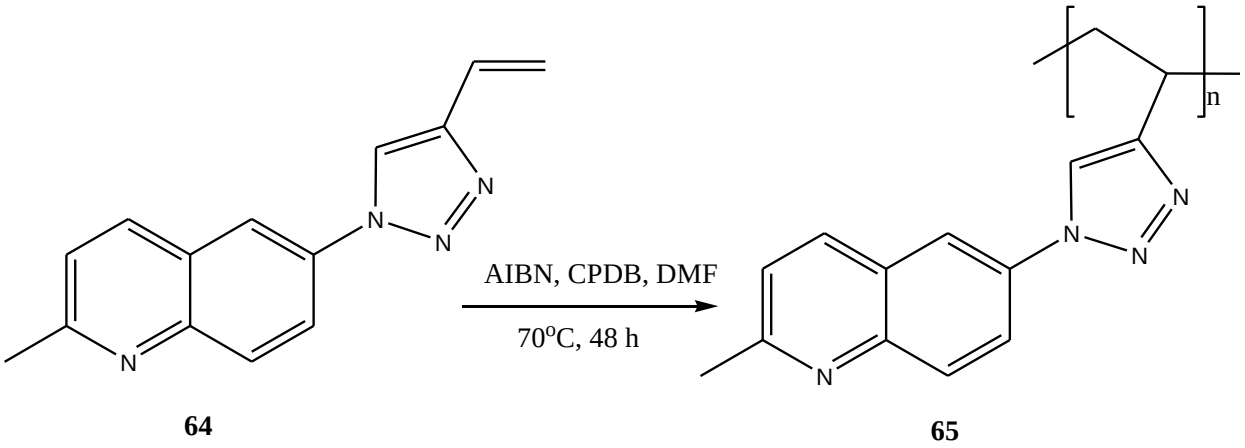

64 **65**

Scheme 3.5: Synthesis of the RAFT polymer (**65**)

The targeted molecular weights of the quinoline-based polymers were 5000 g mol^{-1} and 10000 g mol^{-1}. The later allowed the calculation of the theoretical amount of the monomer required for each reaction run using the formula shown below when the efficiency of the RAFT agent is assumed to be 100%.

$$M_n = Conv.(\%) + \left(\frac{[M]_0}{[CTA]}\right) M_m + M_{CTA}$$

After precipitation in methanol and toluene, and purification by washing with hexane, the resulting polymers were characterized by ^{1}H-NMR spectroscopy (Figure **3.9**).

The broad signals observed in the range 6.8-8.5 ppm were assigned to the overlapping proton signals of the quinoline, triazole and CPDB units.

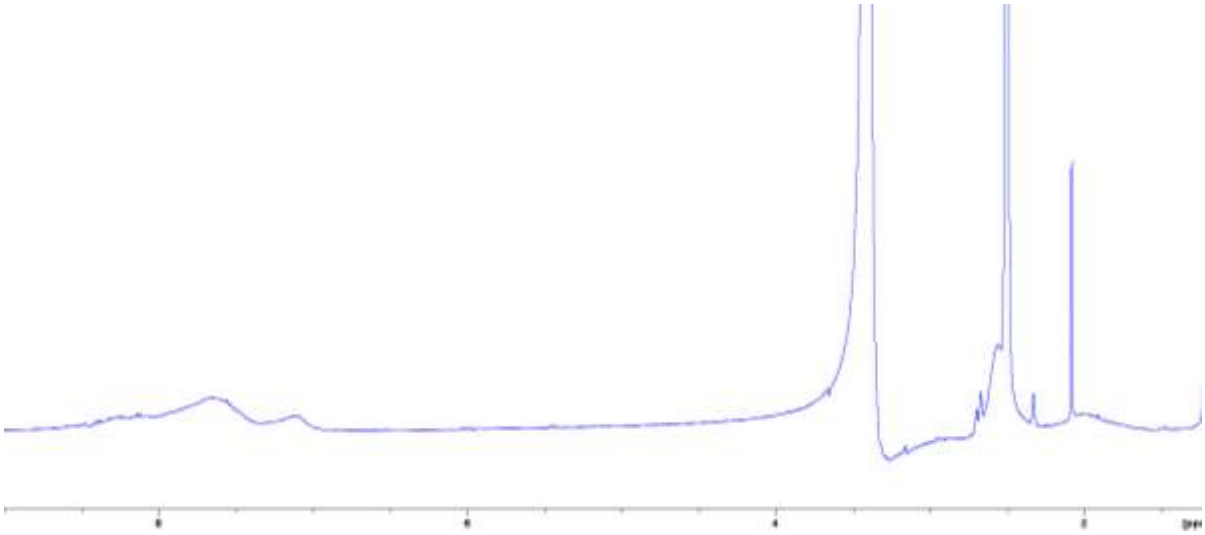

Figure 3.9: ^{1}H-NMR spectrum of RAFT polymer (**65**) in DMSO

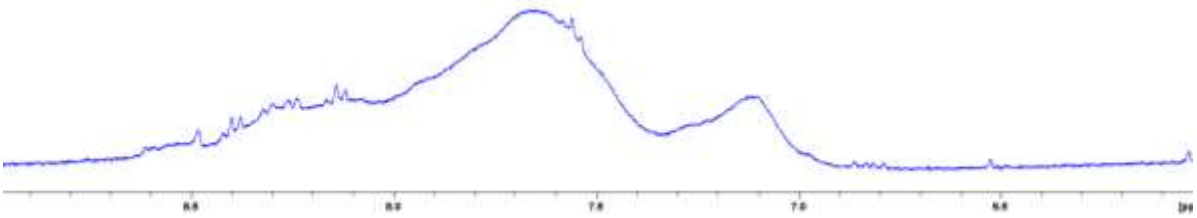

Figure 3.10: Partial ^{1}H-NMR spectrum of RAFT polymer (**65**) in DMSO

The success of the RAFT polymerization was also illustrated by the FT-IR spectrum of the polymer as compared with that of the starting monomer (Figure **3.11**).

The FT-IR spectrum of the polymer showed the presence of the functional groups from CPDP (**81**) such as the C-N at 2391 and C=S at 1130 cm^{-1} as shown in the expanded FT-IR spectrum (Figure **3.12).**

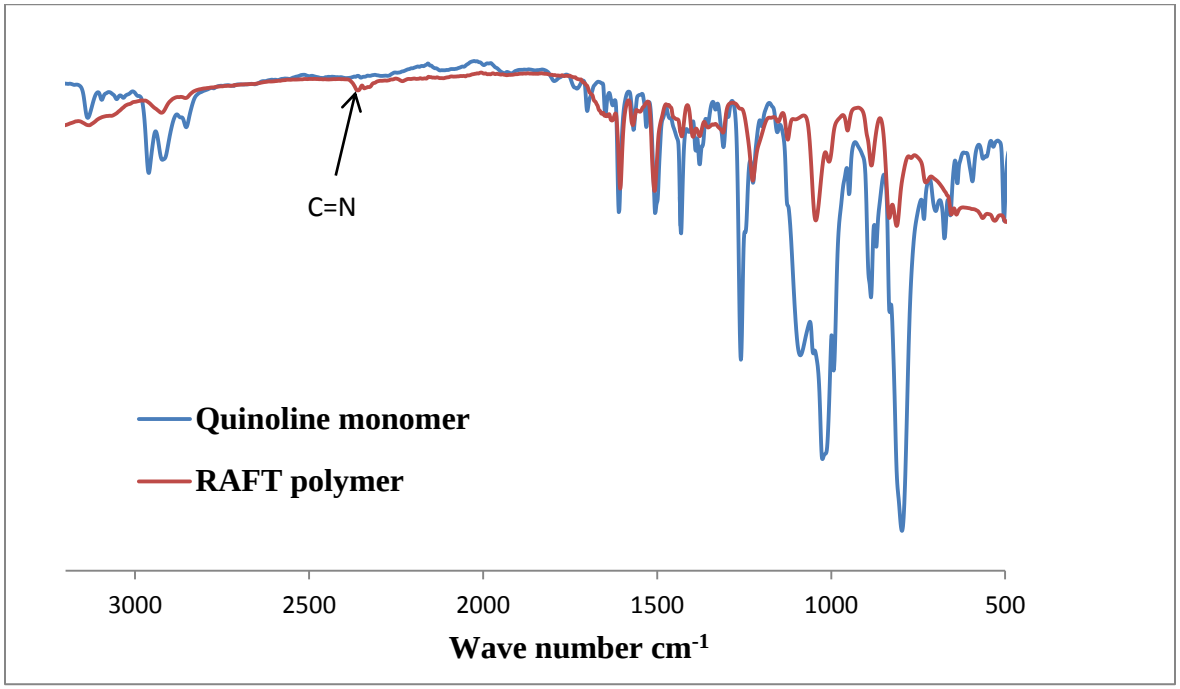

Figure 3.11: FT-IR spectrum of triazole-quinoline based monomer (**64**) and RAFT polymer (**65**)

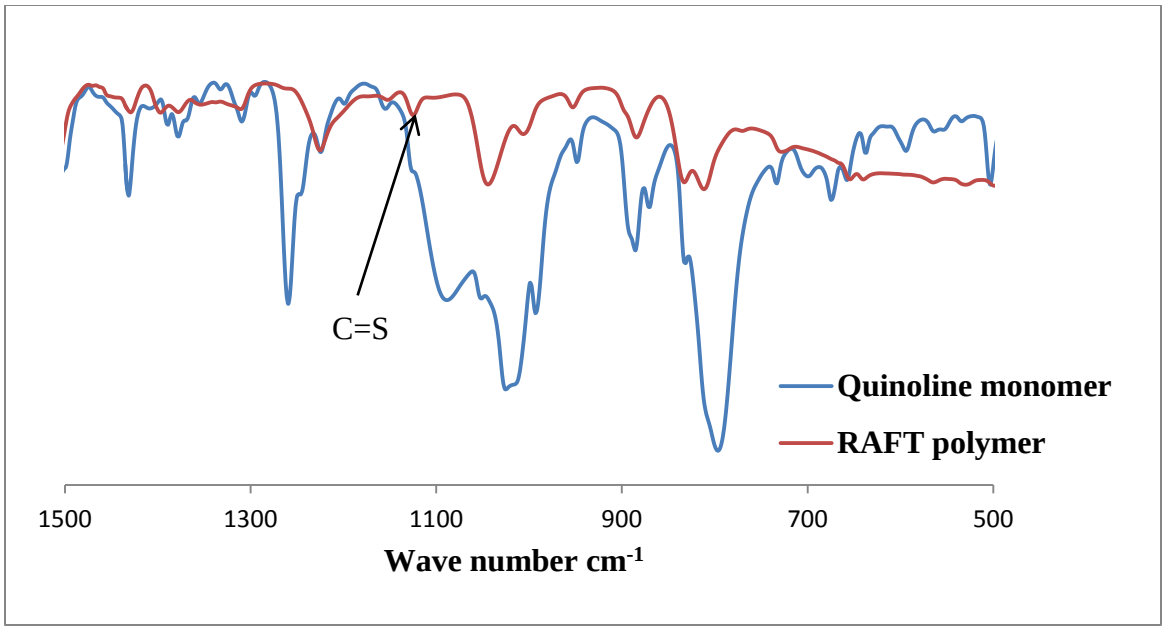

Figure 3.12: Expanded FT-IR spectrum of quinoline-based monomer (**64**) and RAFT polymer (**82**)

3.3.3. Gel permission chromatography (GPC) analysis of the polymers

In order to know the number average molecular mass (M_n), weight average molecular mass (M_w) and polydispersity indexes (PDI) of synthesized polymer Gel Permission Chromatography (GPC) was performed. The later were investigated at 40^0C using DMA as eluent and the results are summarized in table **3.1** below. The instrument was calibrated with linear PMMA standards and the resulting GPC chromatograms at a concentration of 1.0 x 10^{-4} molL^{-1} are shown in Figures **3.13**, **3.14** and **3.15** respectively.

POLYMER	M_n **(Daltons)**	M_w **(Daltons)**	**PDI** (M_w / M_n)
Styrene	3,445	5,426	1.575062
Copolymer	1,701	2,517	1.475255
RAFT polymer	7,647	9,787	1.279806

Table 3.1: Summary of GPC data of synthesized polymers in DMA at 40^0C.

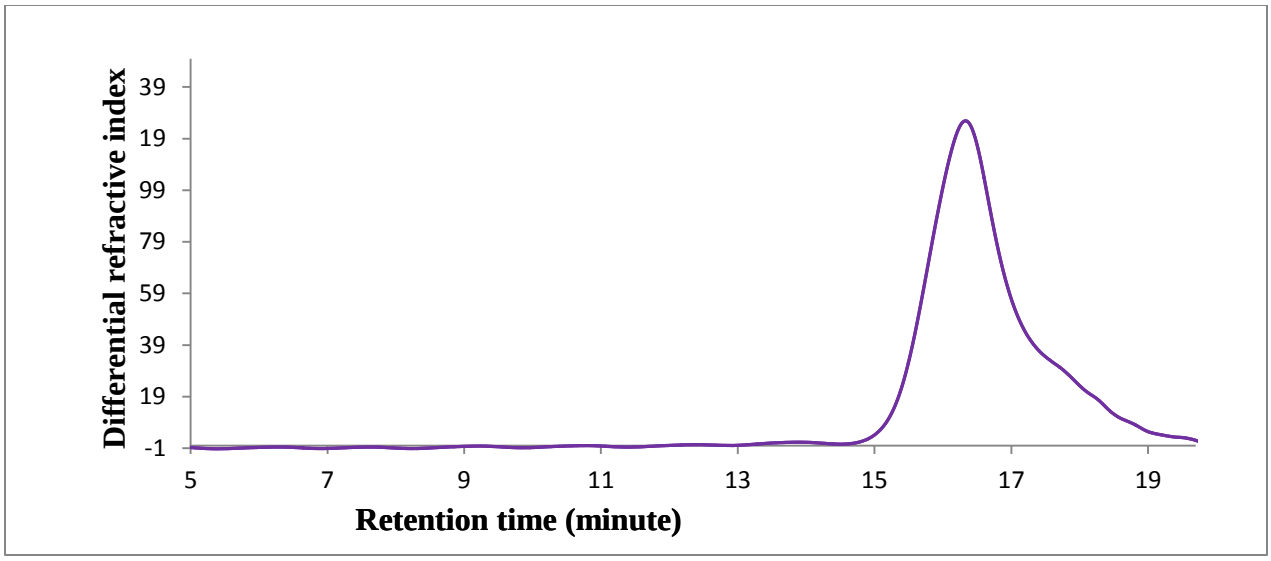

Figure 3.13: GPC chromatograms of polystyrene in DMA at 40^0C (concentration 1.0 x 10^{-4} $molL^{-1}$).

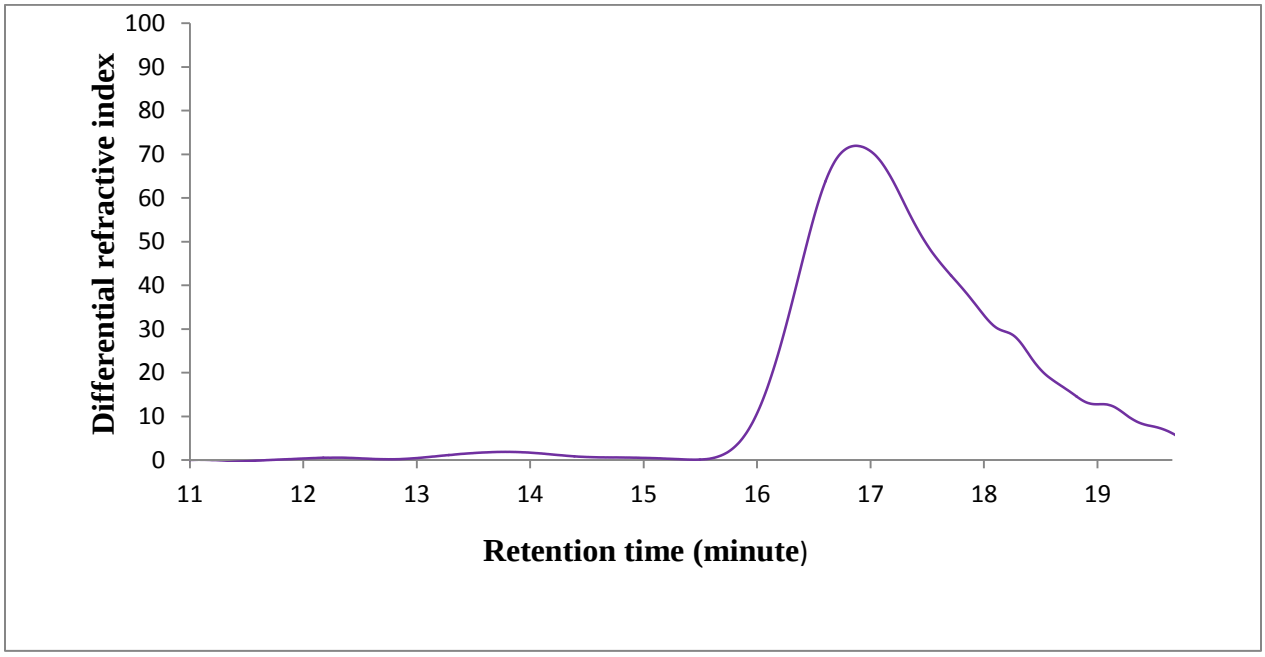

Figure 3.14: GPC chromatograms of quinoline-styrene Copolymer in DMA at 40^0C (concentration 1.0 x 10^{-4} $molL^{-1}$).

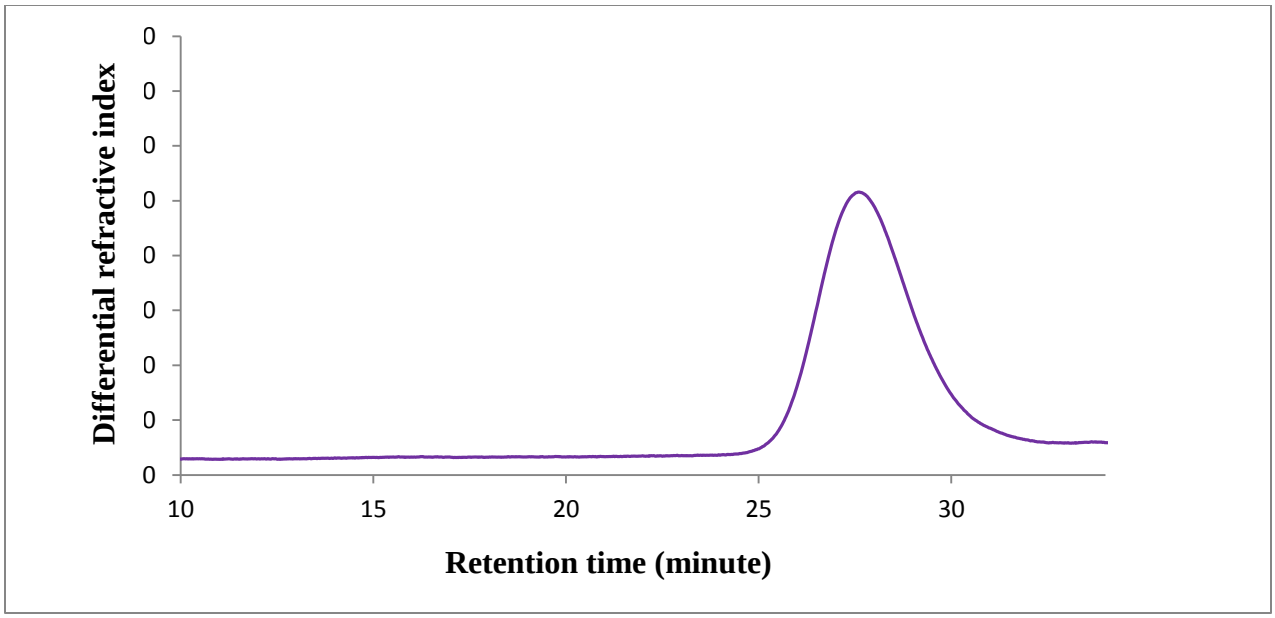

Figure 3.15: GPC chromatograms of RAFT polymer in DMA at 40^0C (concentration 1.0 x 10^{-4} $molL^{-1}$)

3.3.4. Thermal stability of the polymers

In order to evaluate the thermal stability of RAFT polymer (**65**) and copolymer (**78**) thermogravimetric (TG) and derivative thermogravimetric (DTG) was carried out. Those thermal studies were performed at a heating rate of 10°C min^{-1} in nitrogen atmosphere in the range 20-800 ^{o}C. The resulting curves are shown in the Figure **3.16**, **3.17** and **3.18** for thermogravimetric and derivative thermogravimetric studies respectively. The major change in mass for the polymers was observed at from 341 ^{o}C for copolymer while for RAFT polymer was at 349^{o}C. This change in thermal stability is due to introduction of styrene monomer which makes the quinoline-based polymer less heat resistant. The investigation of residual mass percentage at 600 ^{0}C showed a residual mass percentage of 47% for RAFT polymer (**65**) and 30% for copolymer, indicating reduction in rigidity for quinoline-based polymer when styrene monomer is introduced in polymer chain.

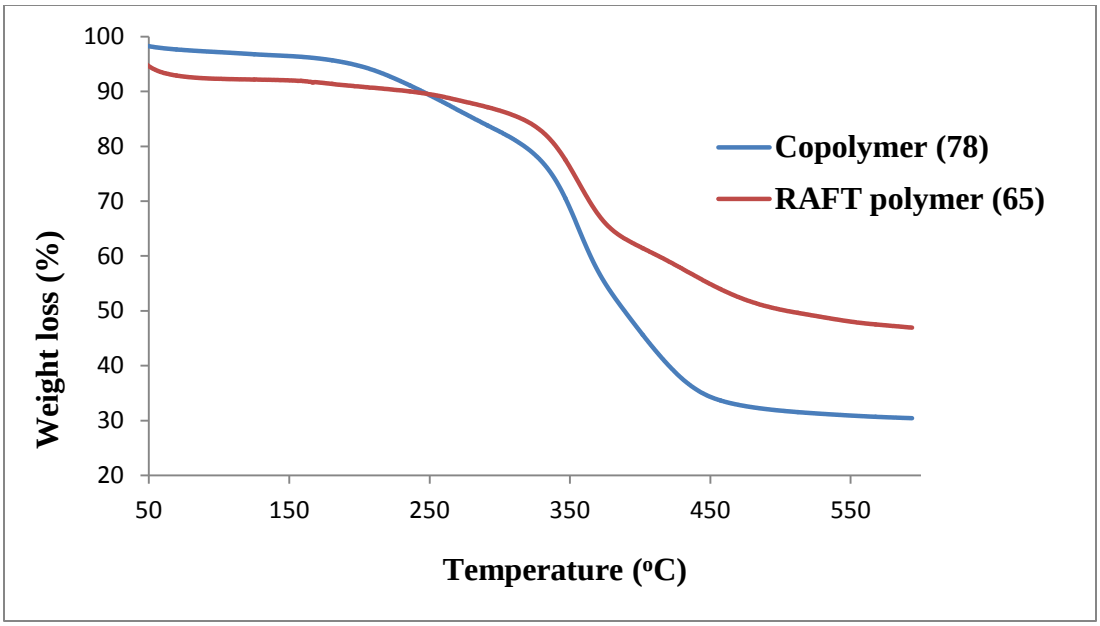

Figure 3.16: Thermogravimetric (TG) curves of RAFT polymer (**65**) and copolymer (**78**) at a heating rate of 10°C min^{-1} in nitrogen atmosphere

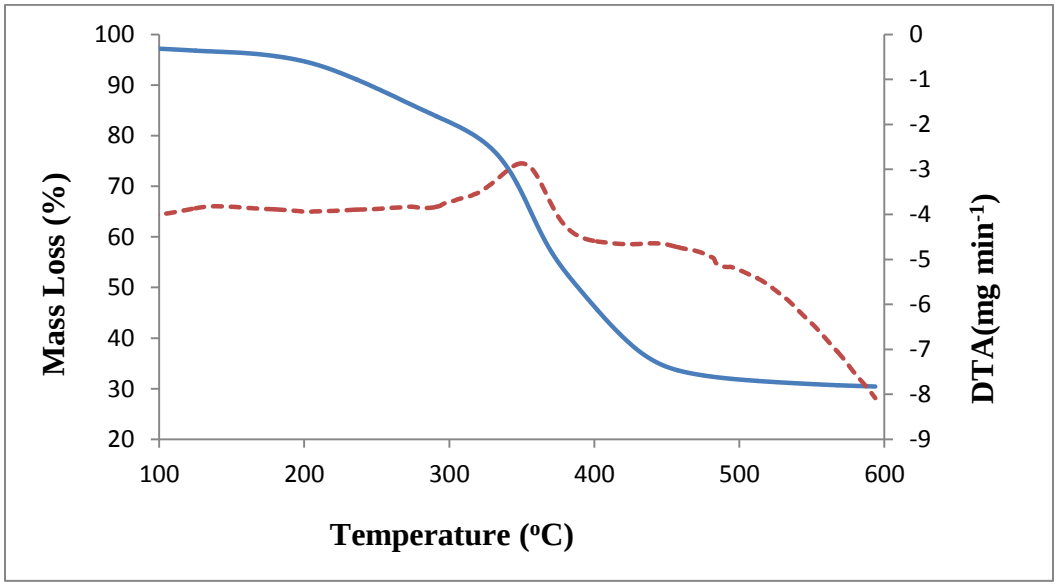

Figure 3.17: Thermogravimetric (TG) and DTG curves for copolymer (**78**) at a heating rate of 10°C min^{-1} in nitrogen atmosphere**.**

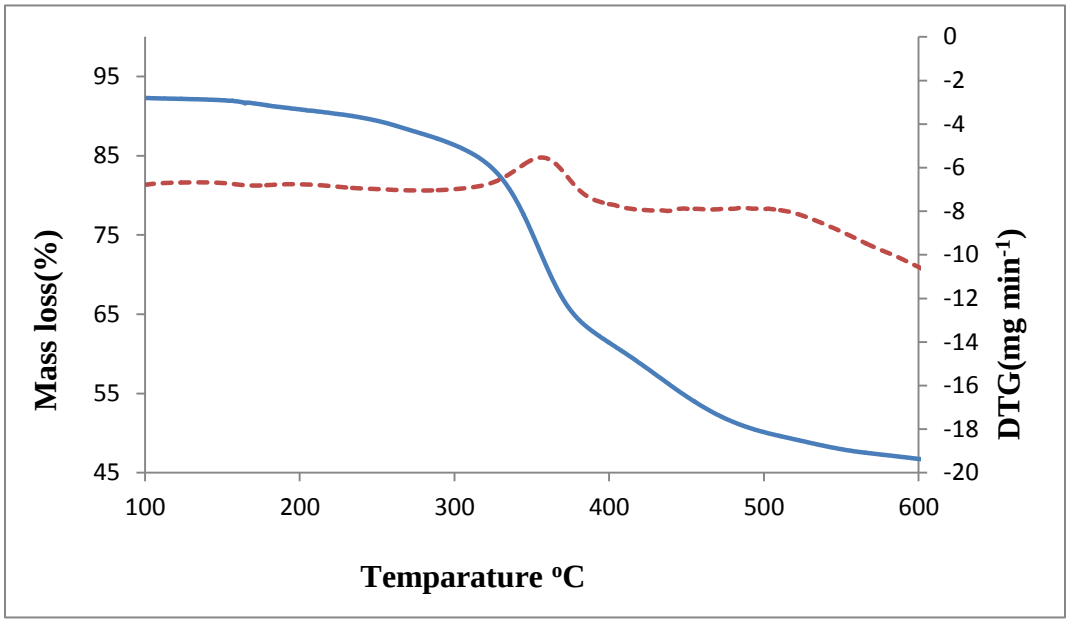

Figure 3.18: Thermogravimetric (TG) and DTG curves for RAFT polymer (**65**) at a heating rate of 10°C min^{-1} in nitrogen atmosphere**.**

3.4. Photophysical properties of the quinoline derived compounds (64, 68, 69, and 74) and its polymers

Quinoline derivatives represent a major class of heterocycles which are well known in polymer chemistry, optolectronics, and electronics for their outstanding mechanical properties.[25] The quinoline backbone is an electron-deficient fused heteroaromatic ring, and its derivatives are known to exhibit high electron mobility, outstanding thermal and oxidative stabilities as well as good photoluminescence efficiencies. Various electron-acceptor polysubstituted quinolines have been studied for their excellent photophysical properties when directly connected to an electron donor or *via a* π-conjugated spacer. This results in the alternating donor-acceptor structures which enable optical,[158] nonlinear optical.[159] Redox,[160] and electroluminescent properties[161] to be tuned over a wide range.

Most quinoline derivatives are known for their poor fluorescence even in the presence of non-transition metal ions.[162] This poor fluorescence intensity is attributed mostly to the photo-induced electron transfer (PET) effect described early, or to the formation of aggregates or excimers. Though this effect results in the reduction of fluorescence intensity, it allows the design of ''turn on'' chemosensors for transition metals ions in which the PET effect is inhibited by metal coordination. Consequently, different quinoline-containing compounds including oligomers and polymers with one or multiple binding sites have been designed and used as chemosensors for transition metals.

More extensive conjugation in quinoline-based systems may lead to enhanced fluorescence effects. Various conjugated chemical structures, including the triazole ring system, may be introduced into the quinoline chromophore to enhance its fluorescence properties.

3.4.1. Photophysical properties of quinoline derived compounds [(64),(69), (70) and (74)]

3.4.1.1. UV-Vis absorption properties of the quinolone-derived compounds (64), (68), (69), and (74)

UV-Vis absorption spectra of the quinoline derivatives (**64**), (**69**), (**70**) and (**74**) were recorded at room temperature as dilute solutions in DMF (1.12×10^{-6} $molL^{-1}$ (Figure **3.19**). All the absorption spectra showed an absorption band between 285nm and 310 nm which can be assigned to π-π* transitions of conjugated systems.

All recorded spectra showed less intense and lower energy absorption bands at different wavelengths. These bands were assigned to charge transfer effect of the substituents on the quinoline ring system which have been chemically modified in the course of the monomer synthesis. The highest red shift among those small bands was observed in the amino-bearing quinoline compound (**69**) followed by azide-bearing quinoline compound (**70)**. The two triazole-bearing molecules [(**64**) and (**74**)] showed the same absorption bands at the higher energy compared to their precursors. This observation suggests that the amino group is a much stronger electron-donating species than the other groups introduced to the quinoline ring system. Therefore intramolecular charge transfer effects are expected to be much stronger in the amino-bearing quinoline moiety than in other compounds.

This evidence was emphasized by the absorption spectra of the two related molecules the vinyl monomer (**64**) and its precursor (**74**) which showed the same absorption bands for charge transfer, but with different intensities due to different substitution on the triazole ring.

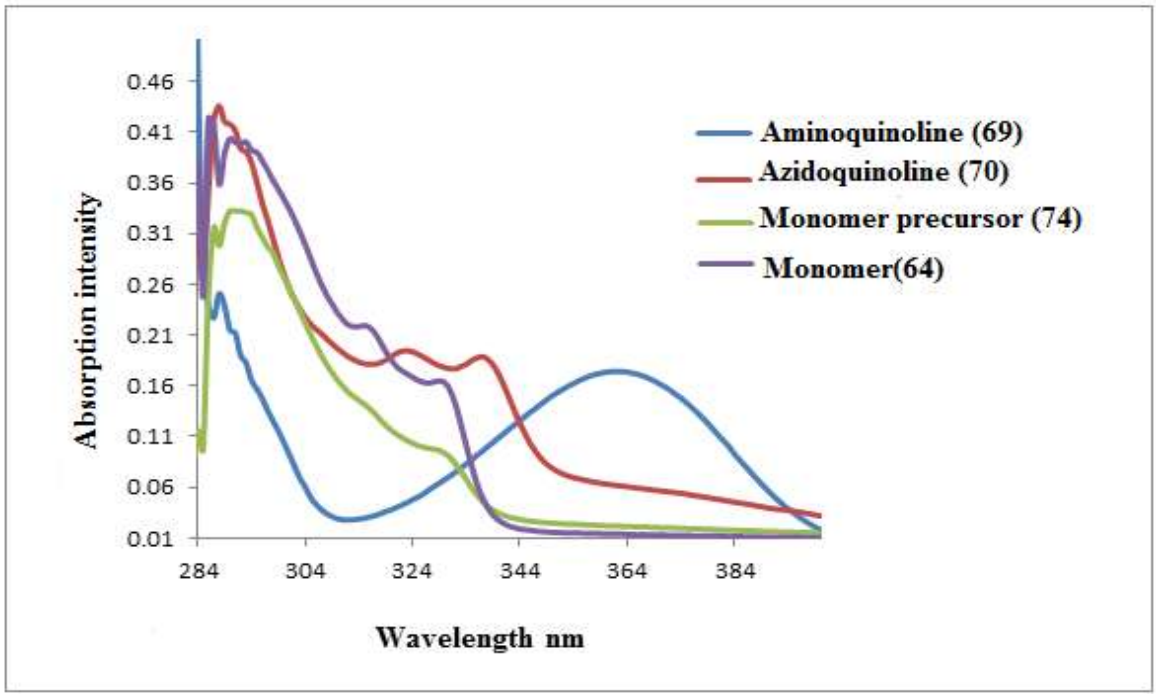

Figure 3.19: UV-Vis spectra of the quinoline compounds (**64**), (**69**), (**70**) and (**74**) in DMF at 25 ^{o}C, at a concentration of 1.12 x 10^{-6} molL^{-1}.

3.4.1.2. Emission properties of quinoline derived compounds (64), (69), (70) and (74)

The emission spectra of these compounds were also recorded in the same solvent (DMF) and at the same temperature (25 ^{o}C) and concentration as for the absorption spectra, and the results are shown in Figure **3.20**.

Due to the presence of basic nitrogen atoms in the quinoline ring system as well as in the triazole ring the emission properties of the synthesized quinoline compounds (**64**), (**69**), (**70**) and (**74**) showed a dependence on the external factors rather than the expected influences from conjugation. All the compounds showed maximum emission at 429 nm when the samples were excited at 376 nm. The amino-bearing quinoline compound (**69**) showed higher fluorescence intensity compared to the others, which is due to the establishment of intermolecular hydrogen bonding between the amino hydrogens and the nitrogen atoms of the quinoline ring system.

These interactions reduce the likely fluorescence quenching due to the photo-induced electron transfer (PET) effect from the nitrogen lone pair of the amino group.

The next highest fluorescence intensity was observed from the emission spectra of the azide-bearing quinoline compound (**70)**. This is due to the reduced electron donating ability of the azide compared to the amino group which reduces its contribution towards the PET effect. The two triazole-bearing compounds (**64** and **74**) showed less fluorescence intensity compared to the other simple molecules. The introduction of the triazole ring system into quinoline tends to extend the conjugation from which we can expect a fluorescence enhancement. On the other hand, the incorporation of an electron-rich moiety like the triazole ring increases the probability for photo-induced electron transfer which reduces the fluorescence intensity. This fact was verified by comparing two triazole-bearing quinoline compounds (**64** and **74**) which differ structurally only on two terminal carbons. The monomer (**64**) which is the double bond terminated compound was found to fluoresce more weakly than its precursor (**74**) which possesses an alcohol function group. This difference can be explained in terms of electron density on triazole unit. The higher the electron density the greater the chance for the PET effect to occur. The monomer has higher electron density on the triazole unit compared to its precursors due to the double bond, therefore the PET effect is likely to be more significant in monomer than in its precursor.

In addition to this effect, the monomer precursor (**74**) has a hydroxyl group which can participate in hydrogen bonding. This effect can reduce the efficiency of the PET effect and result in increased fluorescence intensity of the monomer precursor (**74**) compared to the vinyl monomer (**64**).

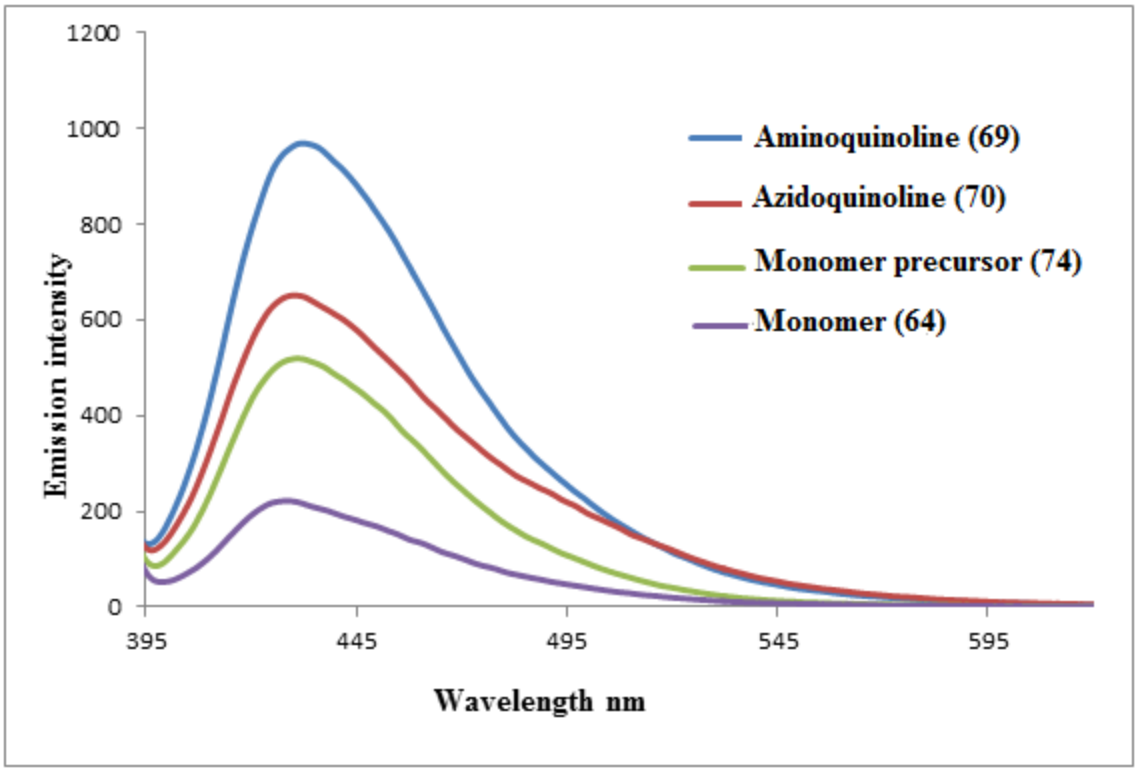

Figure 3.20: Fluorescence spectra of the quinoline compounds [(**64**), (**69**), (**70**) and (**74**)] in DMF at 25 ^{o}C, at the concentration of 1.12 x 10^{-6} molL^{-1} with an excitation wavelength of 376 nm.

3.4.2. Photophysical properties of the quinoline-containing polymers

3.4.2.1. UV-Vis absorption spectra of the quinoline-containing polymers

The *UV-Vis* absorption spectra of the synthesized polymers were obtained in a dilute DMF solution of each polymer (0.008 g L^{-1}) at room temperature using styrene as a reference polymer. The results are shown in the Figure **3.21**. All the polymers containing the quinoline chromophore absorbed at 330 nm which is attributed to π-π* transitions in the conjugated backbones. These results also show that the incorporation of the quinoline moiety into the copolymer did not affect the maximum absorption of the quinoline chomophore.

Though the spectra of all the investigated polymers except polystyrene showed the absorption at 330 nm, their intensities are a function of the amount of quinoline chomophore in the polymer chains.

Polystyrene showed no absorption under these conditions. However, incorporation of the quinoline functionality to form a copolymer resulted in an improved absorption.

The RAFT polymer absorbed more strongly than the monomer, which can be attributed to the contribution from the end-groups from the RAFT agent.

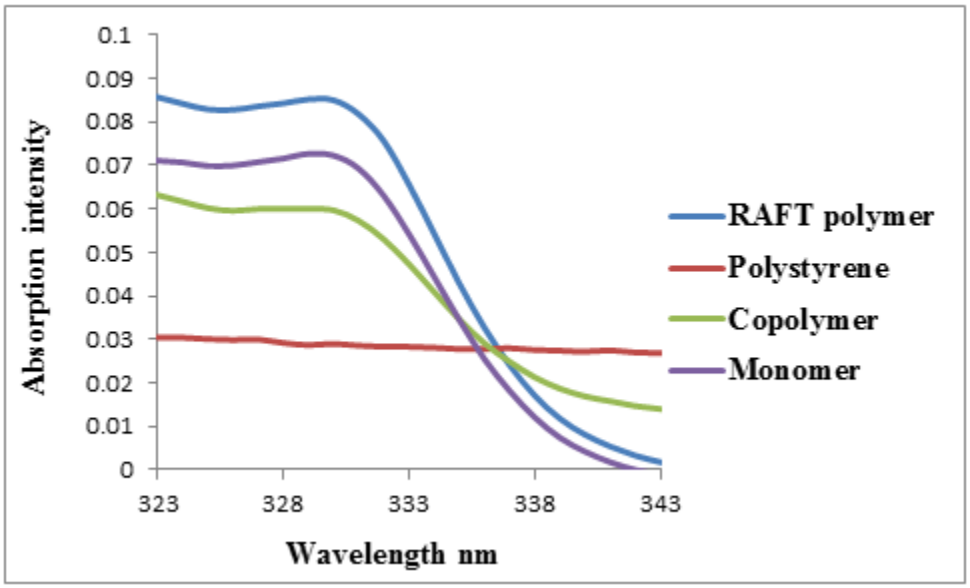

Figure 3.21: *UV-Vis* spectra of synthesized polymers [(**65**), (**77**) and (**78**)] in DMF at 25 ^{o}C, at a concentration of 0.008 g L^{-1}.

3.4.2.2. Emission spectra of the quinoline-containing polymers

In order to extend the investigation of the impact of the quinoline chromophore on the polymer chain, the emission properties of the polymers were examined. The emission spectra of the synthesized polymers were recorded under the same conditions (in DMF at 25^{o}C) and concentration (0.008 gL^{-1}) as their absorption spectra (0.008 gL^{-1}). All the samples were excited at 376 nm using polystyrene as a standard and the results obtained are shown in Figure **3.22**.

All the polymers showed an emission maximum at 422 nm which is associated with a π-π* transition of the conjugated quinoline chromophore. Polymers containing the quinoline chromophore also showed a small emission band at 485 nm, characteristics of excimer formation or aggregates.[163]

The emission intensity was expected to be a function of the amount of quinoline chomophore present in a chain. However, the experimental results show a reversed pattern for the emission intensities.

The quinoline RAFT polymer which was expected to exhibit a higher intensity compared to the other polymers and starting monomer, was found to emit less intensely. This effect is attributed to a quenching effect from the RAFT agent due the superposition of the RAFT agent absorption and the quinoline fluorescence emission, which allows energy transfer from quinoline to the RAFT agent. This quenching was confirmed by comparing the fluorescence emission of the RAFT polymer and the quinoline-containing polymer obtained from random polymerization as shown in the Figure **3.23**. The latter showed enhanced fluorescence emission compared to the RAFT polymer which underwent quenching from the RAFT agent.[164]

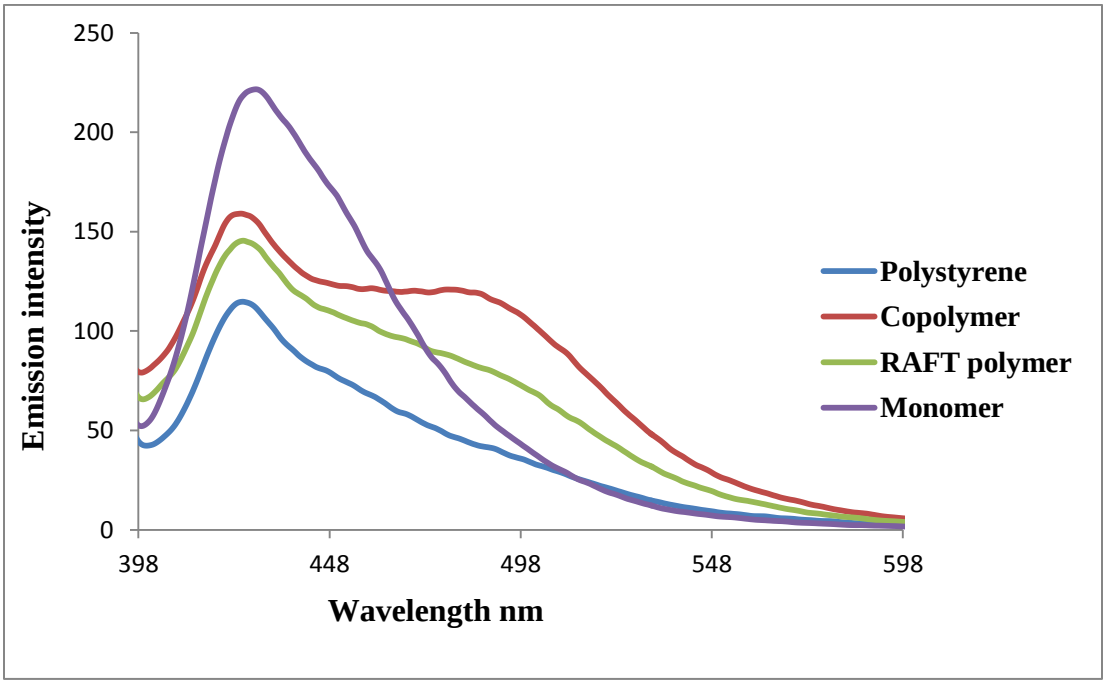

Figure 3.22: Fluorescence spectra of synthesized polymers [(**65**), (**77**) and (**78**)] in DMF at 25 ^{o}C, at a concentration of 0.008 gL^{-1} with an excitation wavelength of 376 nm

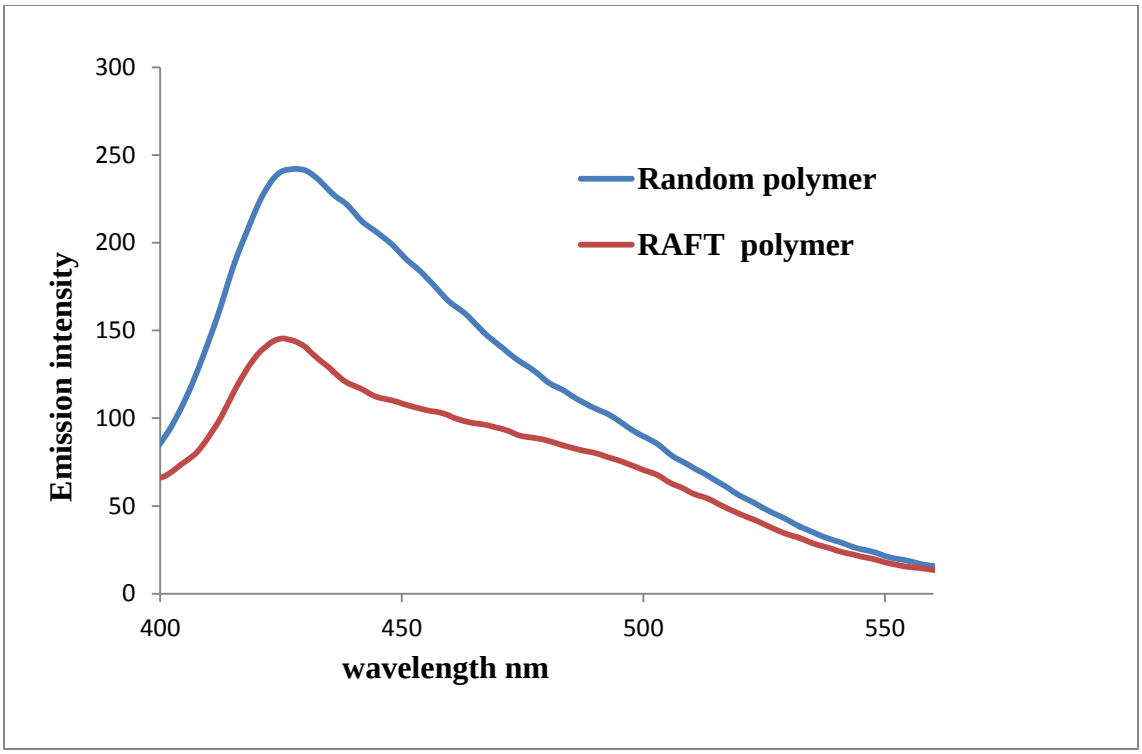

Figure 3.23: Fluorescence spectra of RAFT (**65**) and random polymer (**75**) in DMF at 25^{o}C. The concentration of the polymer was 0.008 $gL^{-1}$and the excitation wavelength was 376 nm.

3.5. Preliminary studies on complexation of quinoline polymers with Zn, Cd, Hg, Fe, and Ni

Transition metal ions can exhibit biological effects in animals and can present a major part of an environmental pollutant, even at very low concentration. In order to assess health risks and environment monitoring, we need efficient tools and methods to detect these ions. Although traditional techniques approved by environment protection agencies (*e.g.* EPA) for determining transition metal ions in water seem to be promising,[165] they suffer from extensive sample preparation and expensive equipment requirements. The latter problem has been addressed by the development of organic sensors which require only a fluorometer.

Basically a fluorescent sensor should have a receptor (recognition site) bonded to a fluorophore translating the recognition event into a fluorescence signal.[166]

The metal ion can be detected *via* three ways. The first method involves the fluorophore with less or no fluorescence properties, which becomes more fluorescent when bonded with the metal ions.

This effect can be attributed to the induced conformational restriction resulting from the interaction between fluorophore and metal ion.[167] The second method involves fluorescence quenching in which a species with increased fluorescence properties in the absence of metal ions of interest and becomes less or display no fluorescence in the presence of a metal ion. This effect is due to the energy transfer,[168] or electron transfer mechanism[169]occurring during fluorophore-metal ion bond formation.

The third method for transition metal ion detection involves the emission spectrum of the analyte solution by considering shifts in its emission maximum.[170]

The quinoline-based sensor has recently attracted attention from many researchers concerned with transition metal,[171] and anion recognition,[172] due to their easy synthesis, sensitivity and stability.

Typical quinoline based chemosensors are summarized in Figure **3.24** and can be synthesized by any of the methods described earlier. The Photophysical properties of quinoline chemosensors can be tuned over a wide range in solution depending on the nature of the substituents R_1, R_2, R_3, R_4, and R_5. This is often achieved by changing the receptor group in the 2 (R_1) and 8 (R_5) positions and electron withdrawing or electron group in the 4 (R_2), 5 (R_3), and 6 (R_4) positions.[173]

e.g.

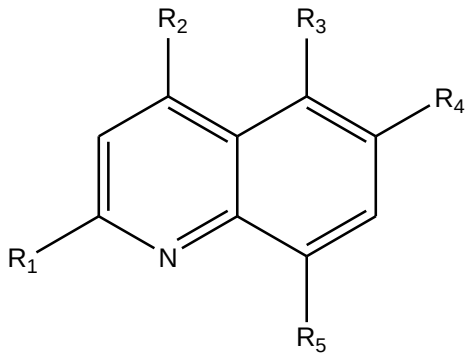

R1	R2	R3	R_4	R5
$-CH_3$	CO_2Me	Cl	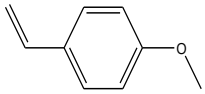	OH

Figure 3.24: Typical quinoline-based chemosensors

In order to increase the sensitivity of the quinoline-based sensor, the quinoline chromophore has been incorporated in various structural polymer chains. The relative flexibility associated with the polymeric materials and the arrangement of their main or pendant chains allow them to bring closer the binding sites and facilitate metal ion complexation.

To investigate the complexation capability of the quinoline-based polymer, five transition metal ions have been studied. These include transition metals ion which are essential for life such as Zn(II), and Fe(II) and other which are environmental pollutants, *e.g.* Hg(II), Cd(II), and Ni(II).

3.5.1. Fluorescence studies of the quinoline-based polymer (65) in presence of selected transition metal ions

In order to understand the fluorescence behaviour of the triazole-quinoline polymer in the presence of the selected transition metal ions mentioned above, the fluorescence properties of the sample containing both polymer and ion were investigated and the results are shown in the Figure **2.25**.

The spectra were obtained with dilute solutions of the quinoline-based polymer (1.12×10^{-6} $molL^{-1}$) in DMF. The study was carried out at room temperature by exciting the sample at 376 nm followed by measuring its emission from 200 nm to 700 nm.

Upon addition of 3μl of the appropriate transition metal ion solution (0.0062 $molL^{-1}$) to the quinoline-based polymer solution, fluorescence intensity of the polymer was found to increase in all cases except for Fe(II). The highest fluorescence intensity was observed for Ni(II) followed by Zn(II) and Hg(II) which were similar, and lastly Cd(II) with the lowest fluorescence enhancement. The quenching of Fe(II) is due to its coordination to the receptor sites of the triazole-quinoline polymer which disturbs the electron distribution of the polymer and consequently promotes intersystems crossing. The latter enhances phosphorescence and quenches fluorescence.

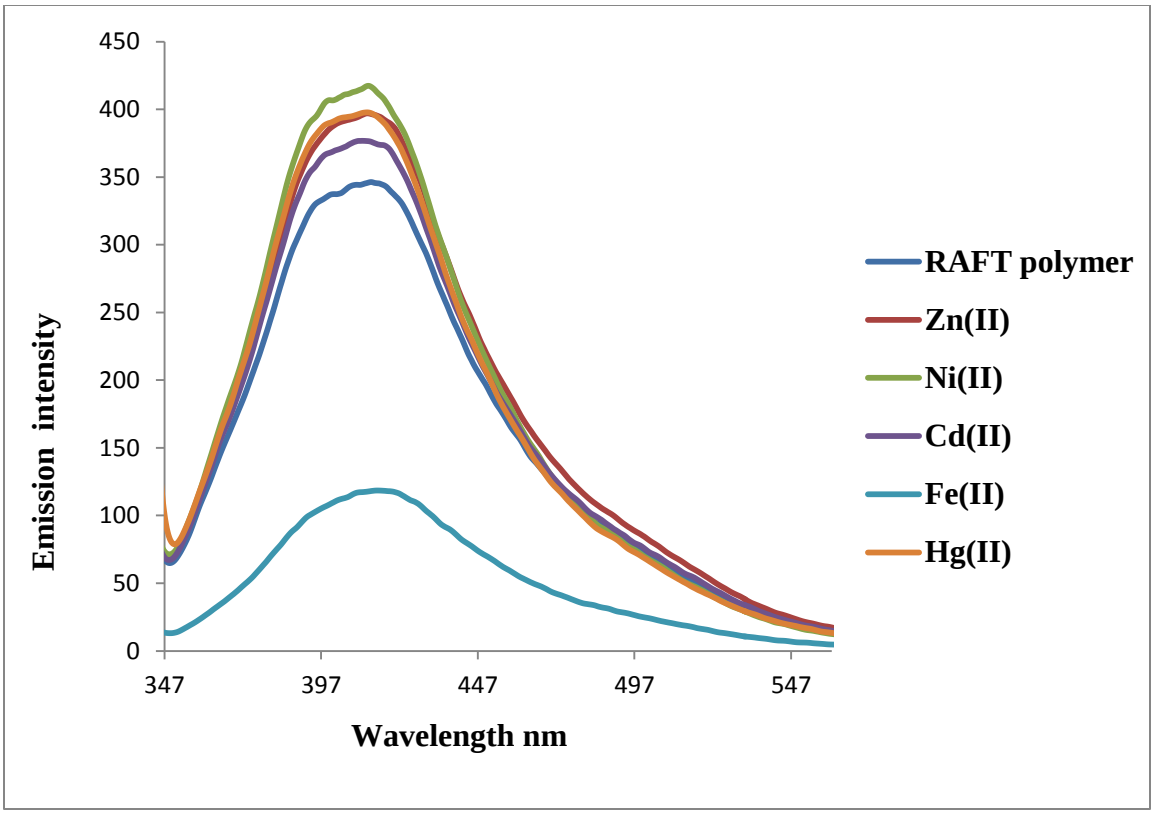

Figure 3.25: Fluorescence spectra of the quinoline-based polymers (**65**) in presence of selected transition metal ions

The results obtained suggest that the synthesized quinoline-based polymer can be used as sensor for paramagnetic Ni(II) which has been classified as one of thirteen priority metal pollutants,[174] Zn(II) and Hg(II) which are mostly detected by simple molecules,[175,176] but in this case some chemical modifications on the polymer backbone is necessary to minimize the fluorescence interference between the two cations.

Since the fluorescence enhancement of Cd(II) differs from Zn(II), this polymer could possibly act as a selective sensor for Cd(II) since most designed organic sensors for this ion suffer from Zn(II) interference owing to their chemical similarities.[177] Fe(II) detection by this type of polymer as a selective turn-off fluorescence sensor, seems to be practically difficult due to enhanced fluorescence quenching by this ion.

3.5.2. *UV-Vis* absorption studies of the quinoline-based polymer (65) in presence of selected transition metal ions

The absorption spectra of the quinoline-based polymer in the presence of the selected transition metal ions was also monitored using the same conditions and concentrations as for its emission spectra. To an aliquot of the quinoline-based polymer solution 3µl of each transition metal ion solution was added and the *UV-Vis* absorption spectrum was then recorded Figure (**2.26**).

All the complexed polymers absorbed in the same range as the original polymer and all complexed polymers showed less absorption than the original polymer, except the one involving Fe(II) which showed higher absorption than the original polymer and Zn(II) which showed almost the same absorption as the original polymer.

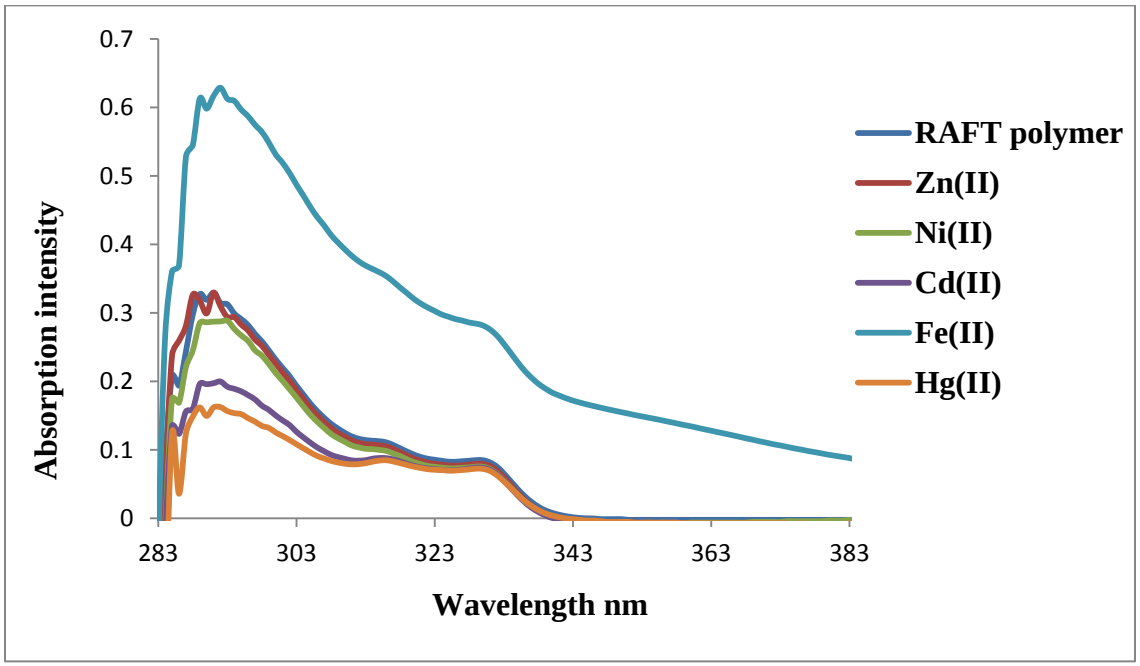

Figure 3.26: Absorption spectra of triazole-quinoline polymers (**65**) in presence of selected transition metal ions

Chapter 4

Conclusion

The aim of this research was to synthesize the branched fluorescent quinoline-triazole polymers in which the quinoline moiety is incorporated on the pendant chains. Different molecular weight quinoline-based polymers and a copolymer were successfully synthesized using Reversible Addition-Fragmentation chain Transfer polymerization (RAFT), and conventional free radical vinyl polymerization from a fluorescent vinyl quinoline-based monomer.

The desired fluorescent vinyl quinoline-based monomer **(64)** was synthesized in multiple steps from commercially available 4-nitroaniline and crotonaldehyde. The quinoline backbone was formed using the Skraup-Doebner-Von Miller method. Various reactions including metal-mediated reduction, diazotization-azidation, and Cu(I)-catalyzed Huisgen's 1,3-dipolar cycloaddition of terminal alkynes and azide ("click" reaction) were used for chemical modifications of the substituents on the quinoline backbone.

The photophysical properties of the quinoline componds and polymers were investigated in DMF solvent. The absorption properties of the quinoline compounds appeared to be a function of the electron-donating ability of the substituent on the quinoline backbone. On the other hand the emission properties showed to be dominated by external factors rather than the expected influences from the conjugation systems. The absorption studies of the polymers showed that the maximum absorption intensities depend on the quinoline chomophores present in the chain while maximum emission intensities were reversed due to the quenching in RAFT polymer (**65)**. A preliminary study on the complexation of the quinoline polymers with selected transition metals showed that our quinoline-based polymer can be used as a chemosensor for transition metals.

Future work will include the following:

- Modification of the end-groups of the RAFT polymers and comparison of their fluorescence properties.

- Effect of solvent polarity on the photophysical properties of the quinoline-based polymers.
- Application of other controlling polymerization methods (ATRP, NMP) on our novel quinoline-based vinyl monomer (**64)**.
- Ratiometric fluorescence studies of the quinoline-based polymers in the presence of transition metals.

Chapter 5

Experimental

5.1. General

Commercial grade solvents and reagents were purchased from Sigma Aldrich or Merck, and used as received without further purification. All the reactions were accomplished under atmospheric air. Potentially dangerous azides[178] were synthesized according to the established protocol. The completion of the reactions was monitored by thin layer chromatography (TLC) on commercial Merck aluminium plates coated with silica gel 60 F_{254}. Colum chromatography was performed using Merck silica gel (particle size 0.040-0.063 mm, 230-400 mesh). NMR spectra were recorded on 400 MHz Bruker Advance DPX spectrometer in $CDCl_3$ and d_6-DMSO at room temperature, using tetramethyl silane as an internal reference. Chemical shift values are expressed in parts per million (ppm) while coupling constants (*J)* are given in Hz.

FT-IR spectra were recorded in the range 4000-400 cm^{-1} using Opus software (version 6. 5. 6) on a Bruker Platinum Tensor 27 ATR-IR spectrophotometer.

The melting point data were determined using a Lasec Hot Stage apparatus. The UV-Vis spectra were recorded on a Perkin Elmer Lambda 35 UV-Vis spectrometer using a 1cm quartz cell while emission spectra were recorded on a Perkin Elmer LS 45 fluorescence spectrometer. The elemental analysis for carbon, hydrogen and nitrogen was performed using a Vario EL (ElementarAnalysensystem GmbH) instrument.

Single crystal X-ray crystallographic structure were determined using a Bruker Kappa Apex II diffractrometer in the conventional ω–2θ scan mode and monochromatic Mo-Kα radiation (λ = 0.71073 Å).

5.2. Experimental procedures

5.2.1. Synthesis of vinyl monomer (64)

5.2.1.1. Synthesis of 2-methyl-6-nitroquinoline (68)

A 250 ml three necked round bottom flask equipped with magnetic stir bar was charged with concentrated hydrochloric acid (44.8 ml, 10.2 M), *p*-nitroaniline (1.2 g, 8.9 mml) and glacial acetic acid (0.5 ml, 8.9 mml) which was heated to reflux for 30 min where upon, potassium iodide (0.123 g, 0.740 mmol) and 10 ml of toluene was added. This was followed by dropwise addition of crotonaldehyde (1.5 ml, 17.8) in toluene (2 ml) over a period of 1h and mixture was heated to reflux further for 6 h. After cooling the reaction mixture to room temperature, the crude products were precipitated out using concentrated ammonia /dilute sodium hydroxide solution. After drying at reduced pressure the crude product was purified by column chromatography on silica gel (7:3 ethyl acetate: hexane) to afford the product as light yellow solid in 60% yield. M_P.: 169 ^oC; FT-IR, ν_{max} (cm^{-1}): 3099 (Ar-H), 2970 (CH_3), 1336 and 1529 (NO_2); ^{1}H-NMR (400 MHz, $CDCl_3$), δ (ppm): 2.74 (s, 3H, H-11), 7.38 (d, *J* = 8.48 Hz, 1H, H-3), 8.06 (d, *J* = 9.2 Hz, 1H, H-8), 8.16 (d, *J* = 8.6 Hz,1H, H-4), 8.37 (d, *J* = 9.04,1H, H-7), 8.67 (s, 1H, H-5); ^{13}C-NMR (100 MHz, $CDCl_3$), δ (ppm): 24.66 (C-11), 122.01 (C-7), 122.93 (C-5), 123.30 (C-3), 124.23 (C-10), 129.32 (C-8), 136.77 (C-4), 144 (C-6), 148.88(C-9), 162.27 (C-2).

5.2.1.2. Synthesis of 2-methyl-6-aminoquinoline (69)

To a 250 ml round bottom flask equipped with magnetic stir bar, concentrated hydrochloric acid (20 ml) and 2-methyl-6-aminoquinoline (1 g, 5.32 mmol) were added. After cooling the reaction mixture in ice, granulated tin (2. g, 17 mmol) was added, and the reaction was heated at 50 ^oC until the tin metal had reacted. The reaction mixture was allowed to cool to room temperature followed by removal of metal residues by filtration.

The filtrate was basified with sodium hydroxide (40 ml) and extracted with chloroform (3x 50 ml) to give a crude product which was further purified by column chromatography on silica gel (1:1ethyl acetate: hexane) to give yellow solid product in 65 % yield. M_P: 187 ^oC; FT-IR, ν_{max} (cm^{-1}) : 3317, 3188 (NH_2), 2929 (CH_3); ^{1}H-NMR (400 MHz, $CDCl_3$), δ (ppm): 2.59 (s, 3H, H-11), 3.81 (s, 2H, NH_2), 6. 8 (s, *J* = 2.4 Hz, 1H, H-5), 7.05 (d, *J* = 8 Hz, 1H, H-7), 7.09 (d, *J* = 8.44 Hz, 1H, H-3), 7.73 (d, *J* = 8.44 Hz, 1H, H-4), 7.77(d, *J* = 8.2 Hz, 1H, H-8);

^{13}C-NMR (100 MHz, $CDCl_3$), δ (ppm): 24.83 (C-11), 107.73 (C-5), 121.43 (C-3), 122.27 (C-10), 127.80 (C-7), 129.57 (C-8), 134.26 (C-4), 142.78 (C-6), 143.93 (C-9), 155.08 (C-2).

5.2.1.3. Synthesis of acidic ionic liquid [H- NMP] HSO_4 (72)

To a cold solution of 1-methyl-2-pyrrolidone (0.97 ml, 10 mml) in dichloromethane (15 ml), sulphuric acid (0.53 ml, 98%) was added dropwise over a period of 10 min. The reaction mixture was then allowed to stir at room temperature for 4 h, and the solvent was removed under reduced pressure. The product was further dried at 70 ^oC under vacuum for 1 h to afford a colourless oil product. FT-IR, ν_{max} (cm^{-1}): 3400–2500 (NH), 1697 (C=O); ^{1}H-NMR (400 MHz, DMSO), δ (ppm): 1.88 (m, 2H, H-3), 2.17 (t, 2H, H-4), 2.50 (s, 1H, NH), 2.68 (s, 3H, H-5), 3.47 (t, 2H, H-2).

5.2.1.4. Synthesis of 2-methyl-6-azidoquinoline (70)

A 250 ml round bottom flask equipped with a magnetic stir bar, was charged with $[H\text{-}NMP]^+$ HSO_4^- (0.79 g, 4 mmol) and 2-methyl-6-aminoquinoline (0.158 g, 1 mmol) in a mixture of THF and water (20 ml, 1:1), and then was cooled in an ice bath. To the mixture, $NaNO_2$ (0.175 g, 2.536 mmol) was added and the mixture was stirred for 30 minutes to allow diazonium salt formation. Then NaN_3 (0.163 g, 2.507 mmol) was added slowly to allow azidation reaction to take place. After 30 min of vigorous stirring, THF was removed under reduced pressure and water (30 ml) was added to separate the ionic residues from $NaNO_2$ and NaN_3.

The crude azide was extracted with chloroform (3 x 30 ml) which was then removed under reduced pressure to give a black crude product. The product was purified by column chromatography on silica gel (9:1, hexane: ethyl acetate) to give brown oil product in 40 % yield. FT-IR, ν_{max} (cm^{-1}): 3067 (Ar-H), 2958 (CH_3), 2100 (N_3); ^{1}H-NMR (400 MHz, $CDCl_3$), δ (ppm): 2.67 (s, 3H, H-11), 7.22 (d, *J* = 8.48 Hz, 1H, H-3), 7.28 (d, *J* = 8.16 Hz, 1H, H-7), 7.9 (s, 1H, H-5), 7. 90 (d, *J* = 8.44,1H, H-4), 7.96 (d, *J* = 8.84 , 1H, H-8); ^{13}C-NMR (100 MHz, $CDCl_3$), δ (ppm): 23.99 (C-11), 114.24 (C-3), 121.32 (C-6), 121.95 (C-10), 126.06 (C-5), 129.28 (C-8), 134.46 (C-7), 136.57 (C-4), 144.17(C-9), 157.39 (C-2).

5.2.1.5. Synthesis of 1-(1-(2-methylquinolin-6-yl)-1H-1, 2, 3-triazol-4-yl) ethanol (74)

A mixture of 2-methyl-6-azidoquinoline (0.1 g, 0.5 mmol), 3-butyn-2-ol (0.038 g, 0.543 mmol), PMDETA (0.1086 mmol), $CuSO_4.5H_2O$ (8.66 x 10^{-3}g, 0.0543 mmol) in a minimum amount of water, and sodium ascorbate (0.022 g, 0.1086 mmol) in a minimum amount of water was placed in a 100 ml round bottom flask containing 20 ml of THF. The mixture was vigorously stirred at room temperature for 12 h. THF was then removed under reduced pressure and water (20 ml) was added to remove the inorganic residues. After product extraction using chloroform (3 x 30 ml) followed by concentration, the crude product was purified by column chromatography on silica gel (7:3 ethyl acetate: hexane) to afford white solid product in 50% yield. (M_P : 140 ^oC); FT-IR, ν_{max} (cm^{-1}): 3132 (Ar-H), 1606 (Ar-C=C), 1558 (N=N), 3328 (OH); ^{1}H-NMR (400 MHz, $CDCl_3$), δ (ppm): 1.71 (d, *J* = 6.52 Hz, 3H, H-4'), 2.55 (s, 1H, OH), 2.80 (s, 3H, H-11), 5.22 (q, 1H, H-3'), 7.41 (d, *J* = 8.36 Hz, 1H, H-3), 8.06 (s, 1H, H-5), 8.07 (d, *J* = 4.64 Hz, 1H, H-7), 8.15 (d, *J* = 9.52 Hz, 1H, H-4), 8.16 (s,1H, H-1'), 8.19 (d, *J* = 9.12 Hz , 1H, H-8); ^{13}C-NMR (100 MHz, $CDCl_3$), δ (ppm): 23.28 (C-4'), 25.39 (C-11), 63.28 (C-3'), 118.18 (C-5), 118.58 (C-1'), 122.22 (C-3), 123.48 (C-6), 126.49 (C-10), 130.72(C-8), 134.14 (C-7), 136.39 (C-4), 153.27 (C-9, C-2'), 160.37 (C-2).

5.2.1.6. Synthesis of vinyl monomer (64)

To a two necked round bottomed flask equipped with a magnetic stirrer, Dean Stark apparatus and reflux condenser was added 1-[1-(2-methylquinolin-6-yl)-1H-1,2,3-triazol-4-yl] ethanol (1 g, 4 mmol), *p*-toluene sulfonic acid monohydrate (0.5 g, 2.6 mmol) and toluene (60 ml). The reaction mixture was heated to reflux at 110 ^{o}C for a period of 4 h and then allowed to cool to room temperature. Then the reaction mixture was neutralized with sodium hydroxide solution (30 ml, 3 M) resulting in two layers. The organic layer was collected, washed with water (3 x 30 ml) and dried over anhydrous sodium sulphate. After concentration under reduced pressure, the crude product was collected and purified by column chromatography on silica gel (4:1, ethyl acetate : hexane) to afford a light yellow solid product in 50 % yield. Anal. Calcd: C, 71.1; H, 5.12; N, 23.71. Found: C, 66.94; H, 4.34; N, 22.33,); (M_P: 156 ^{o}C); FT-IR, ν_{max} (cm^{-1}): 3157 (Ar-H), 2970(CH_3), 1612 (Ar-C=C): ^{1}H-NMR (400 MHz, $CDCl_3$), δ (ppm): 2.73 (s, 3H, H-11), 5.38 (d, *J* = 11.16 Hz , H_a-4'), 5.97(d, *J* = 17.72 Hz,1H, H_b-4'), 6.72 (dd, 1H, H-3'), 7.33 (d, *J* = 8.44 Hz, 1H, H-3), 7.99 (d, *J* = 9.68 Hz, 1H, H-7), 8 (s, 1H, H-5), 8.09 (d, *J* = 9.64 Hz, 1H, H-4), 8.12 (d, *J* = 13.16 Hz, 1H, H-8), 8.15 (s,1H, H-1'), ^{13}C-NMR (100 MHz, $CDCl_3$), δ (ppm): 25.21 (C-11), 177.10 (C-5), 118.05 (C-4'), 118.29 (C-1'), 122.29 (C-3), 123.50 (C-6), 125.16 (C-10), 126.53 (C-8), 130.45 (C-7), 134.13 (C-3'), 136.70 (C-2'), 146.78 (C-4), 147.21 (C-9), 160.24 (C-2).

5.2.2. Synthesis of RAFT agent

5.2.2.1. Synthesis of bis(thiobenzoyl) disulphide

A well-dried three-neck round-bottom flask equipped with a condenser and a dropping funnel was charged with dried magnesium turnings (1.25 g, 51 mmol), a small amount of iodine and of freshly distilled THF (10 ml). The mixture was stirred at room temperature and a solution of bromobenzene (5.25 ml, 50 mmol) in freshly distilled THF (40 ml) was added. When the reaction started, the remaining bromobenzene solution was added drop-wise so that the temperature is kept below 40 ^{o}C.

After all the magnesium was consumed the flask was placed in ice, and carbon disulfide (3.00 g, 50 mmol) was added drop-wise through a septum, resulting in an exothermic reaction, with the colour of the solution changing to red.

The reaction mixture was stirred for another 0.5 h at room temperature and then cooled in an ice bath. After a solution of *p*-tosyl chloride (9.50 g, 50 mmol) in dry THF (40 ml) was added drop-wise over 30 minutes, the colour changed from red to purple. After stirring the reaction mixture for 1 h at room temperature the solvent was removed under reduced pressure and residue was kept overnight in a freezer. The solidified residue was washed with distilled water and recrystallized from acetone and acetonitrile to afford purplish-red crystals.

5.2.2.2. Synthesis 2-cyano-2-propyl dithiobenzoate (CPDP)

A 250 ml round-bottom flask equipped with a condenser and magnetic stirrer bar was charged with AIBN (1.45 g, 8.83 mmol), bis(thiobenzoyl)disulfide (1.8 g, 5.87 mmol) and ethyl acetate (70 ml). The reaction mixture was heated to reflux for 18 h where upon ethyl acetate was removed under reduced pressure.

The crude product was collected and purified by column chromatography on silica gel (0.2: 0.98 ethyl acetate: hexane) to afford a purple crystalline in product in 90% yield. ^{1}H-NMR (400 MHz, $CDCl_3$), δ (ppm): 1.86 (s, 3H, H-7,7'), 7.31 (t, *J* = 7.4Hz , H-2,2'), 7.48 (t, *J* = 7.44 Hz,1H, H-3), 7.83 (d, *J* = 7.8, H-1,1'); ^{13}C-NMR (100 MHz, $CDCl_3$), δ (ppm): 26.47 (C-7,7'), 41.76 (C-6), 119.97 (C-8), 126.65 (C-2,2'), 128.56 (C-1,1'), 132.95 (C-3), 144.54 (C-4).

5.2.3. Synthesis of quinoline-triazole polymers

5.1.3.1. Conventional free radical polymerization

(a) Polymerization of 2-methyl-6-(4-vinyl-1H-1,2,3-triazol-1-yl)quinoline

To a pear-shaped Schlenk flask a equipped with magnetic stir bar and septum, a mixture of 2-methyl-6-(4-vinyl-1H-1,2,3-triazol-1-yl)quinoline (0.05 g, 0.21 mmol) and azobisisobutyronitrile (AIBN) (7×10^{-4} g, 4.29×10^{-3} mmol) in DMF (3 ml) was added. The solution was degassed *via* four freeze-thaw cycles and flushed with argon.

The mixture was then heated to reflux for 48 h at 70 ^{o}C and the polymer was then precipitated with methanol (20 ml). The polymer was filtered and washed with hexane (20 ml) to yield a white solid product.

(b) Copolymerization of 2-methyl-6-(4-vinyl-1H-1,2,3-triazol-1-yl)quinoline and styrene (1:1 feeding molar ratio)

A pear-shaped Schlenk flask charged with 2-methyl-6-(4-vinyl-1H-1,2,3-triazol-1-yl)quinoline (0.1 g, 4.3×10^{-4} mmol), styrene (0.044 g, 4.3×10^{-4} mmol), azobisisobutyronitrile (AIBN) (0.014g, 8.5×10^{-5} mmol) and DMF (3 ml) was connected to the pump. The sealed flask was degassed via four freeze-thaw cycles and flushed with argon. The mixture was then heated to reflux for 48 h at 70 ^{o}C and the polymer was precipitated with methanol (20 ml). After filtration and washing with hexane (20 ml) the polymer was collected as a brown soli

5.2.3.2. Controlled method

(a) 5000 molecular weight polymer

To a pear-Shaped schlenk flask a mixture of 2-methyl-6-(4-vinyl-1H-1,2,3-triazol-1-yl)quinoline (0.1g, 0.4 mmol), RAFT agent (CPDP) (4.6×10^{-3} g, 0.002 mmol) and azobisisobutyronitrile (AIBN) (6×10^{-4} g, 4×10^{-3} mmol) in DMF (4 ml) was added. The solution was degassed via four freeze-thaw cycles and flushed with argon. The mixture was then heated to reflux for 48 h at

70 ^{o}C followed by precipitatation of the polymers with methanol (20 ml). After filtration and washing with hexane (20 ml) the polymer was collected as a white solid.

(b) 10000 molecular weight polymer

The method described for 5000 g/mol polymer was followed using 2-methyl-6-(4-vinyl-1H-1,2,3-triazol-1-yl)quinoline (0.1 g, 0.4 mmol), RAFT agent (CPDP) (4.6 x 10^{-3} g, 0.002 mmol) and azobisisobutyronitrile (AIBN) (6 x 10^{-4} g, 4 x 10^{-3} mmol). The polymers were obtained as white solid.

Chapter 6

References

1. Larsen, R.D., Corley, E. G., King, A.O., Carrol, J.D., Davis, P., Verhoeven, T.R., Reader, P. J., Labelle, M., Gauthier, J.Y., Xiang, Y.B., Zamboni, R. J. *J. Org. Chem*., **1996,** 61, 3398.
2. Chen, Y. L., Fang, K. C., Shen, J. Y., Hsu, S. L., Tzeng, C. C. *J. Med. Chem.*, **2001,** 44, 2374.
3. Roma, G., Braccio, M.D., Grossi, G., Mattioli, F., Ghia, M. *J. Med. Chem*., **2000,** 35, 1021.
4. Doube, D., Blouin, M., Brideau, C., Chan, C., Desmarais, S., Eithier, D., Falgueyret, J. P., Friesen, R. W., Girrard, M., Girard, Y., Guay, J., Tagari, P., Young, R. N., *Bioorg. Med. Chem. Lett.*, **1998**, 8, 1255.
5. Maguire, M. P., Sheets, K. R., McVety, K., Spada, A. P., Zilberstein, A. *J. Med. Chem.*, **1994,** 37, 2129.
6. Stille, J. K. *Macromolecules*, **1981**, 14, 870-880.
7. Zhang, X. J., Shetty, A. S., Jenekhe, S. A. *Macromolecules*, **1999**, 32, 7422-7429.
8. Alam, M. M., Jenekhe, S. A. *J. Phys. Chem. B*, **2001**, 105, 2479-2482.
9. Fungo, F., Jenekhe, S. A., Bard, A. *J. Mater Chem.*, **2003,** 15, 1264-1272.
10. Tong, H., Wang, L., Jing, X., Wang, F. *Macromolecules*, **2002**, 35, 7169-7171.
11. Chen, T. A., Jen, A. K. -Y., Cai, Y. M. *J. Chem. Mater*., **1996**, 8, 607-609.
12. Krüger, H., Janietz, S., Sainova, D., Wedel, A. *Macromol. Chem. Phys.*, **2003**, 204, 1607-1615.
13. Wang, S., Liu, Y., Zhang, X. W., Yu, G., Zhu, D. B. *Synth. Met*. **2003**, 137, 1153-1154.
14. Chen, C. H., Shi, J.M. *Coord. Chem. Rev*., **1998**, 171, 161-174.
15. Kulkarni, A. P., Tonzola, C. J., Babel, A., Jenekhe, S. A. *J. Chem. Mater*., **2004**, 16, 4556-4573.
16. Lu, L. D., Jenekhe, S. A. *Macromolecules*, **2001**, 34, 6249-6254.
17. Zhu, Y., Alam, M. M., Jenekhe, S. A. *Macromolecules* **2003**, 36, 8958-8968.
18. Takizawa, K.,Nulwara, H., Thiboult, R. J., Lowenhielm, P., Yoshinaga, K.,Wooley, K. L., Hawker, C. J. *J. Polym. Sci., Part A: Polym. Chem.*, **2008,** 46, 2897-2912.

19. Lutz, J. F. *Angew. Chem. Int. Ed*., **2007**, 46, 1018.
20. Akeroyd, N., Pfukwa, R., Klumperman, B. *Macromolecules*, **2009**, 42, 3014-3018.
21. Thibault, R. J., Takizawa, K., Lowenhielm, P., Helm, B., Mynar, J. L., Fréchet, J. M. J., Hawker, C. J. *J. Am. Chem. Soc.*, **2006**, 128, 12084-12085.
22. Takizawa, K.,Nulwara, H., Thibault, R. J., Lowenhielm, P.,Yoshinaga, K., Wooley, K. L.; Hawker, C. J. *J. Polym. Sci. Part A: Polym. Chem.*, **2008**, 46, 2897-2912.
23. Michael, J. P. *Natl. rep*. **1997**, 14, 605.
24. Campbell, S. F., Hardstne, J. D., Palmer, M. J. *J. Med. Chem.,* **1998**, 31, 1031.
25. Jenekhe, S. A., Lu, L., Alam, M. M. *Macromolecules,* **2001**, 34, 7313.
26. Jenekhe, S. A. Chen, X. L. *science,* **1999,** 283-372.
27. Saito, I., Sando, S., Nakatani, K. *Bioorg. Med. Chem*. **2001**, 9, 2381.
28. Combes, A. *Bull. Soc. Chem. Fr*., **1888**, 49, 89.
29. Buu-Hoi, N.P., Rayer, R., Xuong, N. D., Jacquignos, P. *J. Org. Chem*. **1953**, 18, 1209.
30. Doebner, O., Von Miller, W. *Ber. Dtsch.Chem. Ges*., **1881**, 14, 2812.
31. Gould, R. G., Jacobs, W. A. *J. Am. Chem. Soc.* **1939**, 61, 2890.
32. Skraup, Z. H. *Ber. Dtsch. Chem. Ges*., **1880**, 13, 2086.
33. Friedlander, P. *Ber. Dtsch. Chem. Ges*., **1882**, 15, 2572.
34. Dormer, P. G., Eng, K. K., Farr, R. N., Humphrey, G. R., McWilliams, J. C., Reider, P. J., Sager, J. W., Volante, R. P. J. *Org. Chem*., **2003**, 68, 467.
35. Yadav, J. S., Rao, P. P., Sreenu, D., Rao, R. S., Kumar, V. N., Nagaiah, K.,Prasad, A. R. *Tetrahedron lett*., **2005**, 46, 7249.
36. S. K., Gibbs, R. A. *Tetrahedon Lett*., **2005**, 46, 1647.
37. Mogilaiah, K., Reddy, C. S. *Synth. Commun.*, **2003**, 33, 3131.
38. Palimkar, S. S., Siddiki, S. A., Daniel, T., Lahoti, R. J., Srinivasan, K. V. *J. Org. Chem.*, **2003**, 68, 9371.
39. Jia, C.-S., Zhang, Z., Tu, S, -J., Wang, G.-W. *Org. Biomol. Chem*. **2006**, 4, 104.
40. Tanaka, Y., Hasui, T., Suginome, M. *Org, Lett.*, **2007**, 9, 4407.
41. Brioche, J., Masson, G., Zhu, J. *Org. Lett*., **2012**, 12, 1432.
42. Shen, Q., Wang, L., Yu, J., Liu, M., Qiu, J., Fang, L., Guo, F., Tang, *J. Synthesis*, **2012,** 44, 389-392.

43. Sudha, S., Banditta, D., Pasha, M. A. *International of Scientific & Technology Research*, **2013**, 2, 54-57.
44. Wu, J. L., Cui, X. L., Chen, L. M., Jiang, G. J., Wu, Y. J. *J. Am. Chem. Soc.*, **2009**, 131, 13888.
45. Zhang, Z., Tan, J., Wang, Z. *Org. Lett.*, **2008**, 10, 173.
46. Zhang, Y, Wang, M., Li, P., Wang, L. *Org. Lett.*, **2012**, 14, 2206-2209.
47. Shan, G., Sun X., Xia Q., Rao Y. *Org. Lett.*, **2011**, 13, 5770-5773.
48. Jia, X., Peng, F., Qing, C., Huo, C., Wang, X. *Org. Lett.*, **2012**, 14, 4030-4033.
49. Katritzky, A. R., Rees, C. W., Scriven, E. F. V., Fan, W. Q. *Eds*.; *Elsevier Science*: *Oxford*, **1996**, 4, 1-126.
50. Huigen, R., *1,3-Dipolar Cycloaddition Chemistry*; **1984**. *Wiley New York*.
51. Rostovtsev, V. V., Green, L. G., Fokin, V. V., Sharpless, K. B. *Angew. Chem. Int. Ed*., **2002**, 41, 2596-2599.
52. Torne, C. W., Christensen, C., Meldal, M. *J. Org. Chem*., **2002**, 67, 3057-3064.
53. Evans, R. A. *Aust. J. Chem*., **2007**, 60, 384.
54. Binder, W. H., Sachsenhofer, R. *Macromol. Rapid Commun.*, **2007**, 28. 15.
55. Lutz, J. F. *Angew. Chem., Int. Ed*., **2007**, 46, 1018.
56. Speers, A. E., Adam, G. C., Cravatt, B. F. *J. Am. Chem. Soc*., **2003**, 125, 4686.
57. Beatty, K. E., Xie, F., Wang, Q., Tirrell, D. A. *J. Am. Chem. Soc.*, **2005**, 127, 14150.
58. Deiters, A., Schultz, P. G. *Biorg. Med. Chem. Lett*., **2005**, 15, 1521.
59. Bertrand, P., Gesson, J. P. *J. Org. Chem*., **2007**, 72, 3596.
60. Golas, P. L., Tsarevsky, N. V., Sumerlin, B. S., Matyjaszewiski, K. *Macromolecules*, **2006**, 39, 6451.
61. Girard, C., Önen, E.; Aufort, M., Beauvière, S., Samson, E., Herscovici, *J. Org. Lett*. **2006**, 8, 1689-1692.
62. Zhu, L., Lynch, V. M., Anslyn, E. V. *Tetrahedron*, **2004**, 60, 7267.
63. Rostovtsev, V. V., Green, L. G., Fokin, V. V., Shapeless, K. B., *Angew, Chem. Int. Ed*., **2002**, 41, 2596-2599.
64. Nulwara, H., Takizawa, K., Odukale, A., Khan, A., Thibault, R. J., Taff, B. R., Lipshutz, B. H.; Hawker, C. J. *Macromolecules*, **2009**, 42, 6068-6074.

65. Himo, F., Lovell, T., Hilgraf, R., Rostovstev, V. V., Noodleman, L., Sharpless, K. B., Fokin, V. V. *J. Am. Chem. Soc.*, **2005**, 127, 210-216.

66. Zhan, W.-H., Barnhill, H. N., Sivakumar, K., Tian, H., Wang, Q. Tetrahedron *Lett*, **2005**, 46, 1691-1695.

67. Rodionov, V., Presolski, S., Daz Dı'az, D., Fokin, V.V., Finn, M. G. *J. Am. Chem. Soc*., **2007**, 129, 12705-12712.

68. Li, L., Lopes, P. S., Rosa, V., Figuera, C. A., Amélia, M., Lemos, N. D. A., Duarte,M.T., Avilés T., Gomes, P. T. *Dalton Trans*., **2012**, 41, 5144-5154.

69. Álvarez, J.G., Dìe, J., Gimeno. J. *Green Chem.*, **2010**, 12, 2127-2130.

70. Jiang, L., Wang, Z., Bai, S. Q., Andy Hor, T. S. *Dalton Trans.*, **2013**, 42, 9437-9443|9437.

71. McNulty, J., Keskar, K, Vermula, R. *Eur. J*., **2011**, 17, 14727-14730.

72. McNulty, J., Keskar, K. *Eur. J. Org. Chem.*, **2012**, 28, 5462-5470.

73. Wu, P., Feldman, A. K., Nugent, A. K., Hawker, C. J., Scheel, A., Voit, B., Pyn, J., Fréchet, J. M. J., Shapeless, K. B., Fokin, V. V. *Angew. Chem., Int. Ed*., **2004**, 43, 3928-3932.

74. Rodionov, V., Fokin, V. V., Finn, M. G. *Angew. Chem., Int. Ed*., **2005**, 44, 2210-2215.

75. Liu, M., Reiser, O. *Org. Lett.*, 2011, 13, 1102-1105.

76. Shao, C., Cheng, G., Su, D., Xu, J., Wang, X., Hu, Y. Adv. *Synth. Catal*., **2010**, 352, 1587-1592.

77. Liu, Q., Ji, Y. *Green Chem.*, **2011**, 13, 562-565.

78. Bhosale, S. V., Bhosale, S. V. *Mini-Rev. Org. Chem*., **2007**, 4, 231-242.

79. Ah Shin, J., Lim, Y. G., Lee, K. H. *J. Org. Chem*., **2012**, 77, 4117-4122.

80. Lutz, P. J., Rempp, P., Merrill, E. W. *Polymer Synthesis 3rd Ed*. **2004**, Wiley-VCH, New York.

81. Carothers, W.H. *J.Am.Chem.Soc.*, **1929**, 51. 2548

82. Flory, P.J. *Principles of Polymer Chemistry, Cornell University Press*, **1953**, Ch. 4, p. 106.

83. Odian G. *Principles of Polymerization, 4th Ed.* **2004**, John Wiley & Sons, INC: New York.

84. R.J. Young Chapman & hall. Introduction to polymers **1987,** ISBN 0-412-22170-5.

85. Moad, G., Solomon, D. H. *The chemistry of radical polymerization, 2nd Rev. Ed*. **2006**, Elsevier ISBN 0-08-044286-2.

86. Denisova, E.T., Denisova, T.G., Pokidova, T.S. *Hand-book of Free Radical Initiators*, **2003**. Wiley, New York.

87. Cowie, J. M. G., Valeria, A. *Polymers; Chemistry and Physics of Modern Materials 3rd Ed.* **2008**, Scotland: CRC Press.
88. Bamford, C. H., "Radical Polymerization" pp. 708-867 in Encyclopedia of Polymer Science and Engineering, Vol. 13, H. F. Mark, N.M. Bikales C.G. Overberger, and G. Menges, eds., **1988**, Wiley-interscience, New York.
89. Sarac, A. S., *Prog. Polym. Sci*., **1999**, 24, 1149.
90. Wilson, J. E., *Radiation Chemistry of Monomers, Polymer and Plastics, Chaps.* 1-5, Marcel Dekker, New York, **1974**.
91. Otero and, T. F., Mugarz, M. A. *Makromol. Chem*., **1987**, 188, 2885.
92. Samal, S. K., Nayak, B. *J. Polym. Sci. Polym. Chem. Ed*., **1988**, 26, 1035.
93. Price, G., Norris, D. J., West, P. J., *Macromolecules*, **1992**, 25, 6447.
94. Islamova, R. M., Puzin, Y. I., Kraikin, V. A. , Fatykhov, A. A., Dzhemilev, U. M. *Russ. J. of Appl. Chem.,* **2006,** 79, 1509-1513.
95. Islamova, R. M., Puzin, Y. I., Fatykhov, A. A., Monakov, Y.B. Polym. Sci., **2006,** 48, 130-133.
96. Volg, O., *J. Polym. Sci. Polym. Chem., Ed*., **2000,** 38, 4013.
97. Stevens, M. P. *Polym. Chem.: An Introduction*, **1999**, New York: Oxford University Press.
98. Cunningham M. F., Geramita, K., Ma, J. W. *Polymer*, **2000**, 41, 5385-5392.
99. Szwarc, M., levy M., Milkovic R., *J. Am. Chem. Soc*. **1956**, 78, 2656-7.
100. Ostu,T., Yoshida, M. *Markomol. Chem., Rapid Commun*., **1982**, 3, 127.
101. Ostu, T., Yoshida, M., Tazaki, T. *Makromol. Chem., Rapid Commun*., **1982**, 3, 133.
102. Nicolas, J., Guillaneuf, Y., Lefay, C., Bertin, D., Gigmes, D., Charleux, B. *prog. Polym. Sc.*, **2013**, 38, 63-235.
103. Di Lena, F., Matyjaszewski, K. *Prog. Polym. Sci.,* **2010**, 35, 959.
104. Ji, J., Yan, L. F. *J. macromol. Sci. Part A: Pure Appl. Chem.,* **2010**, 47, 445.
105. Klumpermam, B., Van Den Dungen, E. T. A., Heuts, J. P. A., et al. *Macromol. Rapid Commun.,* **2010**, 31, 1846.
106. Fischer H. *Chem. Rev*., **2001**, 101, 3581-3610.
107. Solomon, D.H., Rizzardo, E., Cacioli, P. *U.S. Patent,* **1986**, 4, 518, 429
108. Odell, P., Veregin, R. P. N., Mishalak, L. M., Brousmiche, D., Georges, M.K., *Macromolecules,* **1995**, 28, 8453-5.

109. Dollin, M. Szkurhan, A. R., Georges, M. K., *J. Polym. Sci., Part A: Polym. Chem.,* **2007**, 45, 5487-93.

110. Hawker, C.J. J. Am. Chem. Soc., **1994**, 116, 11185.

111. Moad, G., Rizzardo, E., *The Chemistry of Radical Polymerization*. **2006**, Amsterdam: Elsevier Ltd.

112. Solomon, D. H., Rizardo, E., Cacioli, P. Polymerization process and polymers produced thereby. US 4, 581, 429, CSIRO, **1986**.

113. Hawker, C. J., Barclay, G. C., Orellana, A., Dao, J., Devonport, W. *Macromolecules*, **1996**, 29, 5245-54.

114. Chiefari, J., Chong, Y.K., Ercole, F., Krstina, J., Jeffery, J., Le, T.P.T., Mayadunne, R.T.A., Meijs, G. F., Moad, C.L., Moad, G., Rizzardo, E., Thang, S. H. *Macromolecules*, **1998,** 31, 5559.

115. Moad, G., Rizzardo, E., Thang, S.H. *Aust. J. Chem*., **2005**, 58, 379-410.

116. Niranjan Yeole. "*Thiocarbonylthio compounds". Synlett*. **2010**, 10, 1572-1573.

117. Mitsukami, Y., Donovan, M., Lowe, A., McCormick, C. *Macromolecules*, **2001**, 34, 2248.

118. Perrier, S., Davis, T.P., Carmichael, A., Haddleton, D.M. *Chem. Commun*., **2002**, 2226.

119. Moad, G., Rizzardo, E., Thang, S.H. *Aust. J. Chem*., **2005**; 58, 379-410.

120. Chong, Y.K., Kristina, J., Le, T.P.T., Moad, G., Postma, A., Rizzardo, E., Thang, S.H. *Macromolecules*. **2003**, 36, 2256.

121. Chiefari, J., Mayadounne, R.T.A., Moad, C.L., Moad, G., Rizzardo, E., Postma, A., Skidnore, M.A., Thang, S.H. *Macromolecules*. **2003**, 36, 2273.

122. Quinn, J. F., Barner, L., Rizardo, E., Davis, T. P. *J. Polym. Sci. Part A: Polym. Chem*., **2001**, 40, 19-25.

123. Muthukrishnan, S., Pan, E. H., Stenzel, M. H., Barner-Kowollik, C., Davis, T. P., Lewis, D., Barner, L. *Macromolecules*, **2007**, 40, 2978-2980.

124. Chong, Y. K., Le, T. P. T., Moad, C. L., Rizzardo, E., Thang, S. H. *Macromolecules,* **1999**, 32, 2071-2074.

125. Matyjaszewski, K., Gnanou, Y., Leibler, L., *Macromolecular Engineering*. *Precise synthesis, materials properties, application.* Wiley-VCH: Weinheim, **2007**.

126. Kato, M., Kamigaito, M., Sawamoto, M., Higashimura, T. *Macromolecules*, **1995**, 28, 1721-1723.

127. Wang, J., Matyjaszewski, K. *J. Am. Soc.*, **1995**, 117, 5614-5615.
128. Van de kuil, L.A., Grove, D.M., Gossage, R.A., Zwikker, J. W., Jenneskens, L. W., Drenth, W., Van Koten, G. *Organometallics*, **1997**, 16, 4985-4994.
129. Matyjaszewski, K. *Curr. Org. Chem*., **2002**, 6, 67-82.
130. Matyjaszewski, K., Xia, *J. Chem. Rev*., **2001**, 101, 2921-2990.
131. Tang, W., Tsarevsky, N.V., Matyjaszewski, K. *J. Am. Chem. Soc.*, **2006**, 123, 598-604.
132. Ouchi, M., Terashima, T., sawamoto, M. *Chem. Rev.*, **2009**, 109, 4963-5050.
133. Seeliger, F.; Matyjaszewiski, K. *Macromolecules*, 2010, 43, 5478.
134. Morick, J., Buback, M., Matyjaszewski, K. *Macromol. Chem. Phys*. **2011**, 212, 2423-2428.
135. Tang, W., Kwak, Y., Braunecker,w., Tsarevsky, N.V., Coote, M. L., Matyjaszewski, K. *J. Am. Chem. Soc*. **2008**, 130, 10702-10713.
136. Vallee B. L., Falchuk K. H. *Physiol. Rev*., **1993**, 73, 79-118.
137. Zhang, Z., Wu, D., Guo, X., Qian, X., Lu, Z., Zu, Q., et al. *Chem Res Toxicol.*, **2005**, 18, 1814-20.
138. De Silva, A. P., Moody, T. S., Wright, G. D. *Analyst*, **2009**, 134, 2385-2393.
139. Adams, D. M., Brus, L., Chidsey, C. E. D., Creager, S., Creutz, C., Kagan, C. R., Kamat, P. V., Laeberman, M., Lindsay, S., Marcus, R. A., Metzger, R. M., Michel-Beyerle, M. E., Miller, J. R., Newton, M. D., Rolison, D. R., Sankey, O., Schanze, K. S., Yardley, J., Zhu, X. *J. Phys. Chem. B*, **2003**, 107, 6668.
140. Banthia, S., Samanta, A., J. Phys. Chem B, **2006**, 110, 6437-6440.
141. Bissell, R. A., De Silva, A. P., Gunaratne, H. Q. N., Lynch, P. L. M., Maguire, G. E. M., McCoy C. P., Sandanayake K. R. A. S. *Top. Curr. Chem*., **1993**, 168, 223-264.
142. Förster, T. *Discuss Faraday Soc. Transfer mechanisms of electronic excitation*, **1957**, 7, 27.
143. Zhang, Y., Guo, X. F., Si, W. X., Jia, L., Qian, X. H. *Org. Lett*., **2008,** 10, 473-476.
144. Zhou, X. Y., Yu, B. R., Guo, Y. L., Tang, X. L., Zhang, H. H., Liu, W. S. *Inorg. chem.*, **2010**, 49, 4002-4007.
145. Xue, L., Li, G. P., Liu, Q., Wang, H. H., Liu, C., Ding, X., He, S., Jiang, H. *Inorg. Chem.*, **2011**. 50, 3680-3690.
146. Ballesteros, E., Moreno, D., Gomez, T., Rodriguez, T., Rojo, J., Garcia-Valverde, M., Torroba, T. *Org. Lett*., **2009**. 11, 1269-1272.

147. Wang, H. H., Xue, L., Qian, Y. Y., Jiang, H. *Org. Lett*., **2010**, 12, 292-295.

148. Han, Z. X., Luo, H. Y., Zhang, X. B., Kong, R. M., Shen, G. L., Yu, R. Q. *Spectrochimica Acta Part A: Molecular and Biomolecular spectroscopy*, **2009**, 72, 1084-1088.

149. Zhou, Z., Yu, M., Yang, H., Huang, K.,Li, F., Yi, T., Huang C. *Chem. Commun*., **2008**. 3387-3389.

150. Wang, S. X., Meng, X. M., Zhu, M. Z. *Tetrahydron. Lett*., **2011**, 52, 2840-2843.

151. De, S., Baruah, J. B. *Der Pharma Chemica*, **2013**, 5, 145-149.

152. Xiaobo H., Jie M., Yu D., Yixiang C., Chengjian Z. *Polymer*, **2010**, 51, 3064-3067

153. Zhang, X., Shetty, A. S., Jenekhe, S. A. *Macromolecules*, **1999**, 3, 7422.

154. Kwon, T. W., Alam, M. M, Jenekhe, S. A. Chem. Matter. **2004**, 16, 4657-4666

155. Doebner, O., Miller, W. *Ber. Dtsch. Chem. Ges.,* **1881**, 14, 2812.

156. Hajipour, A. R., Mohammadsaleh, F. J. Org. Synth., **2011**, 43, 451- 455.

157. Lowe, A. B., McCromick,C. L. *Prog. Polym. Sci*., **2007**, 32, 283-3351.

158.Cui, Y., Zhang, X., Jenekhe, S. A. *Macromolecules,* **1999,** 32, 3824.

159. Yang, C. J., Jenekhe. S. A., Vanherzeele, H., Meth, J. S. *Ind. Eng. Chem. Res.* **1999**, 38, 1759.

160. Agrawal, A. K., Jenekhe, S. A. *Chem. Mater.* **1996**, 8, 579.

161. Zhang, X., Jenekhe, S. A. Macromolecules **2000**, 33, 2069.

162. Montes, V. A., Pohl, R., Shinar, J., Anzenbacher, P, Jr. *Chem. Eur. J.* **2006**, 12, 4523-4535.

163. Jenekhe, S. A., Osaheni, J. A. *Science* **1994**, 265, 765-768.

164. Farinha,J. S., Relógio, P., Charreyre, M. T., Prazeres, T. J. V., Martinho, J. M. G. *Macromolecules*, **2007**, 40, 4680-4690.

165. http://www.epa.gov/safewater/methods/inch-tbl.html.

166. De Silva, A. P. NiMal Gunaratne, H. Q. Gunnlaugsson, T., Huxley A. J. M., McCoy, C. P. Radamacher J. T., Rice T. E. *Chem. Rev.,* **1997**, 97, 1515.

167. McFarland, S. A., Finny, N. S. *J. Am. Chem. Soc.* **2002**, 1178-1179.

168. Fabbrizzi, L., Licchelli, M., Pallavicini, P., Perotti, A, Taglietti, A., Sacchi, D. *Chem. Eur. J.* **1996**, 75-82.

169. Bodenent, B., Fages, F., Delville, M. H. *J. Am. Chem. Soc.* **1998**, 7511-7519.

170. Xia, W. S., Schmehl, R. H., Li, C. J., Mague, J. T., Luo, C. P., Guldi, D. M. *J. Phys. Chem. B*, **2002**, 833-843.

171. Gokel, G. W. Leevy, W. M., Weber, M. E. *Chem. Rev*. **2004**, 104, 2723.

172. Wu, F. Y, Tan, X. F., Wu, Y. M. Zhao, Y. Q. *Spectrochim. Acta A: Mol. And Biomol. Spectrosc*. **2006**, 65, 925-929.

173. Meng, X., Wang, S. X. Zhu, M. *Quinoline-based Flurescence Sensors, Molecular Photochemistry-Various Aspect, Dr. Satyen Saha (Ed),* **2012**, ISBN: 978-953-51-0446-9.

174. Patnaik P. *Handbook of Environmental Analysis: Chemical Pollutants inAir, Water, Soil and Solid Wastes, CRC Press, Boca Raton, FL*, **1997**, 69.

175. Nolan, E. M., Lippard S. *J. Chem. Rev*. **2008**, 108, 3443-80.

176. Mikata, Y. Sato, Y., Takeushi, S., Kuroda, Y. Konno, H., Iwatsuki, S. *Dalton Trans*., **2013**, 42, 9688-9698.

177. Dakternieks, D. *Zinc and Cadmium, Coord. Chem. Rev.* **1990**, 98. 279-294

178. Brase, S., Gil, C., Knepper, K., Zimmermann, V. *Angew. Chem. Int. Ed*. **2005**, 44. 5188-5240.